

Regulation of Skeletal Muscle Mechanics: Chronic Influences On Acute Control

By

Austin Willard Ricci

A dissertation accepted and approved in partial

fulfillment of the

requirements for the degree of

Doctor of Philosophy

In Human Physiology

Dissertation Committee:

Damien M. Callahan, Chair

Michelle Marneweck, Core Member

Andrew C. Fry, Core Member

Nick Willet, Institutional Representative

University of Oregon

Spring 2025

© 2025 Austin Willard Ricci

This work is openly licensed via CC BY-NC-ND

Dissertation Abstract

Austin Willard Ricci

Doctor of Philosophy in Human Physiology

Title: Regulation of Skeletal Muscle Mechanics: Chronic Influences on Acute Control

Skeletal muscle mechanics are dynamically regulated by chronic stressors such as resistance training (RT), age, and circulating sex hormones as well as acute stressors such as muscle activation and fatigue. Regulatory proteins within the sarcomere influence the interactions between myosin and actin and therefore alter muscle function at the most basic level. How these proteins are modified by the interplay between chronic and acute stressors may help explain why certain at-risk populations are unable to maintain muscle function during repeated muscle contractions or exercise. We hypothesized that fatiguing exercise to task failure induces post-translational modifications to key regulatory proteins, MyBP-C and RLC, that are associated with altered contractile function of individual muscle fibers in young recreationally active, young RT, and older adults. It has also been shown that estrogen deficiency leads to reduced RLC phosphorylation and the ability to potentiate force following brief muscle activation, but this has not been studied in humans. A separate study utilized a novel model of estrogen suppression in young females to study the effects of estrogen deficiency independent of age on RLC phosphorylation and whole muscle twitch potentiation in humans. Overall, we found that fatigue paradoxically improved contractile velocity and power in single muscle fibers of young adults, more prominently in RT young adults, but not in older adults. We also found that estrogen suppression in young females may lead to reduced twitch potentiation in vivo. These set of studies shed light on how chronic effectors influence acute control of muscle contractile function at the cellular and whole tissue level.

Publications:

Privett, G. E., **Ricci, A. W.**, Wiedenfeld Needham, K., & Callahan, D. M. (2025). Chronic and Acute Mediators of Passive Viscoelasticity in Human Skeletal Muscle Fibers. *Experimental Physiology*.

Privett, G. E., **Ricci, A. W.**, David, L. L., Wiedenfeld Needham, K., Tan, Y. H., Nakayama, K. H., & Callahan, D. M. (2024). Fatiguing exercise reduces cellular passive Young's modulus in human vastus lateralis muscle. *Experimental Physiology*.

Privett, G. E., **Ricci, A. W.**, Ortiz-Delatorre, J., & Callahan, D. M. (2024). Predicting myosin heavy chain isoform from postdissection fiber length in human skeletal muscle fibers. *American Journal of Physiology-Cell Physiology*, 326(3), C749-C755.

Mongold, S. J., **Ricci, A. W.**, Hahn, M. E., & Callahan, D. M. (2022). Skeletal Muscle Compliance and Echogenicity in Resistance-Trained and Nontrained Women. *The Journal of Strength & Conditioning Research*, 10-1519.

Publications Planned:

Acute Fatigue In Vivo Alters Cellular Contractile Performance in Vitro Dependent on Training Status. **Austin W. Ricci**, Grace E. Privett, Karen W. Needham, Damien M. Callahan. Expected Submission by June 30th. This manuscript will cover the contents of Aim 1. The majority of revisions will rely on top-level decisions such as inclusion/exclusion of figures/supplementary figures as well as revisions to the body of text and discussion to best apply this work to the field and target journal.

Age Mediates the Response to Acute Fatigue In Single Muscle Fibers From Young and Older Adults. **Austin W. Ricci**, Grace E. Privett, Karen W. Needham, Damien M. Callahan. Expected Submission by June 30th. This manuscript will cover the contents of Aim 2. The revisions needed here are unlikely to require additional recruitment, although lack of MHC I fibers in young individuals may limit impact at publication. Regardless, similar to Aim 1, revisions regarding figure inclusion/exclusion and interpretations that are relevant and applicable to the field and target journal will be made.

Estrogen Suppression Reduces Twitch Potentiation Independent of Age. **Austin W. Ricci**, Julissa Ortiz-Delatorre, Damilare Adebayo, Rishi Gulati, Damien M. Callahan. Given updated power analyses with our current effect sizes, it is suggested that a sample size of 22 participants would be the target to achieve 80% power. Thus, we would need to recruit an additional 8 participants. Additionally, muscle biopsies are important to test a primary hypothesis regarding RLC phosphorylation, but likely not a requirement for publication as the most interesting and applicable data thus far are found with E2 and TP. However, at publication, the ability to identify

mechanisms (RLC, fiber type, MHC II area) contributing to this phenomenon would be crucial and improve our impact and change of acceptance to the target journal. Thus, recruiting 8 participants and analyzing the data can be done by September 15th if muscle biopsies are not a requirement, however a longer timeline of ~6months may be more realistic. Final write-up and formatting will likely take at least an additional month. Overall, expected time to submission is estimated to be by January 1st.

Acknowledgments

My deepest appreciation goes to Dr. Damien Callahan who has provided me with unwavering support and a breadth of opportunities as I completed this dissertation project and PhD program at the University of Oregon. He is the definition of a mentor and has not only served as my PhD advisor, but as a role model for what it means to be a good husband, father, and professional. Thank you.

I would also like to thank my outstanding committee members Dr. Nick Willett, Dr. Michelle Marneweck, and Dr. Andrew Fry. Thank you for your insight on this project as it would not be as strong without your guidance.

To Dr. Grace Privett, whose wise words and phrases such as “learn by struggling” accurately describe the nature of our time together. From that first day in Muscle Metabolism where I said I was in your lab and you had no idea who I was, to 6 years of some of the most effective teamwork pulling off what just two grad students shouldn’t be able to do. Thank you for being an amazing colleague and even better friend. Without you there is no way this project would have been completed.

To Julissa, your entrance to the lab and our department could not have happened at a better time. Your intellect, work ethic, and ability to fit right in with our lab environment speaks volumes to the kind of person you are. Your self-proclaimed “toxic positivity” reverberates through the lab and makes every day brighter. Thank you for being a great colleague, for your passion for physiology that allowed us to venture into a new realm of research, and for being such an amazing friend. The only regret is I didn’t get to work with you longer.

To Karen Needham, our lab and many others would not operate without you. The work you do for us is so impactful and your ability to pull off difficult experiments has been

invaluable. Thank you for the countless hours of troubleshooting gels and for keeping all of us so organized. I would also like to thank the rest of our amazing lab group. Dami and Rishi, I wish I was able to work with you both for longer. You are so intelligent and have such deep interests and passions in muscle physiology I cannot wait to see what you accomplish. Thank you for your contributions to our lab and this project, it does not go unnoticed. To our team of undergraduates, Allen Donovan, Ayoloowa Popoola, Jordan Cooper, Alex Batrouny, Navreet Sandhu, Kaitlynn Ping, and Molly Milligan. Some of you were there in the beginning and helped shaped how I mentored, taught, and learned how to conduct research. Others were there closer to the end and without you the final push to completing this project would not have been possible.

I want to thank Phillip Matern, who taught me the importance of scientific teaching and is a big reason I fell in love with muscle physiology. A good educator is able to communicate their knowledge effectively and instills passion in their audience. Phillip has emulated this every year we worked together (and the years I was his student) and I appreciate his dedication as it reminds me that the research we conduct only has an impact if we communicate it honestly and effectively.

To my family and friends, every moment from childhood until now has shaped who I am because of the experiences shared with you. I love you all more than you know and owe so much to you for making this possible. To my lovely wife, Sydney, you are my everything and through the ups and downs of this PhD you have stood by me in support, pushed when I needed pushing, and pulled when I needed pulling. No words can explain my appreciation for what you have done, thank you. I love you. And my baby girl, Reese, you are what I work for, and you are what inspires me to keep going. Your Daddy loves you.

I would like to thank our funding sources, the National Institutes of Health and the Wu Tsai Human Performance Alliance. Without your support, the impactful work this project has produced does not exist. Lastly, our research would not be possible if it were not for the volunteers that participate in human subjects research, thank you for your contribution to science.

Dedication

To my wife.

My dreams have become reality because of the love and support you have given me.

Table of Contents

Dissertation Abstract.....	3
Publications:.....	4
Acknowledgments.....	6
Dedication.....	9
List of Figures.....	14
List of Supplementary Figures.....	16
List of Tables.....	19
1. Introduction and Statement of the Problem	20
2. Literature Review.....	26
2A. The Role of Regulatory Proteins MyBP-C and RLC in Skeletal Muscle Contraction	26
2B. Skeletal Muscle Function is Modified by Fatigue	32
2C. Effects of Resistance Training on Skeletal Muscle Mechanics.....	34
2D. The Effects of Human Aging on Skeletal Muscle Structure and Function	36
2E. Female Sex Hormones Influence Skeletal Muscle Responses and Adaptations	39
3. Aim 1: To assess how fatiguing exercise impacts single muscle fiber contractile function and regulatory protein modification and if this varies by resistance training history or biological sex.	42
3A. Introduction.....	42
3B. Methods.....	45
Study Design:.....	45
Participants:.....	45
Physical Activity Monitoring:.....	46
Knee Extensor Strength, Muscle Morphology, and Fatigue Protocol:	47
Muscle Biopsy and Tissue Processing:.....	48
Single Fiber Mechanical Experiments:.....	49
SDS-PAGE/MHC Isoform Identification:	50
Western Blot:.....	51
Immunohistochemistry:	53
Antibodies:.....	53
Statistical Analysis:.....	54
3C. Results	55

Participant Characteristics, Fiber Type Distribution, and Morphology.	56
Fatiguing Exercise and Whole Muscle Performance.	58
Single fiber contractile performance in non-trained and resistance trained males and females.	60
Effects of in vivo fatigue on permeabilized single fiber contractile performance in vitro ...	62
Phosphoproteomic and Western Blot Analysis of MyBP-C and RLC.	63
3D. Discussion	64
Single fiber morphology and contractile function in resistance trained and non-trained males and females.	65
Fatiguing exercise improves single fiber velocity and power dependent on training and biological sex.	68
Effects of Resistance Training and Fatigue on RLC and MyBP-C Phosphorylation.	71
Limitations	74
Conclusion	75
4. Aim 2: To assess how chronological age mediates the effects of fatiguing exercise on single muscle fiber contractile function and regulatory protein modification.	76
4A. Introduction	76
4B. Methods	79
Study Design:	79
Participants:	79
Physical Activity Monitoring:	80
Knee Extensor Strength, Muscle Morphology, and Fatigue Protocol:	80
Muscle Biopsy and Tissue Processing:	81
Single Fiber Mechanical Experiments:	82
SDS-PAGE/MHC Isoform Identification:	84
Western Blot:	85
Immunohistochemistry:	86
Antibodies:	87
Statistical Analysis:	87
4C. Results	88
Participant Characteristics, Fiber Type Distribution, and Morphology.	89
Fatiguing Exercise and Whole Muscle Performance.	91

Single fiber contractile performance in non-trained and resistance trained males and females.	92
Effects of in vivo fatigue on permeabilized single fiber contractile performance in vitro. ..	94
Western Blot Analysis of MyBP-C and RLC.....	95
4D. Discussion	95
Single fiber morphology and fiber type distribution in young and older males and females.	97
Single fiber contractile function is not different between young and older adults.	98
Fatiguing exercise improves single fiber contractile function in an age-dependent manner.	100
Limitations	102
Conclusion	103
5. Aim 3: To investigate the role of estrogen in mediating post-activation potentiation independent of age.	104
5A. Introduction	104
5B. Methods	106
Study Design:.....	106
Participants:.....	107
Menstrual Cycle Tracking:.....	108
Physical Activity Monitoring:.....	108
Habituation Session and Ultrasonography:.....	108
Experimental Study Session:	110
Dynamometry Data Analysis:	111
Muscle Biopsy and Tissue Processing:	111
Western Blot:.....	112
SDS-PAGE/MHC Isoform Identification:	112
Immunohistochemistry:	113
Antibodies:	114
Statistical Analysis:.....	114
5C. Results	115
Anthropometrics, Activity Level, and Whole Muscle Performance	115
Serum and Plasma 17 β -Estradiol and Progesterone	116

Twitch Characteristics, Potentiation, and RLC Phosphorylation.....	118
5D. Discussion	120
Mechanisms Influencing Twitch Potentiation.....	120
Updated Analysis Following Post-Study Methodological Considerations.....	122
17 β -Estradiol May Impact Twitch Potentiation in Young Females	125
Limitations	126
Conclusions.....	128
6. Final Discussion and Conclusions	129
Supplementary Figures	135
References.....	145

List of Figures

Figure 1. Area (A) and Area Fraction (B) of MHC I (white bars) and MHC II (gray bars) fibers via immunohistochemistry in NT and RT males and females. A. Each dot represents the average fiber area from a single individual and bars represent the group mean. B. Each dot represents the area fraction for a single individual and bars represent the group mean. C. Representative image of NT (left) and RT (right) males (top) and females (bottom) histology. *significantly different from NT male at $p < 0.05$, #significantly different than NT female at $p < 0.05$, ‡significantly different from RT female at $p < 0.05$, ††† $p < 0.001$ 56

Figure 2. CSA (A.), maximum isometric force (B.), maximum isometric tension (C.), maximum loaded shortening velocity (D.), and maximum contractile power (E.) in MHC IIA (left) and MHC IIA/IIX (right) single fibers of the non-fatigued VL of NT (white bars) and RT (gray bars). Circles represent a single fiber value from a single individual. Bars represent the estimated marginal mean. p-values indicate the presence of significance between NT and RT in that fiber type..... 59

Figure 3. Maximum isometric tension (A.), maximum loaded shortening velocity (B.), and maximum contractile power (C.) in MHC IIA (left) and MHC IIA/IIX (right) single fibers of the non-fatigued (white bars) and fatigued (gray bars) VL of NT males and females. Circles represent a single fiber value from a single individual. Bars represent the estimated marginal mean. p-values indicate the presence of significance between non-fatigued and fatigued in that fiber type. 60

Figure 4. Maximum isometric tension (A.), maximum loaded shortening velocity (B.), and maximum contractile power (C.) in MHC IIA (left) and MHC IIA/IIX (right) single fibers of the non-fatigued (white bars) and fatigued (gray bars) VL of RT males and females. Circles represent a single fiber value from a single individual. Bars represent the estimated marginal mean. p-values indicate the presence of significance between non-fatigued and fatigued in that fiber type..... 61

Figure 5. Phosphorylation of MyBP-C (A.), RLC-2f (B.), and RLC-2s (C.) in the non-fatigued (closed circles) and fatigued (open circles) VL of NT (left) and RT (right). Each dot represents an individual's value and connecting lines between NF and F samples. (D.) Phosphoproteomic analysis of RLC and MyBP-C via LC/MS in RT Males. Each dot shows fold change from average NT phosphoenrichment and x indicates group mean fold change. p-values indicate significance level of main effect of training status. *indicates significantly different from NT at $FDR < 0.05$, ** $FDR < 0.001$ 62

Figure 6. Histological analysis of fiber morphology and fiber type distribution in Younger (white) and Older (gray) males (open) and females (textured). A. Average fiber area of MHC I or MHC II. B. Area fraction of MHC I or MHC II expressed as a percent. C. Percentage of total fibers analyzed in a sample that expressed MHC I or not MHC I (MHC II). D. Representative image of Young (left) and Older (right) male (top) and female (bottom). Dots represent an

individuals contribution to the group mean, which is represented as a bar. p-values denote significantly different by sex (A) or age (B,C). 89

Figure 7. CSA (A.), maximum isometric force (B.), maximum isometric tension (C.), maximum loaded shortening velocity (D.), and maximum contractile power (E.) in MHC IIA (left) and MHC IIA/IIX (right) single fibers of the non-fatigued VL of Young (white bars) and Older (gray bars). Circles represent a single fiber value from a single individual. Bars represent the estimated marginal mean. p-values indicate the presence of significance between Young and Older in that fiber type. 92

Figure 8. Maximum isometric tension (A.), maximum loaded shortening velocity (B.), and maximum contractile power (C.) in MHC I, I/IIA, IIA, and IIA/IIX single fibers of the non-fatigued (white bars) and fatigued (gray bars) VL of Older participants. Circles represent a single fiber value from a single individual. Bars represent the estimated marginal mean. p-values indicate the presence of significance between non-fatigued and fatigued in that fiber type..... 93

Figure 9. Phosphorylation of MyBP-C (A.), RLC-2f (B.), and RLC-2s (C.) in the non-fatigued (closed circles) and fatigued (open circles) VL of young (left) and older (right). p-values indicate significance level of main effect of training status. 95

Figure 10. A. Serum Estradiol (white bars) and progesterone (gray bars). B. Twitch torque before (closed circles) and after (open circles) 10s MVIC. C. Twitch torque before (closed circles) and after (open circles) 10sMVIC expressed as a % of baseline. Yellow dot represents HC participant on oral contraceptive. Each circle represents an individual data point and bars represent group mean. *** indicates significantly different from baseline at $p < 0.001$ 117

Figure 11. Twitch potentiation (A) and Twitch RTD potentiation (B) in EU, HC, and OF. Twitch potentiation on Day 1 (closed circles) vs Day 2 (open circles) in EU, HC, and OF (C). Relationship between Serum E2 and Twitch Potentiation (D). Yellow dot indicates HC participant on oral contraceptive. Each circle represents an individual data point and bars represent the group mean. *** indicates significantly different by Day at $p < 0.001$ 118

Figure 12: RLC-2s (A) and RLC-2f (B) phosphorylation before (white bars) and after (gray bars) 10sMVIC. Circles represent a single individual and bars represent the group mean. 120

List of Supplementary Figures

Supplementary 1. Comparison of different methods to assess fiber type in histology and SDS-PAGE. A. Relative abundance of MHC I, MHC IIA, and MHC IIX in NT and RT males and females. B. Association between Relative Abundance and Area Fraction of MHC I and MHC II fibers. C. Association between Relative Abundance and Fiber type distribution of MHC I and MHC II fibers. D. Representative image of MHC homogenate samples via SDS-PAGE. ** indicates difference in MHC IIX abundance at $p < 0.01$ 134

Supplementary 2. CSA (A.), maximum isometric force (B.), maximum isometric tension (C.), maximum loaded shortening velocity (D.), and maximum contractile power (E.) in MHC IIA single fibers of the non-fatigued VL of NT (white bars) and RT (gray bars) males (left) and females (right). Circles represent a single fiber value from a single individual. Bars represent the estimated marginal mean. p-values indicate the presence of and level of significance. 135

Supplementary 3. CSA (A.), maximum isometric force (B.), maximum isometric tension (C.), maximum loaded shortening velocity (D.), and maximum contractile power (E.) in MHC IIA/IIX single fibers of the non-fatigued VL of NT (white bars) and RT (gray bars) males (left) and females (right). Circles represent a single fiber value from a single individual. Bars represent the estimated marginal mean. p-values indicate the presence of and level of significance. 136

Supplementary 4. Maximum isometric tension (A.), maximum loaded shortening velocity (B.), and maximum contractile power (C.) in MHC IIA single fibers of the non-fatigued (white bars) and fatigued (gray bars) VL of NT males (left) and females (right). Circles represent a single fiber value from a single individual. Bars represent the estimated marginal mean. p-values indicate the presence of significance between non-fatigued and fatigued in that fiber type. 137

Supplementary 5. Maximum isometric tension (A.), maximum loaded shortening velocity (B.), and maximum contractile power (C.) in MHC IIA/IIX single fibers of the non-fatigued (white bars) and fatigued (gray bars) VL of NT males (left) and females (right). Circles represent a single fiber value from a single individual. Bars represent the estimated marginal mean. p-values indicate the presence of significance between non-fatigued and fatigued in that fiber type. 137

Supplementary 6. Maximum isometric tension (A.), maximum loaded shortening velocity (B.), and maximum contractile power (C.) in MHC IIA single fibers of the non-fatigued (white bars) and fatigued (gray bars) VL of RT males (left) and females (right). Circles represent a single fiber value from a single individual. Bars represent the estimated marginal mean. p-values indicate the presence of significance between non-fatigued and fatigued in that fiber type. 138

Supplementary 7. Maximum isometric tension (A.), maximum loaded shortening velocity (B.), and maximum contractile power (C.) in MHC IIA/IIX single fibers of the non-fatigued (white bars) and fatigued (gray bars) VL of RT males (left) and females (right). Circles represent a single fiber value from a single individual. Bars represent the estimated marginal mean. p-values indicate the presence of significance between non-fatigued and fatigued in that fiber type.
 138

Supplementary 8. A. Phosphorylation of RLC-2f (left) and MyBP-C (right) in flash frozen (FF) and mechanically prepared tissue. B. RLC-2f phosphorylation following sham (white bars) or alkaline phosphatase (AP, gray bars) incubation to confirm phosphorylated bands. C. Western blot images of experiment A (top) and B (bottom) for RLC-2f..... 139

Supplementary Figure 9. Phosphoproteomic analysis of differentially phosphorylated residues from NT and RT NF and F samples. A. NT males vs RT males. B. NT females vs RT females. C. NF vs F in RT males. D. NF vs F in RT females. C. NF vs F in NT males. D. NF vs F in NT females. Each dot represents an individual residue and its fold change from RT male (A), RT female (B), NF (C,D,E,F). Red dots are significantly increased phosphorylation, blue dots are significantly decreased phosphorylation, and black dots are non-significant..... 139

Supplementary 10. Comparison of different methods to assess fiber type in histology and SDS-PAGE. A. Relative abundance of MHC I, MHC IIA, and MHC IIX in Young and Older males and females. B. Association between Relative Abundance and Area Fraction of MHC I and MHC II fibers. C. Association between Relative Abundance and Fiber Type Distribution of MHC I and MHC II fibers. D. Representative image of MHC homogenate samples via SDS-PAGE. p-value indicates significantly different by age (A), # MHC IIX abundance different from Older male (A)
 140

Supplementary 11. CSA (A.), maximum isometric force (B.), maximum isometric tension (C.), maximum loaded shortening velocity (D.), and maximum contractile power (E.) in MHC IIA single fibers of the non-fatigued VL of Young (white bars) and Older (gray bars) males (left) and females (right). Circles represent a single fiber value from a single individual. Bars represent the estimated marginal mean. p-values indicate the presence of significance between Male and Female in that fiber type. 141

Supplementary 12. CSA (A.), maximum isometric force (B.), maximum isometric tension (C.), maximum loaded shortening velocity (D.), and maximum contractile power (E.) in MHC IIA single fibers of the non-fatigued VL of Young (white bars) and Older (gray bars) males (left) and females (right). Circles represent a single fiber value from a single individual. Bars represent the estimated marginal mean. p-values indicate the presence of significance between Male and Female in that fiber type. 142

Supplementary 13. Average area of MHC I (white bars) and MHC II (gray bars) fibers (A). Relationship between average MHC I (B) and MHC II (C) fiber area and twitch potentiation. Each circle represents a single individual and bars represent the group mean..... 143

Supplementary 14. Twitch torque potentiation (A) and twitch RTD potentiation (B) excluding two EU participants outside the luteal phase. Relationship between E2 and twitch potentiation in young females only (C). Yellow dot highlights HC participant on oral contraceptive. Each dot represents an individual's value and bars represent the group mean. p-value represent effect of group for A and B, and represents association between E2 and twitch torque potentiation.

..... 143

List of Tables

Table 1. Anthropometric and Activity Data of Young NT and RT Participants.....	54
Table 2. Fatigue Data and Whole-Muscle Performance in NT and RT Participants ...	57
Table 3. CSA and MHC Isoform Distribution of Single Fibers Analyzed in NT and RT Participants.....	58
Table 4. Anthropometric and Activity Data of Young and Older Participants.....	88
Table 5. Fatigue Data and Whole-Muscle Performance in Young and Older Participants	91
Table 6. CSA and MHC Isoform Distribution of Single Fibers Analyzed in Young and Older Participants.....	91
Table 7. Anthropometric and Activity Data of EU, HC, and OF Participants	115
Table 8. Whole-Muscle Performance and Twitch Characteristics in EU, HC, and OF Participant	116
Table 9. Blood 17β -Estradiol (E2) and Progesterone (P4) Concentrations in EU, HC, and OF Participants.....	116

1. Introduction and Statement of the Problem

Skeletal muscle is a highly complex and dynamic tissue whose core function is to generate force and shorten, providing locomotion. Underlying its function is the sarcomere, a highly ordered hexagonal lattice of overlapping thick and thin filaments comprised of numerous proteins, most notably actin and myosin, that interact to generate force and shorten. A key function of skeletal muscle is its regulation, driven in part by regulatory proteins that directly or indirectly alter the motor function of myosin, playing an important role in maintaining physical function under myriad conditions. The most notable acute influence on skeletal muscle function is fatigue, the reversible reduction in force and power generating capacity following repeated or prolonged activation (Callahan et al., 2009). Acute fatigue is primarily attributed to the accumulation of intracellular metabolites, proton (H^+) and inorganic phosphate (P_i), brought about by elevated and prolonged ATP hydrolysis during cross-bridge cycling (Debold, 2012). It is these metabolites that synergistically act to depress force and shortening velocity, despite saturating calcium (Ca^{2+}) (Nelson et al., 2014). During muscle activation, and especially during repeated activation such as fatiguing exercise, intracellular and extracellular signaling via Ca^{2+} and β -adrenergic stress may lead to post-translational modifications to sarcomeric regulatory proteins, further complicating skeletal muscle regulation. Skeletal muscles complex nature arises in part by its dependence and influence on other organ systems such as nervous and endocrine, therefore teasing out the contributions of these systems independent of muscle-specific responses and adaptations, perhaps even levels of muscle organizational structure, remains an important strategy to uncover the mechanisms responsible for altered contractile function. Single muscle fiber assays provide a unique approach to this problem, allowing insight into the inherent function of the muscle outside of external influences such as neuromuscular excitation

contraction coupling or endocrine/metabolic factors. These preparations allow for control of the intracellular environment, attributing differences in fiber function across groups to the properties of the cells themselves and the intracellular proteins that govern muscle contraction. Elucidating the intracellular mechanisms that describe altered contractile function remains a critical frontier of skeletal muscle physiology, as these mechanisms may serve as targets for therapeutic or rehabilitative interventions across multiple populations, especially in groups that are at increased risk for mobility impairments and injury such as older adults (Enns & Tiidus, 2010; Janssen et al., 2002) and female athletes (Anderson et al., 2019; Deitch et al., 2006), respectively.

In addition to responding to acute stimuli, skeletal muscle also adapts to chronic influencers such as repeated exercise training, chronological aging, and exposure to sex hormones. Exercise training, specifically resistance training, is a beneficial tool to improve and/or maintain muscle mass and function. It is well established that resistance training is the primary driver of hypertrophy, an increase in muscle size via increased cellular cross-sectional area (Schoenfeld, 2010). Overall, resistance trained individuals generate more absolute strength and power than non-trained individuals over a range of muscle groups, yet hypertrophy alone is not sufficient to explain the inter-individual variability in strength adaptations (Erskine et al., 2014). Relative strength and power are also generally increased following resistance training (Privett, Ricci, Needham, et al., 2024; Widrick et al., 2002), supporting the notion that increased muscle size is not the only determinant of skeletal muscle performance adaptations. In the context of aging, muscle size does not fully explain the reduction in muscle strength and power either. Motor neuron loss (Power et al., 2014), intramuscular adipose content (Akazawa et al., 2022), and preferential atrophy of fast twitch MHC II fibers and the shift in fiber type distribution towards MHC I (Lexell et al., 1983) all play a critical role in the reduction in muscle

function, specifically muscle power. In fact, the loss in strength is velocity dependent in that older adults maintain isometric strength when normalized for muscle size (Callahan & Kent-Braun, 2011). However, strength during dynamic contractions, especially at higher velocities, is greatly reduced compared to younger adults (Callahan & Kent-Braun, 2011). Dynamic contractions are critical for tasks of daily living as they are what allow for ambulation, sit-to-stands, and climbing stairs. Furthermore, repeating these dynamic contractions, i.e. fatiguing exercise, results in more power loss for older compared with younger adults, despite having greater fatigue resistance during prolonged or intermittent isometric contractions (Callahan & Kent-Braun, 2011). The decline in power during fatiguing exercise is arguably more important than baseline level reductions. Fatigability in older adults does not simply occur during intense exercise as can be argued for younger adults or athletes, instead tasks of daily living and routine physical activity may become fatiguing, not only reducing independence but increasing risks for falls and injury (Mueller-Schotte et al., 2016).

A common theme amongst aging musculoskeletal research is that females experience greater deficits in muscle mass and function across the lifespan. These disparities by sex have often been attributed to the loss of estrogen following menopause. 17β -Estradiol (E2) is the main circulating estrogen during the female menstrual cycle and is known to regulate muscle mass and function. As a steroid hormone, estradiol can pass through the phospholipid bilayer of skeletal muscle membranes and bind to nuclear estrogen receptors, ER α and ER β , and G-protein coupled estrogen receptors (GPER's), (Heldring, 2007) altering protein expression and intracellular signaling cascades. Circulating E2 can fluctuate up to 5-fold during each menstrual cycle, reaching values >500 pg/mL (Elliott-Sale et al., 2021), however it is unknown if muscle structure and function varies significantly within a menstrual cycle as E2 peaks and valleys or if chronic

exposure to these peaks is sufficient for maintaining a certain muscle phenotype. Following menopause, E2 levels drop significantly to <10pg/mL while estrone (E1), produced by adipocytes rather than the ovaries, becomes dominant (Coelingh Bennink, 2004).

Postmenopausal females exhibit lower muscle size, strength and power than younger females (Callahan & Kent-Braun, 2011), and reduced cellular hypertrophy following resistance training (Bamman et al., 2003a). In females aged 50-57 years, those that undergo estrogen replacement therapy have greater muscle cross-sectional area (CSA) and strength (Taaffe et al., 2005). It is possible the regulation of muscle mass may be attributed to differences in protein synthesis as postmenopausal females on year-long estrogen replacement therapy exhibited increased expression of proteins along the IGF-1 signaling cascade (Pöllänen et al., 2010), a critical pathway for muscle mass regulation. For premenopausal females, the use of hormonal contraceptives (HC) is common and provide an added layer of complexity regarding the effects of circulating estrogen on muscle-specific outcomes. HC's contain synthetic variations of estrogen (ethinyl estradiol, EE) and/or progesterone (progestin) to suppress ovulation and prevent pregnancy. Combination pills taken orally often contain both EE and progestin, however other options, often termed "mini pills", contain only progestin. Another class of HC's include subdermal implants, Implanon™ and Nexplanon®, that contain only progestin and release this hormone for an extended period, usually 3-5 years. Hormonal intrauterine devices (IUD) are inserted into the uterus and release progestins as well, however these progestins act directly on the uterus and do not have a notable effect on circulating estrogen (Jin et al., 2022). Combined oral contraceptives that contain both EE and progestin act to suppress endogenous E2 and progesterone production while providing a supplement of both synthetic estrogen and progesterone. Two independent systematic reviews of the current literature suggest that exercise

performance may be trivially reduced during early follicular phase, when E2 is relatively low, (McNulty et al., 2020), or when taking oral combined EE and progestin contraceptive (Elliott-Sale et al., 2020). However, much of the literature has highlighted oral contraceptive use, whereas progestin only contraceptives such as subdermal implants may provide a unique insight into estrogen suppression in young females.

Chronic adaptations to muscle structure and function may impact acute responses to muscle activity. This dissertation aims to assess 3 chronic effectors (resistance training, age, and estrogen) on the acute control of muscle function (fatiguing exercise and 10-second MVIC) and how this may vary by biological sex. Females have shown to exhibit greater fatigue resistance than males during isometric contractions, however female athletes sustain soft tissue injuries such as anterior cruciate ligament (ACL) tears at significantly higher rates than male athletes (Anderson et al., 2019). Older adults also exhibit greater isometric fatigue resistance than younger adults, yet fatigue dramatically more during dynamic contractions (Callahan & Kent-Braun, 2011). Taken together, there exists a possibility that acute fatigue-induced changes to inherent muscle function may explain differences in fatigability between younger and older males and females. We propose that modifications to sarcomeric regulatory proteins during fatiguing exercise impact the force and power generating capacity of single muscle fibers that allow younger adults to better maintain muscle power compared to older adults during exercise. In this set of studies, we assessed the force, velocity, and power of single muscle fibers and phosphorylation of key regulatory proteins from the non-fatigued and fatigued vastus lateralis in resistance trained (RT) and non-trained (NT) males and females. We also repeated this study in healthy older males and females for comparison to our NT younger adults. Further, loss of estrogen has been associated with a reduction in the baseline phosphorylation of myosin

regulatory light chain (RLC) and its ability to potentiate force following muscle activation in a phenomenon termed post-activation potentiation (PAP). This unique phenomenon allows for increased performance at the whole muscle and joint level, which may act to limit fatigue and by extension falls and injury risk. While much of the literature provides a clear mechanistic link between estrogen deficiency and RLC phosphorylation in rodent ovariectomy models, whether this extends to humans is largely unknown. In this final study, we utilized a novel study design of estrogen suppression in humans by comparing eumenorrheic young females during the mid-luteal phase of the menstrual cycle (high E2), younger females taking progestin only HC (low E2), and postmenopausal females (low E2) to identify the role of reduced circulating E2 independent of age on RLC phosphorylation and PAP.

2. Literature Review

2A. *The Role of Regulatory Proteins MyBP-C and RLC in Skeletal Muscle Contraction*

Regulatory proteins decorate the thin and thick filaments and allow for acute control of force and kinetics at the level of the cross-bridge. Two such proteins that have been widely studied in both cardiac and skeletal muscle are regulatory light chain (RLC) and myosin binding protein C (MyBP-C). These proteins are of interest as they are downstream targets of intracellular signaling, Ca^{2+} and PKA, that are upregulated during exercise.

MyBP-C is a ~125-140kDa thick filament associated protein that exists within the inner two thirds of each half sarcomere, “c-zone”, each spaced approximately 40nm apart along the axis of the thick filament in a ratio of 1 MyBP-C : 3 myosin (Heling et al., 2020a; Robinett et al., 2019). Three isoforms of MyBP-C exist: cardiac (cMyBP-C; MYBPC3), slow skeletal (ssMyBP-C; MYBPC1), and fast skeletal (fsMyBP-C; MYBPC2). These isoforms are similar in that they contain a series of 7 immunoglobulin (Ig) and 3 fibronectin (Fn) domains, termed C1-C10, however cMyBP-C contains an additional N-terminal Ig domain, C0 (Barefield & Sadayappan, 2010). For all isoforms, a linker region, M-motif, exists between C1-C2. MyBP-C can bind both actin and myosin, regulating thin filament sensitivity as well as myosin’s motor function in a phosphorylation dependent manner (Colson, 2019; Heling et al., 2020a). MyBP-C is phosphorylated mainly by cyclic AMP dependent protein kinase (protein kinase A, PKA) and additionally by protein kinase C (PKC) (Ackermann & Kontogianni-Konstantopoulos, 2011). While fsMyBP-C has no known phosphorylation sites, ssMyBP-C has 3 phosphorylatable residues in the proline-alanine rich region near the C1 domain and 1 in the M-motif, while cMyBP-C contains the opposite (Barefield & Sadayappan, 2010). Most studies investigating the structure and function of MyBP-C have been focused on the cardiac isoform, likely due to the

profound implications of MyBP-C mutations in hypertrophic cardiomyopathy (HCM). Of all the mutations associated with HCM, 40% reside within cMyBP-C (Carrier et al., 2015). Since the link has been made between MyBP-C and HCM, extensive work has been done in the role of post-translational modification to cMyBP-C with respect to sarcomeric function in cardiac muscle, yet only more recently has interest been gained in the skeletal isoforms. PKA-mediated phosphorylation has been shown to modulate the structure and function of both cardiac and skeletal MyBP-C (Bunch et al., 2019; Robinett et al., 2019). In vitro preparations of cardiac native thick and thin filaments have shown that actin sliding velocity is reduced in the c-zone, but phosphorylation of cMyBP-C allowed for an attenuation of this reduced velocity (Previs et al., 2016). This suggests that cMyBP-C provides a drag effect on thin filament shortening that is attenuated by phosphorylation (Previs et al., 2016). The suspected structural change during phosphorylation is a reduced extensibility of cMyBP-C towards the thin filament, relieving the drag effect and increasing filament shortening velocity (Previs et al., 2016). Ca^{2+} , however, may antagonistically tune contractility as cMyBP-C phosphorylation exhibited its greatest effects at low Ca^{2+} (Previs et al., 2016). Similar findings have been shown in permeabilized skeletal muscle fibers where Robinett et al. 2019 demonstrated that slow fibers experience a greater transient force overshoot than fast fibers assessed by slack-restretch protocol. Transient force overshoot is a phenomenon that occurs in permeabilized muscle fibers following a protocol by which the fiber is rapidly slacked after achieving peak isometric force to remove all existing cross bridges, then restretched to original length to assess the rate of cross bridge attachment. The finding that slow fibers had a larger transient force overshoot suggests that they can form new cross bridges in response to this mechanical perturbation (Robinett et al., 2019), but is opposite hypotheses based on previous work that this overshoot is due to an increase in the

cooperativity of activation and that fast fibers are more cooperative than slow fibers (Campbell, 2006; McDonald, 2000). MyBP-C, as evidenced in cardiac muscle, can sequester myosin heads in a way that reduces the binding affinity of myosin to actin (Previs et al., 2016). Therefore, incubation of permeabilized fibers with PKA allows for the ability to test fiber-type specific responses in cross-bridge kinetics to ssMyBP-C phosphorylation. When subjected to a slack-restretch protocol, slow fibers doubled their force overshoot in response to PKA at low Ca^{2+} (Robinett et al., 2019). Fast and slow fibers exhibited the same response at saturating Ca^{2+} , presumably due to the notion that no additional cross-bridges would be available. Similar to cardiac, skeletal fibers increased loaded shortening velocity in the c-zone when incubated with PKA compared with native state in the presence of low but not high Ca^{2+} (Robinett et al., 2019). Lambda phosphatase (LP) treatment was shown to do the opposite and inhibit loaded shortening velocity within the c-zone, again at low Ca^{2+} (Robinett et al., 2019). Overall, in human skeletal muscle, ssMyBP-C is a tunable protein that regulates cross-bridge kinetics in a phosphorylation-dependent manner.

Myosin regulatory light chain (RLC) is a thick filament associated protein that modulates skeletal muscle contractility. This dumbbell shaped regulatory protein lies in the lever arm region of the myosin S1 fragment and modulates the extensibility of the myosin head towards or away from the thin filament (Rayment et al., 1993). Unlike smooth muscle, striated muscle (cardiac and skeletal) does not largely depend on RLC for muscle activation. Instead, RLC tunes contractility in a phosphorylation-dependent manner. During skeletal muscle contraction, large Ca^{2+} transients increase the sarcoplasmic Ca^{2+} concentrations, thereby activating calmodulin. The Ca^{2+} /calmodulin complex activates the skeletal specific Ca^{2+} /calmodulin dependent kinase, myosin light chain kinase (skMLCK), which phosphorylates serine residues 14 and 15 on RLC

(Blumenthal & Stull, 1980). In general, RLC phosphorylation increases the extensibility of myosin towards the thin filament thus increasing Ca^{2+} sensitivity and submaximal force (Sweeney & Stull, 1990).

skMLCK activation occurs rapidly upon muscle activation, however dissociation kinetics of Ca^{2+} from calmodulin are nearly 4 times slower than that of binding (Bowman et al., 1992). This allows for prolonged skMLCK activity after relaxation of skeletal muscle and provides a “memory effect” of sustained RLC phosphorylation within the muscle that increases contractility upon subsequent activations. Additionally, the maximal rates of RLC dephosphorylation by myosin light chain phosphatase (MLCP) are up to 50 times slower than that of phosphorylation, and there appears to be more MLCK than MLCP in skeletal muscle which further contributes to sustained RLC phosphorylation (Manning & Stull, 1982; Moore & Stull, 1984). Contractions to induce RLC phosphorylation, commonly referred to as conditioning contractions, are not required to involve fused tetany evidenced by studies showing a single twitch is a sufficient amount of Ca^{2+} to activate skMLCK and resultant sustained RLC phosphorylation (Klug et al., 1986; Moore & Stull, 1984). However, single twitches do not maximally activate skMLCK and therefore a lower fraction of RLC will be phosphorylated. As a result, RLC phosphorylation is both time and frequency dependent. Lastly, there are larger concentrations of MLCK in fast skeletal muscle than slow, and slow muscle requires a higher frequency and duration of stimulation to achieve the same RLC phosphorylation as fast muscle (Klug et al., 1986; Moore & Stull, 1984; Westwood et al., 1984).

The mechanistic link between skMLCK and RLC phosphorylation is evidenced in pre-clinical models of skMLCK knockout mice. When compared to wild type (WT) mice, skMLCK-KO extensor digitorum longus (EDL) stimulation in either short (1min) or long term (5min) does

not result in RLC phosphorylation (Gittings et al., 2011). Additionally, twitch force is minimally potentiated in the early phase of stimulations (<1min), whereas WT mice exhibit ~37% increase in twitch force (Gittings et al., 2011).

In vitro assays of permeabilized single fibers show that addition of skMLCK increases RLC phosphorylation and causes a left-ward shift in the force-pCa curve, suggesting increases in force at submaximal, but not maximal Ca^{2+} concentrations (Persechini et al., 1985; Sweeney & Stull, 1986). Early evidence in rabbit psoas permeabilized fibers suggest that the increases in force following titrated RLC phosphorylation are directly proportional to ATPase activity, which implies that this response is due to an increase in the number of cycling cross-bridges and not an increase in the force per cross-bridge (Sweeney & Stull, 1986). At the cross-bridge level, RLC phosphorylation increases the kinetics of cross-bridge attachment, evidenced by increased f_{app} , however has little to no effect on g_{app} , suggesting no effect on detachment kinetics (Metzger et al., 1989; Sweeney & Stull, 1990). Furthermore, the rate of tension redevelopment following isotonic shortening and restretch, k_{tr} , are higher in phosphorylated fibers across a range of pCa (Sweeney & Stull, 1990). Despite no effect of RLC phosphorylation on detachment kinetics, in vitro motility assays have shown reductions in actin sliding velocity under basal conditions (Greenberg et al., 2010). It is possible this may be explained simply by a larger number of strongly bound myosin heads to actin, reducing sliding velocity. It is important to note that the lack of effect of RLC phosphorylation on actin sliding velocity, single fiber shortening velocity (Persechini et al., 1985), or whole muscle contractile velocity (Butler et al., 1983; Palmer & Moore, 1989) are all under unloaded conditions. Less is known about the effects of RLC phosphorylation on loaded shortening velocity in single fibers and this would provide greater insight into muscle mechanics in vivo.

The cellular and molecular studies of RLC phosphorylation in pre-clinical models have provided substantial insight into the mechanisms of muscle contraction, however it is necessary to translate these findings to the whole tissue. Further, the application of this research to human locomotion requires an investigation beyond steady-state isometric contractions and into the dynamic nature of human muscle performance. Thus, studies of stretch-shortening cycles in rodent muscle have proved useful in uncovering the effects of RLC phosphorylation on loaded shortening in both concentric and eccentric work and power. In mouse EDL, work loops following conditioning contractions of increasing frequencies showed that dynamic work and power was increased along with isometric force in line with increasing RLC phosphorylation (Xeni et al., 2011).

Nearly all the mechanistic work at the cellular level regarding RLC has been conducted in animals. Little to no studies of human single fibers have contributed, thus most of the research revolves around the practical applications of RLC phosphorylation at the whole muscle level. The majority is related to the phenomenon of post activation potentiation (PAP), which is an enhancement of force following voluntary or electrically stimulated contractions. M.E. Houston and colleagues were the first to relate RLC phosphorylation and PAP in humans (Grange & Houston, 1991; Houston et al., 1985, 1987; Houston & Grange, 1991; Stuart et al., 1988). Through these studies, it was found that isometric twitch force is potentiated following either electrically stimulated or maximum voluntary isometric contractions. Although similar findings are found in humans compared to animals, there is large variability in the magnitude of potentiation following a conditioning contraction. It seems likely that this is influenced by the heterogeneity of human skeletal muscle, and the fiber type dependence of RLC phosphorylation. However, in contrast to animals, the same conditioning stimulus has been shown to increase

RLC phosphate content of both slow and fast isoforms in humans (Houston et al., 1987). There does not exist enough data to definitively state that phosphorylation-mediated contractile improvements are or are not isoform specific in humans.

2B. Skeletal Muscle Function is Modified by Fatigue

Skeletal muscle fatigue, as defined by an acute reduction in the force and power generating capacity following repeated or prolonged activation (Callahan et al., 2009), is largely attributed to the accumulation of intracellular metabolites, proton (H^+) and inorganic phosphate (P_i), brought about by elevated and prolonged ATP hydrolysis during cross-bridge cycling (Debold, 2012). Permeabilized muscle fibers activated in fatigued conditions (30mM P_i and 6.2 pH) exhibit reduced contractile function despite saturating Ca^{2+} concentrations [30,9,8]. P_i is thought to manifest its effects through inhibition of the power stroke and reduce the number of strongly bound cross bridges (Debold et al., 2013, 2016). Specifically, elevated P_i reduces force by way of rebinding myosin to a strong, yet weaker state when myosin is bound to actin but before ADP release from myosin (Cooke & Pate, 1985; Takagi et al., 2004). Motility assays have shown that the actin filament sliding velocity is reduced under fatiguing pH (Debold et al., 2008), confirming that low pH directly affects myosin's interaction with actin. Laser trap assays have confirmed that the time myosin is bound to actin (t_{on}) is prolonged under low pH conditions, specifically due to a slowed rate of ADP release from myosin (Debold et al., 2008). While prolonged t_{on} would indicate greater duty ratio, producing greater isometric force which is contrast to single fiber studies (Cooke et al., 1988), Debold et al. 2008 argue that the slowed rate of ATPase activity (Cooke et al., 1988) could reduce the duty ratio that leads to an insignificant change to maximal force seen in single fibers. Data show that P_i and H^+ act synergistically to

depress peak power by 63%, a near two-fold decrease compared to P_i (26%) or H^+ (34%) alone [30,12,23](Debold et al., 2004; Knuth et al., 2006; Nelson et al., 2014). It is difficult to understand which mechanisms are predominating in vivo, however, some combination of the two, reflected by di-protonated phosphate ($H_2PO_4^-$), accurately predicts fatigue during repeated maximum voluntary contractions in humans (Lanza et al., 2007).

Fatigue may also interact with regulatory proteins to alter muscle mechanics. Single fibers in a fatigued environment experience a rightward shift in the force-pCa curve, (Nelson & Fitts, 2014), possibly through competition between H^+ and Ca^{2+} for Troponin C (Parsons et al., 1997). An in vitro fatigue protocol (100Hz stimulation for 100ms, every 2s for 5min) on whole mouse soleus muscle increased phosphorylation of sMyBP-C at Ser59 and Thr84, with no change at Ser62 or Ser204 compared to young wild type mice (Ackermann et al., 2015). Ser59 and Thr84 are phosphorylated by PKA and PKC, respectively (Ackermann & Kontogianni-Konstantopoulos, 2011). During fatiguing exercise, large Ca^{2+} transients may lead to increased activity of PKC (Rose et al., 2004), and a rise in cyclic AMP (cAMP) downstream of β -adrenergic signaling leads to increased PKA activity. It may be that fatiguing exercise leads to downstream phosphorylation of MyBP-C and RLC that aim to sustain dynamic muscle work power in vivo. It is also possible that chronic influencers such as resistance training, aging, or circulating estrogen may alter phosphorylation of these proteins at baseline and, importantly, the ability to phosphorylate during sustained muscle activation.

2C. Effects of Resistance Training on Skeletal Muscle Mechanics

Resistance training is a form of exercise training that involves repetitive dynamic joint movements against predetermined loads. This form of training is utilized clinically to increase muscle mass and strength, although there is a myriad of other health benefits (Westcott, 2012). The increase in muscle mass associated with resistance training is termed hypertrophy, the growth of a muscle by an increase in fiber area rather than number of fibers (Schoenfeld, 2010).

12 weeks of resistance training in young males increased fiber CSA, absolute force, and absolute power (Widrick et al., 2002). These enhancements seem to be due to increased muscle size as specific tension and normalized power show no increases following training (Widrick et al., 2002). The same outcomes were seen following a 14-week resistance training program, with similar relative increases in both young and old males and females (Claflin et al., 2011).

Amongst older adults, 12 weeks of resistance training increases normalized power and unloaded shortening velocity in men (Trappe et al., 2000), but not women (Trappe et al., 2001). However, more long-term training of 12 months increased specific force and unloaded shortening velocity in elderly women (Parente et al., 2008). Cross-sectional studies of chronic resistance training history show that body builders and weightlifters have a larger fiber CSA with greater associated force and power, yet again when normalized for muscle size the fibers perform similarly to non-trained adults (Shoepe et al., 2003), except in body builders where they also exhibited slight increases in specific tension (D'Antona et al., 2006). Interestingly, unloaded shortening velocity within a fiber type tends to be unchanged (D'Antona et al., 2006), which suggest that improvements to muscle power arise from increases in size and force generating capacity.

Contrary to these findings, recent work has found that a group of body builders had lower single fiber specific tension and power than control fibers, despite increases in CSA, absolute force, and

absolute power (Meijer et al., 2015). In line with these findings, one study has suggested that when measuring contractile properties of large fibers, typically from populations such as body builders, the CSA may be overestimated (Monti et al., 2020). In permeabilized fibers, it is generally accepted that fibers swell around 20% of initial volume (Moss, 1979). However, Monti et al. suggest that larger fibers may swell disproportionately more than smaller fibers and thus normalized values of force, i.e. tension, may be artificially reduced. In their study of 6 male body builders and 6 controls, fibers from body builders had lower normalized force, however when correcting for fiber swelling normalizing to the average CSA from histological cross-sections, the differences were abolished.

There does not appear to be data regarding RLC phosphorylation changes with chronic resistance training. However, PAP seems to benefit resistance trained athletes more than recreationally active or sedentary young individuals. For example, resistance trained athletes saw larger potentiation of lower body power during squat than recreationally active males and females following conditioning exercise (Chiu et al., 2003). In older adults, 12 weeks of resistance training increased PAP (Hicks et al., 1991). One potential explanation for an increase in PAP following training is the increased ability to resist fatigue during the conditioning contraction and/or exercise. Many studies utilize a sustained maximal voluntary isometric contraction (MVIC) followed immediately by single twitches (twitch potentiation) or dynamic power movement (performance enhancement). Albeit short term, an MVIC or other conditioning activity may be enough of a stimulus to induce some amount of fatigue in non-trained individuals that mask the effects of RLC phosphorylation-induced force or power potentiation. Of course, increased MHC II area following resistance training may provide a larger relative

abundance of RLC-2f compared RLC-2s, which could allow for increased phosphorylation of RLC from baseline thus enhancing performance.

It has been shown that maximal chronic stimulation of skeletal muscle and treadmill running in rats elicited rises in β -adrenergic receptor density (Farrar et al., 1997). While it is unknown how chronic training regimens may affect regulatory protein modification, it is logical that repeated exposure to adrenergic signaling may cause adaptation in receptor density or sensitivity. This would have large implications in that rehabilitative regimens may be able to target specific training modalities that modulate adrenergic signaling not only in muscle but balance the cardiovascular responses to exercise.

2D. The Effects of Human Aging on Skeletal Muscle Structure and Function

Aging is associated with a reduction in muscle mass and strength, commonly referred to as sarcopenia. Although older adults retain relative isometric torque, power during dynamic contractions are reduced compared to younger adults when normalized for muscle size (Callahan et al., 2009; Callahan & Kent-Braun, 2011; M. S. Miller et al., 2013a). However, this reduced contractile performance cannot be solely explained by reductions in muscle size. Although whole muscle CSA is reduced in older adults (Lexell et al., 1995), fiber CSA is generally unchanged (Frontera et al., 2000, 2008; Hvid et al., 2010), despite a few studies suggesting the potential for reductions (D'Antona et al., 2003; Korhonen et al., 2006; Larsson et al., 1997). However, some studies have indicated that CSA of MHC I fibers are larger in older adults compared with young (M. S. Miller et al., 2013a). Furthermore, aging is associated with the preferential atrophy of MHC II fibers (Lexell et al., 1995), whereas acute disuse in older adults is associated with a shift in fiber type distribution towards MHC II (D'Antona et al., 2003). Taken with the notion that

inactivity reduces single fiber CSA (D'Antona et al., 2003), it is possible that the age-related decline in activity level contributes to altered fiber area in some studies and thus physical activity needs to be a large consideration when drawing conclusions.

Single fiber studies provide valuable insight into the inherent contractile properties of the muscle outside of the influence of muscle architecture, neural recruitment patterns, and metabolic activity. Specific tension and unloaded shortening velocity (V_o) have been shown to decrease with age in both MHC I and IIA fibers from males and females (D'Antona et al., 2003; Frontera et al., 2000; Larsson et al., 1997; Ochala et al., 2007; Yu et al., 2007). Interestingly, some studies show no change in tension or V_o (Frontera et al., 2008; Korhonen et al., 2006; Trappe et al., 2003). Cross bridge kinetics seem to be slowed with age as evidenced by prolonged t_{on} in MHC IIA fibers (M. S. Miller et al., 2013a). There also exists evidence for reduced actin sliding velocity using isolated myosin from older adults (D'Antona et al., 2003; Höök et al., 2001), however this seems to be isoform dependent as MHC IIA actin sliding velocity was unchanged. The variation in responses to aging between studies may be reflected in the commonly overlooked influence of activity level. Acute disuse is associated with an increased shortening velocity (D'Antona et al., 2003), whereas resistance training is associated with increases in force and power in older adults (Trappe et al., 2000, 2001). Therefore, it is critical to control for activity type, intensity, and duration when comparing single muscle fibers from older and younger individuals.

Regulatory proteins within the sarcomere may influence the response of single fiber performance to aging. Specifically, aging has been associated with a reduction in RLC phosphorylation in rats (Gregorich et al., 2016) and humans (Gelfi et al., 2006), despite increased activity level compared to younger adults. Older females have shown reduced RLC-2f

phosphorylation compared to younger adults and older males (M. S. Miller et al., 2013a).

Although animal models suggest RLC phosphorylation is generally unique to the fast isoform, it is not clear if that is the case in humans and some evidence would suggest that it is not (Houston et al., 1987). Therefore, reductions in cross bridge kinetics and shortening velocity in both MHC I and IIA with age track with proposed reductions in RLC phosphorylation, regardless of RLC isoform. Older adults exhibit a reduced force potentiation following a conditioning stimulus (Hicks et al., 1991; Petrella et al., 1989), indicating a reduced ability to phosphorylate RLC. It is possible that reduced RLC-2f abundance due to reduced MHC II area plays a role in reduced twitch potentiation. Moreover, when expressed as a relative increase from baseline twitch, it is possible that if less knee extensor muscle mass is comprised of MHC II (and thus RLC-2f) containing fibers that relative increase in RLC-2f phosphorylation and resultant twitch potentiation will be reduced. Consistent with this, resistance training in older adults increased twitch potentiation (Hicks et al., 1991) and may be due to increased MHC II area, however it is also possible this is simply a better ability to resist fatigue during the conditioning stimulus. As mentioned previously, MyBP-C is phosphorylated by both PKA and PKC. It is unclear whether age impacts β -adrenergic signaling in skeletal muscle. In rats, it does not appear that β -receptor density changes with age, however when exposed to the same treadmill running exercise for 6 months, young but not old rats increased skeletal muscle β -receptor density (Farrar et al., 1997). Therefore, it is possible that chronic effectors of contraction-induced adaptations may be blunted in older individuals. Aging has also been associated with reduced cytosolic PKC in rat soleus muscle (Ishizuka et al., 1993). Therefore, it is possible that aging may result in a blunted ability to phosphorylate proteins downstream of PKA and PKC such as MyBP-C in comparison to younger adults.

2E. Female Sex Hormones Influence Skeletal Muscle Responses and Adaptations

In menstruating females, the aromatase enzyme converts testosterone to estradiol, most notably 17 β -estradiol (Chidi-Ogbolu & Baar, 2019). As a steroid hormone, estradiol can pass through the phospholipid bilayer of skeletal muscle membranes and bind to nuclear estrogen receptors (Heldring et al., 2007). Circulating estradiol can fluctuate up to 5-fold during each menstrual cycle (Elliott-Sale et al., 2021). Thus, if any effects of estradiol exist on skeletal muscle structure and function, then timing of training regimens, clinical treatments, and research studies need to address the variation within an individual in order to better serve and understand female health. Furthermore, cycle length between individuals considered to be eumenorrheic can vary from 21-35 days and estradiol peaks can be up to 3 times higher or lower between these individuals (D'Souza et al., 2023). Although this complicates the study of females, it serves as a stark reminder of the complexity of human biology and should be viewed as evidence to better design research studies to accurately investigate female health.

Skeletal muscle is sensitive to estradiol and has been widely studied in animal models. Estrogen deficiency via ovariectomy (OVX) in mice has resulted in a reduction in both whole muscle and single fiber CSA (Kitajima & Ono, 2016). Administration of exogenous estrogen following OVX resulted in a recovery of fiber and muscle CSA, drawing the mechanistic link between estrogen and muscle size (Kitajima & Ono, 2016). Interestingly, these OVX mice had lower MHC IIA fibers and more MHC IIB which suggests similar response as in disuse atrophy. In regards to muscle contractility, OVX has been associated with reduced single fiber specific tension (Moran et al., 2007) and actin-myosin kinetics (Colson et al., 2015), that are recovered with estradiol administration. At the whole muscle level, isometric and dynamic torque is

reduced in ER α -knockout (Cabelka et al., 2019) and associated with increased fatigability during isometric and dynamic contractions (Cabelka et al., 2019; Collins et al., 2018) and poor recovery of force (Collins et al., 2018). Interestingly, these have been seen in predominantly slow-twitch soleus muscle, whereas fast-twitch extensor digitorum longus (EDL) exhibit no change (Collins et al., 2018). Thus, evidence supports that estrogen signaling is an important regulator of skeletal muscle contractility, not just by amount of estradiol available but also in its capacity to signal downstream within the muscle.

In humans, much of the work in sex hormones has been performed in the context of aging. Strength training studies have suggested that postmenopausal females have reduced response to anabolic stimuli (Bamman et al., 2003b), however in older females on hormone replacement therapy (HRT), specifically estrogen, anabolic responses are similar to premenopausal females (Hansen & Kjaer, 2014). Much of these differences can be attributed to the decline in muscle protein synthesis (Pöllänen et al., 2010). Muscle atrophy, especially with age, is dependent on the balance of protein synthesis and degradation, therefore declines in estrogen with age may affect muscle protein synthesis and subsequently lead to disproportionate muscle atrophy compared to females on HRT or males. A large cross-sectional study of 840 postmenopausal females found that those on HRT had larger muscle CSA and isometric grip strength (Taaffe et al., 2005). The relationship between whole muscle performance and menstrual cycle in females comes with inconclusive results. Aerobic exercise performance does not seem to be altered by circulating hormones (Taylor et al., 2024), and high intensity hamstring and quadriceps isometric and isokinetic torque across the menstrual cycle is similar (Janse de Jonge et al., 2001). While one study has shown that vastus lateralis motor unit firing rates were different (Piasecki et al., 2023), these were not related to muscle performance. Lastly, in highly trained female athletes, neither

oral contraceptive or eumenorrheic menstrual cycle phase altered grip strength, counter movement jump performance, or 20m sprint (Dasa et al., 2021). Despite these inconclusive findings, it may be that chronic estrogen suppression or deficiency such as oral contraceptive use or menopause, respectively, serve as more important in regulating muscle mechanics than acute fluctuations in the menstrual cycle.

Estrogen has been shown to play a significant role in RLC phosphorylation and subsequent force potentiation in pre-clinical models. OVX mice exhibited reduced RLC phosphorylation that was recovered with addition of exogenous estradiol (Lai et al., 2016). In C2C12 cells, increasing exogenous estradiol concentrations linearly increases RLC phosphorylation (Lai et al., 2016). Furthermore, post tetanic potentiation is reduced with OVX and again restored with estradiol administration, but interestingly not different between sham control administered with vehicle vs estrogen (Lai et al., 2016). However, the increase in maximal rate of force development during twitch potentiation is lower in OVX than OVX + estrogen, but sham animals with exogenous estrogen also exhibited increased maximal rate of force development compared to vehicle administration (Lai et al., 2016). ER α -knockout mice have also exhibited reduced post tetanic potentiation and significant reductions in RLC phosphorylation (Collins et al., 2018). Older adult postmenopausal females have shown reduced RLC phosphorylation compared to older adults but importantly to young females (M. S. Miller et al., 2013a), which may be related to loss of estrogen however data is limited in humans.

3. Aim 1: To assess how fatiguing exercise impacts single muscle fiber contractile function and regulatory protein modification and if this varies by resistance training history or biological sex.

3A. Introduction

Chronic resistance training increases muscle mass along with force and power generating capacity (Schoenfeld et al., 2017) yet despite similar training history, relative strength and power remains lower in females (Bartolomei et al., 2021; Perez-Gomez et al., 2008). It is possible that disparities in cellular level adaptations to resistance training may explain these outcomes, although the literature is mixed. 12 weeks of resistance training in young males increased fiber CSA, absolute force, and absolute power (Widrick et al., 2002). These enhancements seem to be due to increased muscle size as specific tension and normalized power show no increases following training (Widrick et al., 2002). The same outcomes were seen following a 14-week resistance training program, with similar relative increases in both young and old males and females (Claflin et al., 2011). Amongst older adults, 12 weeks of resistance training increases normalized power and unloaded shortening velocity in men (Trappe et al., 2000), but not women (Trappe et al., 2001). However, more long-term training of 12 months increased specific force and unloaded shortening velocity in elderly women (Parente et al., 2008). Reduced strength and power have been shown to increase risk for soft tissue injury (de la Motte et al., 2019) and female athletes have a significantly greater incidence of soft tissue injury, such as anterior cruciate ligament (ACL) rupture, than their male counterparts (Anderson et al., 2019; Deitch et al., 2006). The acute reduction in force and power generating capacity following repeated or prolonged muscle activation, i.e. muscle fatigue, may contribute to lower-limb injury risk during

sport or training and rehabilitation programs, although it remains unclear whether this stems from central or peripheral mechanisms (Bourne et al., 2019). However, the compounding effects of peripheral muscle fatigue and existing sex-based differences in relative strength and power may explain the higher injury risk among female athletes.

Females are generally less fatigable than males during isometric contractions (Hunter, 2014). This is thought to be due in part to the larger relative area of Type 1 fibers in females (Hunter, 2014; A. E. Miller et al., 1993). Additionally, during prolonged isometric contractions, intramuscular forces act to occlude the exercising muscle thus reducing perfusion and leading to a larger accumulation of metabolites (Seals et al., 1988). Males typically produce larger absolute torques than females, which may lead to occluding more muscle mass and ultimately leading to less perfusion and additional metabolite buildup. Less is known about sex-based differences in fatiguability during dynamic contractions, although recent studies have shown them to be muscle group and shortening velocity dependent. For example, when strength and power of the elbow flexor muscles of males and females were compared during a dynamic fatiguing task at 20% maximum voluntary isometric contraction (MVIC) torque, the time to failure was longer in females than males at slow velocities (60deg sec^{-1}) (Yoon et al., 2015). However, when instructed to perform this same task as fast as possible, fatiguability was not different between the sexes (Senefeld et al., 2013). These studies have identified mechanisms inherent to the muscle contractile apparatus that may be responsible for observations of sex-based differences in fatigue.

The accumulation of intracellular metabolites that are known to reduce force and power, such as proton (H^+) and inorganic phosphate (P_i) (Debold et al., 2016), are likely not the sole contributors to the alterations in skeletal muscle contractile performance during or following muscle fatigue. Acute changes to the phosphoproteome have been reported in skeletal muscle

following repeated or prolonged muscle activations. For example, myosin regulatory light chain is phosphorylated following transient increases in sarcoplasmic Ca^{2+} concentrations during prolonged muscle activation (Gittings et al., 2011), resulting in enhanced myofilament Ca^{2+} sensitivity (Persechini et al., 1985; Sweeney & Stull, 1986) and myosin kinetics (Metzger et al., 1989; Sweeney & Stull, 1990) in vitro. In vivo, RLC phosphorylation following a sustained maximal voluntary contraction (MVC) potentiates force and power in humans (Chiu et al., 2003; Houston et al., 1985; Stuart et al., 1988), and is thought to be the mechanism behind post-activation potentiation (PAP). Additionally, myosin binding protein C (MyBP-C) regulates crossbridge formation by directly interacting with both thick and thin filaments and is phosphorylated by protein kinase A (PKA), resulting in enhanced velocity and power (Robinett et al., 2019). It has been demonstrated that both RLC (Gittings, 2011) and MyBP-C (Ackermann & Kontogianni-Konstantopoulos, 2011) are phosphorylated in mouse fast (extensor digitorum longus, EDL) and slow (soleus) muscle, respectively, following exposure to an in vitro fatigue protocol. Activation-dependent increases in RLC and MyBP-C phosphorylation may act to limit or forestall muscle fatigue in vivo, improving performance during repetitive and strenuous tasks while potentially reducing injury risk in athletes. It is difficult to distinguish in vivo between the primary contributors to fatigue (i.e. metabolites) and the ancillary effects of prolonged activation (i.e. protein phosphorylation). Therefore, measuring the contractile phenotype of single muscle fibers after an in vivo fatiguing protocol offers insight into the inherent function of skeletal muscle, influenced by fatigue-induced modifications to the phosphoproteome that are independent of metabolite accumulation. Understanding the acute changes to both the muscle phosphoproteome and inherent cellular contractile performance in males and females will help elucidate potential mechanisms that explain sex-based differences in fatigability and injury risk.

Therefore, the purpose of this study was to test the effects of a single bout of fatiguing dynamic knee extensions to task failure on the contractile performance of single muscle fibers of the vastus lateralis (VL) from resistance trained (RT) and non-trained (NT) young adults. We used a voluntary dynamic fatiguing exercise protocol in vivo as a tool to modify the intracellular environment and significantly fatigue the knee extensor muscles to explore potential changes to the muscle phosphoproteome and characterize alterations to the inherent contractile performance of single muscle fibers in vitro. We hypothesized that a single bout of fatiguing exercise to task failure would result in enhanced contractile performance (velocity and power) of permeabilized single fibers under near-optimal intracellular metabolic conditions compared to fibers from the non-fatigued control VL. We also hypothesized that in vivo fatigue would increase the phosphorylation of MyBP-C and RLC compared to the non-fatigued control VL.

3B. Methods

Study Design: A total of 9 non-trained (NT) (4 males; 5 females) and 9 resistance trained (RT) (4 males; 5 females) young adults performed an acute bout of isotonic fatiguing knee extensor contractions at 30% MVIC on their dominant limb. Muscle biopsies from the dominant (fatigued) and non-dominant (control/non-fatigued) limb were performed, and muscle samples were separated for assessment of in vitro cellular contractile performance and western blot to assess phosphorylation of MyBP-C and RLC.

Participants: A total of total of 9 non-trained (NT) (4 males; 5 females) and 9 resistance trained (RT) (4 males; 5 females) young adults participated in the study. All participants completed informed consent and health history questionnaire, prior to inclusion in the study. The

requirement for admission into the RT group was participation in structured resistance training at least 5 days/week, 1hr/session, with a minimum of 3 days/week including lower body resistance training for at least the past 12 months. The requirement for admission into the NT group was no history of structured exercise of any kind. To limit the potential for menstrual cycle-dependent variation in circulating estradiol, all female participants either reported use of hormonal contraceptive or were tested in the pre-follicular phase of the menstrual cycle, (within 5 days of menses onset). Participants reported no orthopedic limitations (severe osteoarthritis, prior joint replacement, etc.), endocrine disease (hypo/hyperthyroidism, Addison's Disease or Cushing's syndrome, etc.), uncontrolled hypertension ($>140/90$ mmHg), neuromuscular disorder, significant heart, liver, kidney or respiratory disease, and/or diabetes. Participants were non-smokers. Finally, participants taking medications known to affect either muscle contractility or beta-adrenergic signaling of neuromuscular activation (including but not limited to beta blockers, calcium channel blockers, and muscle relaxers) were not included.

Physical Activity Monitoring: Habitual physical activity was monitored for approximately 7 days (including at least 1 weekend day) using an ActivPAL (PAL Technologies, UK) triaxial accelerometer affixed to the anterior aspect of the mid-thigh using a waterproof protective barrier (Tegaderm, 3M). Data was categorized according to ActivPAL Daily Summary Outcomes Exports as step count (steps/day) and time spent in 4 different activity categories based on step cadence: time in sedentary (0steps/min), light (<75 steps/min), moderate (≥ 75 steps/min, <125 steps/min), and vigorous (≥ 125 steps/min) activity.

Knee Extensor Strength, Muscle Morphology, and Fatigue Protocol: Participants became familiarized with the BioDex System 3™ Dynamometer (Biodex, USA) on a previous day by performing 3 MVIC and a single fatiguing exercise as described below. On this same day, vastus lateralis (VL) muscle thickness (MT) was measured transversely using B-mode ultrasonography (Philips iE33; Philips, Andover, MA) and a linear-array ultrasound probe transducer (L9-3, 3-9 MHz, 33-mm field of view; Philips, Andover, MA) as the distance between the superficial and deep aponeuroses. Participants were situated in the upright seated position with the hip and knee flexed at 90 degrees (180 degrees = full extension) with the knee joint and dynamometer axis of rotation aligned. Hands were placed on support handles at their side for additional support during exercise and to ensure no hip extension. Range of motion of the knee joint was set to 90 degrees. Participants then performed 3 maximum voluntary isometric contractions (MVIC), with one-minute rest between contractions, for measurement of peak isometric torque and rate of torque development (RTD). Participants were then transferred to the bed for preparation of the muscle biopsy. Following administration of subcutaneous 1% lidocaine HCl injection at the planned site of biopsy and initial incision, the incision was closed with steri-strips (3M) and covered with Tegaderm (3M) to maintain a sterile field. Participants returned to the dynamometer for the isotonic fatiguing exercise protocol. Participants were instructed to “kick out as hard and fast as you can” at 30% of their MVIC along to a metronome at 40bpm with strong verbal encouragement as well as visual feedback of their torque trace in real time. Participants were considered fatigued when their range of motion became significantly reduced by more than 50% on subsequent contractions. Raw analog data was converted to digital using an A/D converter (CED, UK) and recorded using Spike2 software (CED, UK). Digital signals corresponding to position, torque, and velocity were exported and analyzed in a custom MATLAB code

(MATLAB 2022a, MathWorks). Immediately following the last contraction, the volunteer was moved to the bed, incision opened, and the area was sterilized again before performing the biopsy. A biopsy was performed on the contralateral control limb immediately following the fatigued limb biopsy.

Muscle Biopsy and Tissue Processing: Percutaneous needle muscle biopsy of the vastus lateralis muscle was performed as described (Privett et al., 2024). Briefly, following sterilization of the skin, subcutaneous and intramuscular 1% lidocaine injections were delivered. Following the fatiguing exercise, a scalpel blade was used to make a 5mm incision on the vastus lateralis muscle. A 5mm Bergström needle was inserted to the belly of the muscle and manual suction applied to acquire the tissue samples. Muscle samples were then blotted and removed of fat and connective tissue before transfer to either cold (4°C) dissecting solution (120mM NaMS, 5mM EGTA, 0.1mM CaCl₂, 6 mM MgCl₂, 0.25mM KH₂PO₄, 20mM BES, 1.8mM KOH, 1mM DTT, and 5mM ATP-Mg; pH = 7.0) for mechanical analysis or snap frozen in liquid nitrogen (LN₂) and stored at -80°C for isoelectric separation and western blot analysis. Tissue designated for mechanical experiments were dissected at 4°C into bundles of ~100 fibers, tied to glass rods at slightly stretched lengths, and placed in skinning solution (5mM EGTA, 2.5mM MgCl₂, 2.5mM ATP-Na₂H₂, 10mM imidazole, 170mM potassium propionate, EDTA-free protease inhibitor; pH = 7.0) for 24h at 4°C. Next, bundles were transferred into a series of storage solutions (identical to skinning solution but containing 1 mM sodium azide and excluding the protease inhibitor cocktail) with increasing concentrations of glycerol (10%, 25%, 50% v/v) for 2 hours each at 4°C. The 50% glycerol solution contained an EDTA-free protease inhibitor tablet (Thermo

Scientific). Upon final storage in 50% glycerol solution, bundles were kept at -20°C for up to 4 weeks until mechanical analysis.

Single Fiber Mechanical Experiments: Upon day of experiments, one bundle was isolated, trimmed evenly in dissecting solution at 4°C and placed in an additional skinning solution (dissecting solution with 1% Triton-X100 v/v) for 20min at 4°C . Following skinning, the bundle was placed back in dissecting solution at 4°C and fibers were manually dissected at random. Each fiber to be used for mechanical experiments underwent an additional 20min of skinning (dissecting solution with 1% Triton-X100 v/v) at 4°C . Following preparation, each fiber was placed into a large well consisting of relaxing solution (identical to dissecting solution but with the addition of 15mM creatine phosphate (CP), 5mM P_i , 300 units ml^{-1} creatine phosphokinase (CPK)) and tied end to end to a force transducer and a length motor with extended troughs using the Moss clamp technique (Moss, 1979) on a custom apparatus (Aurora Scientific Inc., Aurora, ON, Canada) (Privett, Ricci, David, et al., 2024). The glass-bottomed aluminum bath plate consists of 8 wells temperature controlled by a built-in thermo-electric cooler. The bath plate moves independently from the force transducer and length motor allowing for the transfer of the mounted fiber to different solutions. The bath plate and troughs are mounted to an inverted microscope (Leica Microsystems, Wetzlar, Germany) to track vertically. The fiber was first stretched to a sarcomere length (SL) of $2.65\mu\text{m}$ measured by a Fourier transformation of optical density viewed longitudinally (Aurora Scientific), cross sectional area (CSA) then measured assuming elliptical shape by taking the average of 3 measurements along the length of both the fiber top and side widths. Side widths are viewed through a right-angled prism mounted on the largest bath plate chamber. The fiber was then slacked to set zero force, re-stretched to a SL of

2.65 μ m, upon which fiber length and passive tension was measured, then force was again set to zero to ensure any additional force to be attributed to active contraction, not passive stretch. The fiber was then placed into a second bath containing pre-activating solution (identical to relaxing solution but with EGTA 0.5 mM) for 30sec to provide optimal Ca²⁺ activation upon subsequent transfer into the third bath containing activating solution (identical to relaxing solution but at pCa 4.5). In activating solution, the fiber is allowed to contract maximally until peak force plateaus. Upon maximal activation (force plateau), an isotonic load clamp is performed before returning to relaxing solution. Using the initial fiber length (L_o) and maximum force (F_{max}), the fiber is shortened at progressively higher velocities to achieve 3 different target submaximal loads. This process is repeated until all 5 series of load clamps have been completed (15 load steps in total). The forces are plotted against their associated velocities to generate a force-velocity curve fit with the Hill equation. The Hill fits derive the following parameters: maximum tension (T_{max}), maximum velocity (V_{max}), and maximum power (P_{max}). Fibers were excluded for further analysis if tension dropped >10% from the first to last activation and/or if the SL patterns are disrupted or other evidence of damage is seen. All experiments are performed at 15°C. Upon completion of experiments, the fiber was collected and transferred to an individual tube containing sample preparation buffer (SPB; 2% SDS (v/v), 12.5% Tris/HCl pH 6.8 (v/v), 25% glycerol (w/v), 0.05% β -mercaptoethanol (BME; v/v), drop of 1.0 M bromophenol blue), spun for 30sec @8500RPM, heated for 2min at 65°C, and stored at -80°C for SDS-PAGE.

SDS-PAGE/MHC Isoform Identification: To assess MHC isoform in single muscle fibers, SDS-PAGE was performed. The resolving gel contained 7% acrylamide/Bis (50:1; w/v), 1.5M Tris/HCl (pH 8.8), 1.0 M glycine, 4% SDS, 30% glycerol and the stacking gel contained 4%

acrylamide/Bis (50:1; w/v), 0.5M Tris/HCl (pH 6.8), 0.1M EDTA (pH 7.0), 4% SDS, 5% glycerol. Upon polymerization, upper and lower chamber running buffers consisting of 1X SDS and 0.5X SDS, respectively, were poured prior to protein loading. 20 μ l of solution containing a single fiber was aliquoted into each lane, with a sample homogenate (~2.5mg; 2-5 μ l) from the same volunteer in the center lane as a standard. Gels were run for 3.5 hours at 70V followed by 20 hours at 200V. Following completion of electrophoresis, the gels were stained using a Pierce Silver Stain Kit (BioRAD) and either immediately dried or stored in gel drying buffer (10% glycerol, 20% ethanol) at 4°C for later analysis. MHC isoforms assessed were MHC I, MH IIa, MHC IIx as well as hybridized MHC I/IIa and MHC IIa/IIx. A separate gel was run identical to above, yet only including sample homogenates (~2.5mg; 2-5 μ l) to assess relative abundance of MHC I, IIa, and IIx in each individual and compare across groups.

Western Blot: For semi-quantitative analysis of MyBP-C phosphorylation, frozen biopsy samples are thawed and weighed, homogenized, and extracted in protein extraction buffer (600mM KCl, 150mM KH₂PO₄, 20mM EDTA, 5mM MgCl₂, 3.3mM ATP-Na₂H₂, EDTA-free protease inhibitor, pH 6.7) for 90min on ice. Protein concentration was quantified in the lysate using a Pierce BCA Protein Assay Kit (Thermo Fisher). The sample is then heated to 65°C, and 20 μ g protein is loaded into each well on 4-20% pre-cast SDS-PAGE in Mini-PROTEAN tetra system (BioRAD). Gels are run for 40min at 200V and transferred to a nitrocellulose membrane for 1 hour at 100V in a 1X Tris-glycine buffer with 20% methanol. Ponceau staining is done to confirm a successful transfer, then blocked in TBS Intercept buffer (LI-COR Biosciences, USA) prior to overnight rocking incubation at 4°C in primary antibody. The next day, a second incubation with near-infrared secondary antibodies is performed for 1 hour at room temperature.

All western blots are imaged on a Bio-Rad ChemiDoc™ MP Imaging System (Bio-Rad Laboratories, US) and densitometry analysis performed in Image J.

For semi-quantitative analysis of RLC phosphorylation, frozen tissue samples were weighed prior to homogenization for 5 min using a glass homogenizer chilled periodically in liquid nitrogen. 40mL of sample preparation buffer (8M urea, 80 Tris, 488 Glycine, 0.1% Bromophenol blue, 100 DTT, protease inhibitor tablet (Pierce), 10ul/ml phosphatase inhibitor cocktails 2 and 3 (Sigma) with 50% Glycerol) was added for each milligram of tissue sample. Samples were then homogenized in solution for 5 min at 60°C. After centrifugation at 12000 rpm for 5 min, the supernatant was aliquoted and stored at -80°C for subsequent analysis.

Phosphorylated and non-phosphorylated RLC was separated by charge using 1d isoelectric gel electrophoresis with urea-glycerol gels (stacking gel: 20 Tris-Glycine, 5% Acrylamide stock (29.22% Acrylamide, 0.78% Bis-acrylamide), 20% Glycerol, 0.1% TEMED, 0.03% Ammonium persulfate; resolving gel: 20 Tris-Glycine, 10% Acrylamide, 40% Glycerol, 0.1% TEMED, 0.02% Ammonium persulfate), 10ul per lane, using 1X running buffer (.122M Glycine, 20 Trizma base, pH 8.6) at 400 V, 16 hours at 4°C. Gels were transferred to a nitrocellulose membrane for 1 hour at 100V in a 1X Tris-Glycine buffer with 20% methanol. Membranes were blocked in TBS intercept buffer (LI-COR Biosciences, USA), then rocked overnight at 4°C in primary antibody. The next day, a second incubation with near-infrared secondary antibodies is performed for 1 hour at room temperature. All western blots are imaged on a Bio-Rad ChemiDoc™ MP Imaging System (Bio-Rad Laboratories, US) and densitometry analysis performed in Image J.

Immunohistochemistry: Muscle bundles (~100 fibers) from the vastus lateralis muscle were blotted and embedded in O.C.T. (Tissue-Tek®, Sakura Finetek, USA) before placed in isopentane precooled with LN₂ and stored at -80°C. Samples were acclimated for 1hr at -20°C before cryo-sectioning at a thickness of 8µm on a Leica Cryostat (Leica CM 1850UV) and placed on glass slides. Samples were covered and dried overnight. The next day, samples were rehydrated for 10min in a PBS/1% BSA solution, followed by incubation in primary antibody overnight. Then, samples were washed twice for 5min each and incubated in secondary antibody for 1hr. Samples were then washed twice for 5min each before and after application of methanol for 10min. Lastly, one drop of SlowFade™ Diamond Antifade Mountant with DAPI (Invitrogen, Waltham, MA) was applied directly on the sample, followed by two drops of permount mounting medium (Electron Microscopy Sciences, Hatfield, PA) on the glass slide and cover slip placed on top. Samples were imaged on a Leica fluorescence microscope (Leica DM4000B) and Leica camera (Leica DFC 360FX) at 10x magnification. Composite image generation and subsequent analyses were performed in ImageJ. Each fiber was carefully traced and area was measured. The mean area of MHC I and not MHC I (MHC II) was calculated for each individual. Area fraction was calculated as the percentage of total muscle area occupied by MHC I and MHC II. Fiber type distribution was determined as the total number MHC I or MHC II containing fibers as a proportion of total fiber number in the sample.

Antibodies: Antibodies used for western blot include Rabbit anti-Myosin Light Chain 2 (Abcam, ab92721, 1:5000), Rabbit anti-MYBPC1 (Abcam, ab124196, 1:2000), Rabbit anti-PKA (Cell Signaling Technologies, 9621, 1:300), IRDye® 800CW donkey anti-rabbit (LI-COR, 926-32213, 1:15000), IRDye® 680RD goat anti-rabbit (LI-COR, 926-68071, 1:15000). Antibodies used for

histology include BA-D5 MIgG2b (DHSB, 1:100), SC-71 MIgG1 (DHSB, 1:100), 6H1 MIgGM (DHSB, 1:100), ab11575 IgG (Abcam, 1:100), Goat anti-mouse IgG2b AlexaFluor 647 (Invitrogen, 1:500), Goat anti-mouse IgG1 AlexaFluor 488 (Invitrogen, 1:500), Goat anti-mouse IgM AlexaFluor 568 (Invitrogen, 1:500), Goat anti-rabbit IgG AlexaFluor 488 (Abcam, ab150077, 1:500).

Liquid Chromatography Tandem Mass Spectrometry (LC-MS): Mass spectrometry was performed on skeletal muscle samples from a subset (n=16, 8NT and 8RT) of individuals, some who were and some who were not included in the single fiber mechanical experiments. The height, weight, and BMI of this group was 174 ± 71 cm, 71 ± 18 kg, 23 ± 2 kg/cm² in the NT and 174 ± 11 cm, 72 ± 10 kg, and 24 ± 2 kg/cm² in the RT, respectively. LC-MS was performed as previously described (Privett, et al., 2024). Briefly, samples were disrupted by shearing with glass beads followed by trypsin protein digest and phosphopeptide purification by binding to TiO₂ beads. Phosphopeptides were then labelled with one of 18 tandem mass tags, combined in a single sample and run via the Orbitrap Fusion mass spectrometer at Oregon health and Science University (Portland, OR) Proteomics Shared Resource (PSR) directed by Ashok Reddy, PhD. Informatics methods as described previously (Plubell et al., 2017) and were used to determine relative changes in phosphorylation of serine, threonine, and tyrosine residues.

Statistical Analysis: Two-way ANOVA with fixed effects of Training and Sex was used to assess differences in anthropometrics, whole muscle function, and fatiguing exercise performance. A two-way Repeated Measures ANOVA with fixed effects of fatigue and training was performed for the comparison of RLC and MyBP-C phosphorylation. To assess differences in single fiber

contractile properties between groups, fatigued vs. non-fatigued, and biological sex, a linear mixed effects model was performed within a fiber type and a random effect of Participant ID. Participant ID allows for each individual participant to be weighted in accordance with the number of fibers they contributed to the total data set. To assess contractile function at baseline, a linear mixed model was performed in non-fatigued fibers with fixed effects of training and sex and random effect of Participant ID, within a fiber type. To assess the effect of fatigue, a linear mixed model was performed within a training group, with fixed effects of condition (non-fatigue/fatigue) and sex and random effect of Participant ID. In the event of a condition by sex interaction effect, independent samples t-test were run for the comparison between non-fatigued and fatigued fibers within a sex. All statistical analyses were performed in SPSS (IBM, SPSS Inc.). To assess phosphoproteomic differences via LC-MS, the mean phosphorylation of a residue was compared between NF and F samples as well as between NT and RT. Significantly differentially phosphorylated residues were identified by a false discovery rate (FDR) <0.05. Statistics for LC-MS were performed in EdgeR software, proprietary to the Orbitrap Fusion.

3C. Results

Table 1: Anthropometric and Activity Data of Young NT and RT Participants.

	n	Height (cm) *	Weight (kg) *	BMI (kg/m ²)	Step Count (steps/day) #	Light Activity (mins/day)	Moderate Activity (mins/day) #	Vigorous Activity (mins/day)	
NT	Female	5	162.1 ± 6.1	55.0 ± 3.2	20.9 ± 0.6	7098±2176	25 ± 8	43 ± 15	0.5 ± 0.6
	Male	4	185.3 ± 13.0	84.0 ± 10.1	24.5 ± 1.2	10013±5001	54 ± 27	72 ± 37	0.7 ± 0.6
RT	Female	5	161.1 ± 3.9	59.9 ± 6.1	23.1 ± 2.1	12358±2531	40 ± 13	96 ± 17	5.1 ± 6.2
	Male	4	184.4 ± 4.8	78.7 ± 10.0	22.8 ± 1.7	12752±3865	45 ± 10	111 ± 24	1.0 ± 1.4

Symbols indicate a significant main effect of * biological sex or # training between groups (p<0.05).
Data are shown as mean ± SD.

Participant Characteristics, Fiber Type Distribution, and Morphology.

A total of 18 young healthy adults participated in this study including 9 NT (5 female and 4 male) and 9 RT (5 female and 4 male). Males were taller ($p < 0.001$) and weighed more ($p < 0.001$) than females but were not different in BMI ($p = 0.074$) (Table 1). There was no effect of training on height ($p = 0.887$), weight ($p = 0.991$), or BMI ($p = 0.623$) (Table 1). As measured via ActivPAL accelerometry in 17/18 participants, RT participants had a higher step count ($p = 0.047$) and more minutes per day spent in moderate-vigorous physical activity ($p = 0.005$) (Table 1). No differences by sex were observed in physical activity.

Immunohistochemical analysis was performed in 16/18 participants to assess fiber type distribution and fiber area. The area fraction of MHC I or II fibers was not different between NT and RT ($p = 0.205$), yet was larger in males, albeit not statistically significant ($p = 0.054$; Figure 1B). Fiber type distribution was also assessed as number of MHC I or II fibers as a percentage of the total number of fibers analyzed in cross-section. In this analysis, fiber type distribution was not different between NT and RT or males and females ($p = 0.191$, $p = 0.593$), similar to area fraction. In a separate sample stored in SDS sample buffer, tissue homogenate was separated via SDS-PAGE and densitometry was performed to assess relative abundance of MHC I, IIA, and IIX. This method also shows no difference in MHC I or II abundance between NT and RT or males and females ($p = 0.151$, $p = 0.090$; Supplementary 1A). However, MHC IIX abundance was greater in NT than RT ($p = 0.005$) but not different in MHC IIA ($p = 0.103$) (Supplementary 1A).

Comparing the two methods fiber type abundance (IHC vs SDS-PAGE), there was an association between area fraction via IHC and relative abundance via SDS-PAGE ($R^2 = 0.373$, $p = 0.012$; Supplementary 1B). Relative abundance via SDS-PAGE was associated with fiber type distribution ($R^2 = 0.354$, $p = 0.015$; Supplementary 1C). Average fiber area was larger for both

MHC I and MHC II in RT compared to NT ($p < 0.001$, $p < 0.001$), and in males compared to females ($p < 0.027$, $p < 0.00$) (Figure 1A). There was a sex by training interaction in both MHC I ($p = 0.021$) and MHC II ($p = 0.004$). RT males had larger MHC I and MHC II fiber area than NT males ($p = 0.023$, $p = 0.021$) and RT females had larger MHC I fiber area ($p = 0.039$), but not MHC II fiber area ($p = 0.059$) than NT females (Figure 1A). Neither MHC I or II area were different between NT males and NT females ($p = 0.789$, $p = 0.097$), but were greater in RT males compared to RT females ($p = 0.037$, $p < 0.001$) (Figure 1A).

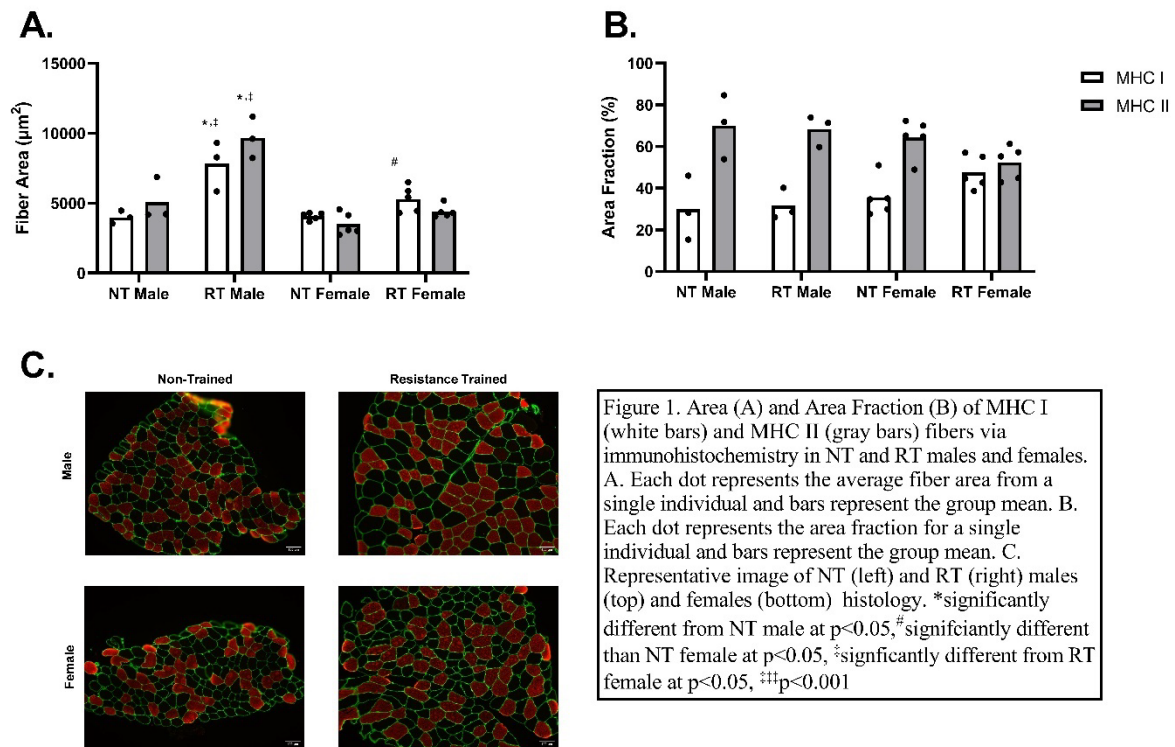


Table 2: Fatigue Data and Whole-Muscle Performance in NT and RT Participants

		n	Time to Fatigue (sec)	Fatigue Ratio (P _f /P _i)	Peak Power (W) *#	Relative Peak Power (W/kg) *#	Peak Torque (Nm) *#	Relative Peak Torque (Nm/kg) *#
NT	Female	5	68±8.8	0.34±0.10	295±33	5.43±0.32	140±8	2.54±0.12
	Male	4	75±29	0.41±0.16	532±95	6.43±1.42	281±44	3.34±0.34
RT	Female	5	99±74	0.36±0.12	383±73	6.19±0.68	195±62	3.20±0.73
	Male	4	74±15	0.29±0.11	779±278	9.90±1.9	353±41	4.57±0.60

Symbols indicate a significant main effect of *biological sex or #training between groups (p<0.05).
Data are shown as mean ± SD.

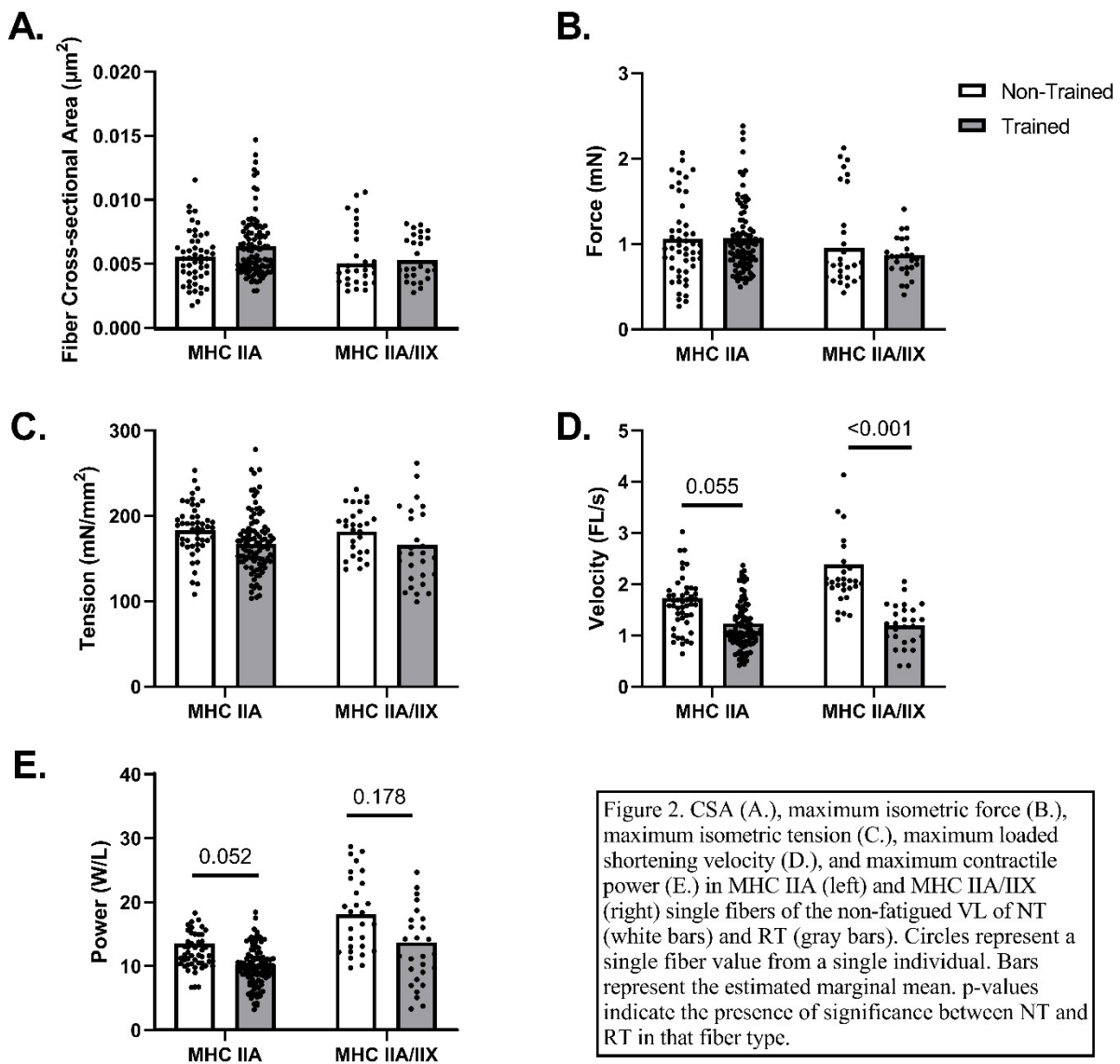
Fatiguing Exercise and Whole Muscle Performance.

Due to data loss during transfer, whole muscle power and time to fatigue are reported in 15/18 and 17/18, respectively. RT participants produced more isometric torque (p=0.008) and power (p=0.037) compared to NT (Table 2). Males also produced more absolute torque (p<0.001) and power (p<0.001) than females (Table 2). Relative torque (p=0.002) and relative power (p<0.001) was greater in RT compared to NT and were greater in males compared to females (p<0.001, p<0.001) (Table 2). RT males generated greater RTD than RT females (p=0.010), NT males (0.028), and NT females (0.050). Relative RTD was not different between RT and NT males (p=0.121), but was greater in NT females compared to RT females (p=0.006). Interestingly, neither the time to fatigue nor the fatigue ratio (representative of power loss) during the exercise protocol were different by training group (p=0.439, p=0.511) or sex (p=0.631, p=0.988) (Table 2).

Table 3: CSA and MHC Isoform Distribution of Single Fibers Analyzed in NT and RT Participants

		n	CSA (mm ²) *#	MHC Isoform Distribution	
				IIA	IIA/X
Non-Trained	Female	88	0.0042 ± 0.0012	57	31
	Male	81	0.0068 ± 0.0019	55	26
Resistance Trained	Female	130	0.0044 ± 0.0013	101	29
	Male	112	0.0080 ± 0.0028	80	32

Data are shown as mean ± SD. * indicates main effects of biological sex and # of training (p<0.05).



Single fiber contractile performance in non-trained and resistance trained males and females.

In the single fibers analyzed for mechanical experiments, data were limited to MHC IIA and MHC IIA/IIX expressing fibers, as the fiber counts for MHC I were low and inconsistent between males and females (males: n=20, females: n=72). Figure 2 depicts single fiber CSA and contractile performance from the non-fatigued control limbs of NT and RT participants. The CSA of MHC IIA and IIA/IIX were not different between RT and NT participants ($p=0.243$, $p=0.769$; Figure 2A), yet was larger in males compared with females ($p<0.001$, $p=0.011$; Supplementary 2A, 3A). F_{\max} was not different in either fiber type between NT and RT fibers ($p=0.946$, $p=0.725$; Figure 2B) but was greater in males than females for MHC IIA ($p=0.003$; Supplementary 2B). T_{\max} was not different in MHC IIA or MHC IIA/IIX between NT and RT ($p=0.193$, $p=0.441$; Figure 2C) or males and females ($p=.518$, $p=0.499$, Supplementary 2C, 3C). Fibers from RT participants exhibited lower V_{\max} in MHC IIA ($p=0.055$), although non-significant, and MHC IIA/IIX ($p=0.001$) (Figure 2D). Similar trends, although non-significant, were seen with P_{\max} ($p=0.052$, $p=0.178$; Figure 2E) compared to fibers from the NT participants. MHC IIA/IIX fibers from females produced greater V_{\max} compared to males ($p=0.022$, Supplementary 3D), yet V_{\max} in MHC IIA ($p=0.875$; Supplementary 2D) or P_{\max} in both MHC IIA and MHC IIA/IIX were not different between the sexes ($p=0.385$, $p=0.992$; Supplementary 2E, 3E).

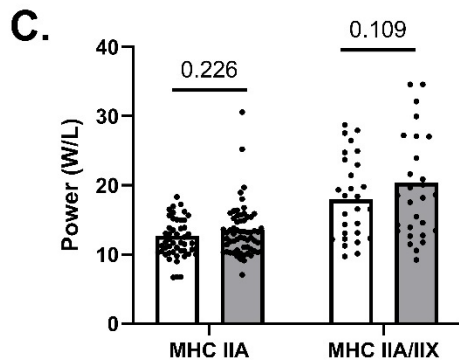
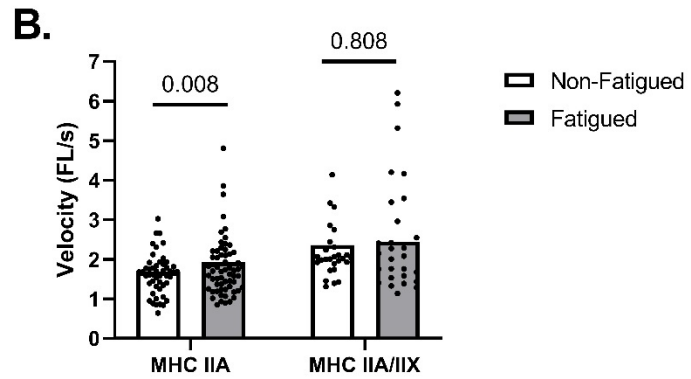
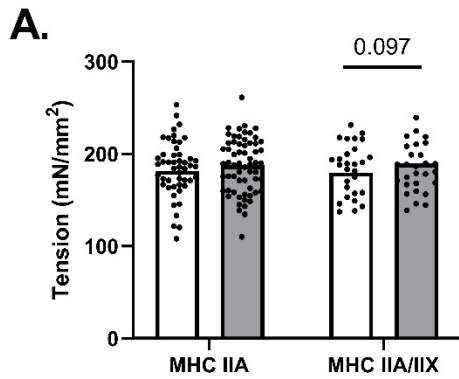


Figure 3. Maximum isometric tension (A.), maximum loaded shortening velocity (B.), and maximum contractile power (C.) in MHC IIA (left) and MHC IIA/IIX (right) single fibers of the non-fatigued (white bars) and fatigued (gray bars) VL of NT males and females. Circles represent a single fiber value from a single individual. Bars represent the estimated marginal mean. p-values indicate the presence of significance between non-fatigued and fatigued in that fiber type.

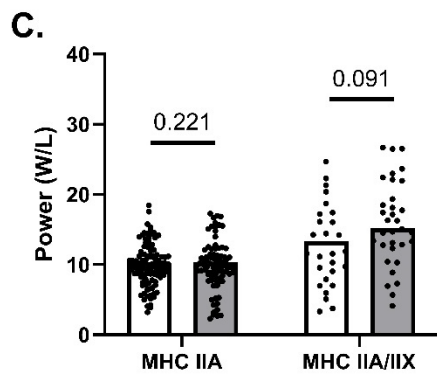
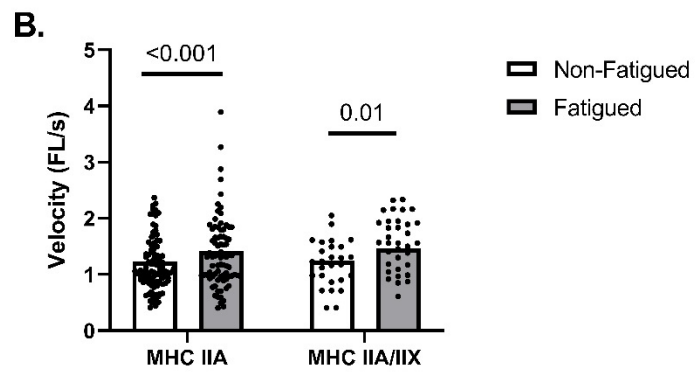
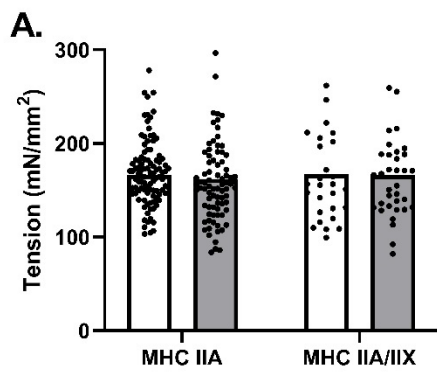


Figure 4. Maximum isometric tension (A.), maximum loaded shortening velocity (B.), and maximum contractile power (C.) in MHC IIA (left) and MHC IIA/IIX (right) single fibers of the non-fatigued (white bars) and fatigued (gray bars) VL of RT males and females. Circles represent a single fiber value from a single individual. Bars represent the estimated marginal mean. p-values indicate the presence of significance between non-fatigued and fatigued in that fiber type.

Effects of in vivo fatigue on permeabilized single fiber contractile performance in vitro.

Figures 3 and 4 depict contractile performance in single fibers from the non-fatigued control and fatigued limbs of NT and RT participants, respectively. In the NT participants, fibers from the fatigued limb had no significant effect on T_{\max} on either fiber type ($p=0.217$, $p=0.097$; Figure 3A). A fatigue by sex interaction effect in MHC IIA/IIX fibers necessitated repeating the statistical analysis within each sex and suggests no change in females ($p=0.338$; Supplementary 5A) but increased T_{\max} in males ($p=0.006$; Supplementary 5A). V_{\max} was greater in fatigued MHC IIA fibers ($p=0.008$), but not MHC IIA/IIX ($p=0.808$) compared with non-fatigued fibers (Figure 3B). P_{\max} was not different between non-fatigued and fatigued fibers in either fiber type ($p=0.226$, $p=0.109$; Figure 3C).

In the RT participants, fatigue did not have an effect on MHC IIA and MHC IIA/IIX T_{\max} ($p=0.240$, $p=0.889$; Figure 4A), but exhibited increased V_{\max} ($p<0.001$, $p=0.01$; Figure 4B). P_{\max} was not different between non-fatigued and fatigued MHC IIA or MHC IIA/IIX fibers ($p=0.220$, $p=0.091$; Figure 4C), yet a significant fatigue by sex interaction effect in MHC IIA/IIX fibers ($p=0.043$) followed by linear mixed model approach within a sex suggest a greater P_{\max} in male fatigued fibers ($p=0.021$) not seen in females ($p=0.696$) (Supplementary 7C).

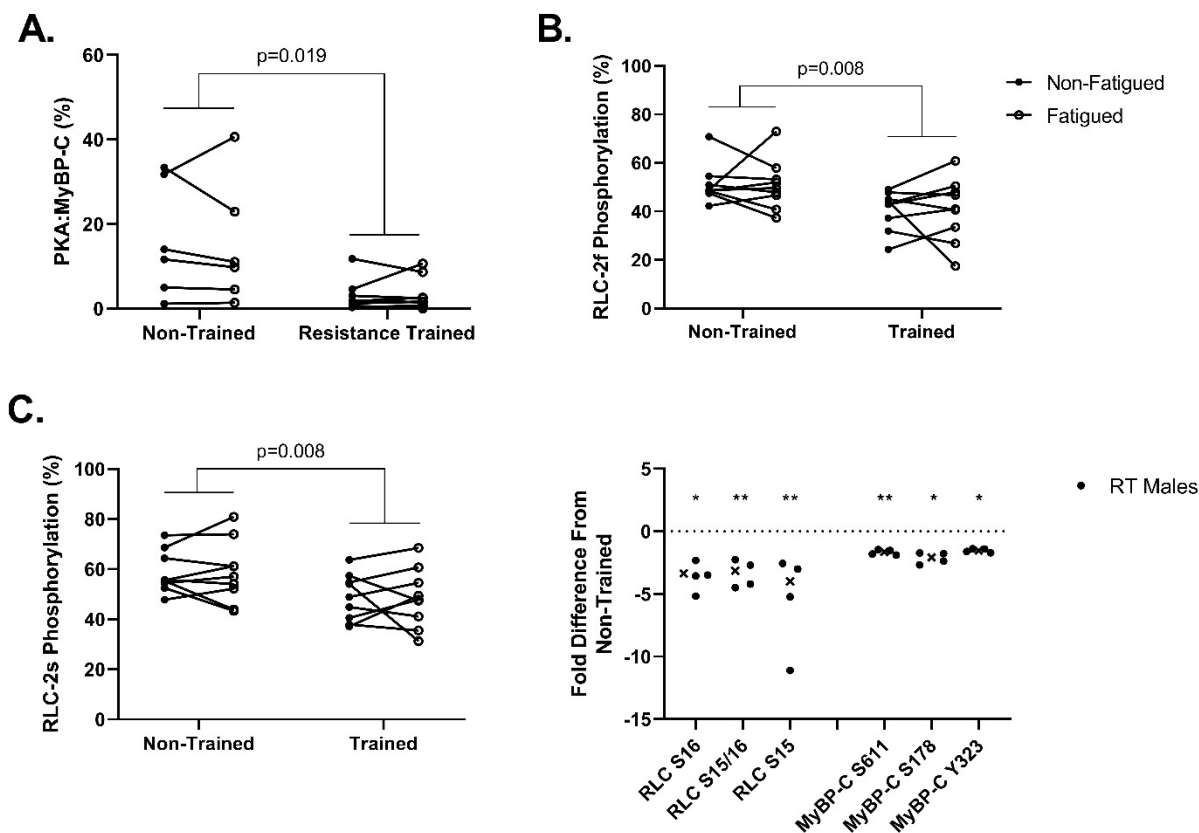


Figure 5. Phosphorylation of MyBP-C (A.), RLC-2f (B.), and RLC-2s (C.) in the non-fatigued (closed circles) and fatigued (open circles) VL of NT (left) and RT (right). Each dot represents an individual's value and connecting lines between NF and F samples. (D.) Phosphoproteomic analysis of RLC and MyBP-C via LC/MS in RT Males. Each dot shows fold change from average NT phosphoenrichment and x indicates group mean fold change. p-values indicate significance level of main effect of training status. *indicates significantly different from NT at FDR<0.05, **FDR<0.001

Phosphoproteomic and Western Blot Analysis of MyBP-C and RLC.

Western blot analysis of MyBP-C phosphorylation (as denoted by PKA:MyBP-C) was not different by fatigue ($p=0.739$) but was greater in NT compared with RT participants ($p=0.019$) (Figure 5A). Phosphorylation of RLC-2f and RLC-2s were also not different by fatigue ($p=0.968$, $p=0.966$), but greater in NT than RT participants ($p=0.004$, $p=0.008$) (Figure 5B,C). Phosphoproteomic analysis identified >8500 residues. In the global dataset, we saw significantly greater differences between training groups than we did by fatigue (Supplementary

Figure 9). RLC and MyBP-C had multiple residues with lower phosphorylation in RT compared to NT in males (FDR<0.05) (Figure 5D).

3D. Discussion

This study examined the chronic effect of resistance training history and the acute effect of muscle fatigue on single muscle fiber contractile function and phosphorylation of sarcomeric regulatory proteins, MyBP-C and RLC from the vastus lateral muscle. In this study sample of 9 NT (5F, 4M) and 9RT (5F, 4M), height and weight, but not BMI, were greater in males than females yet no differences were present between training groups (Table 1). The RT group reported rigorous resistance training history including at least 5 days per week of weightlifting for at least 1 hour and 3 of those days focused on lower body resistance training. As a confirmation of activity level, RT participants had a greater step count and more time spent in moderate activity compared to the NT group (Table 1). Both absolute and relative whole muscle peak torque and peak power was greater in RT compared to NT, and in males compared to females (Table 3). Time to fatigue was not different between groups, which indicates that the sex and training dependent differences in single fiber function following fatiguing exercise may not be impacted by the duration of the exercise. It is well established that females exhibit better fatigue resistance during isometric contractions (Hunter, 2014), however recent literature suggests that fatiguing exercise performed at high velocities does not result in sex differences (Senefeld et al., 2013), which the data presented in this study support. Our chosen task of high velocity dynamic contractions to task failure allows for the muscle to be greatly fatigued regardless of the duration, in an effort to utilize this method as a tool to modify the intracellular

environment and test our central hypotheses that in vivo fatigue will alter the muscle phosphoproteome and single muscle fiber contractile performance.

Single fiber morphology and contractile function in resistance trained and non-trained males and females.

The lack of sufficient MHC I-containing fibers in our current sample provides a limitation in our ability to test fiber type dependent responses to fatiguing exercise, thus our analyses were restricted to MHC IIA and MHC IIA/IIX fibers. There were nominally less MHC I fibers in males (n=20) compared to females (n=72) in both the NT and RT groups. Females typically have a higher number and greater relative area of MHC I fibers compared to males (Hunter, 2014; A. E. Miller et al., 1993), but this is unlikely to be the sole contributor. Our previous work suggests that if dissected at random, an experimenter is less likely to isolate an MHC I compared to an MHC II fiber (Privett et al., 2024). This is likely the main contributor to the current dataset presented as relative MHC abundance measured from tissue homogenate via SDS-PAGE suggest a ~39% and ~29% MHC I abundance in females and males compared to ~25% and ~9% of the fibers analyzed, respectively (Table 3).

Prior literature has documented that resistance trained individuals possess fibers that are larger in CSA and produce greater absolute force and power. For example, 12 weeks of resistance training in young males increased fiber CSA, absolute force, and absolute power (Widrick et al., 2002). These enhancements seem to be due to increased muscle size as specific tension and normalized power show no increases following training (Widrick et al., 2002). The same outcomes were seen following a 14-week resistance training program, with similar relative increases in both young and old males and females (Claflin et al., 2011). However, these are

relatively short training durations compared to the study group in this dataset, who have been resistance training for greater than 12 months. In the current study, the CSA and F_{\max} of analyzed fibers were not different between RT and NT groups (Table 2, Figure 2A,B). Thus, we performed immunohistochemistry in order to measure both MHC I and MHC II fiber area in a more representative sample from these groups. The average fiber area was greater in RT compared with NT and in males compared with females, as was expected. However, RT females did not have greater MHC II fiber area. All RT participants reported high physical activity including 3 days/week of lower limb resistance training. The use of physical activity monitoring via ActivPAL accelerometers confirmed that RT individuals spent more time in moderate-vigorous activity compared to NT (Table 1), and this was true of the RT females especially as they spent over double the amount of time per day in moderate-vigorous activity and >5,000 more steps per day than NT females. However, a limitation of using accelerometry for categorizing physical activity is that it is not directly capable of capturing how much load or total volume is placed on the muscle. Thus, differences in loading during exercise training sessions can influence how resistance trained an individual may be, despite exhibiting similar time spent in moderate-vigorous activity. RT females did exhibit a larger area fraction of MHC I compared to other groups, albeit not statistically significant, suggesting that training regimens may not have been as load intensive compared to RT males. Previous studies have shown that the type of resistance training impacts fiber-type specific hypertrophy. For example, powerlifters or weightlifters who typically utilize weight ranges of >80% 1-repetition maximum (1RM) tend to have a larger area of MHC II fibers compared with bodybuilders who utilize higher volumes with lower relative loads (Fry, 2004). Although these individuals did not classify themselves as powerlifters,

weightlifters, or bodybuilders, it is possible that different training styles and/or training preferences (high repetition/low load vs low repetition/high load) influenced the adaptations.

When normalizing for variations in fiber size, there did not exist differences in isometric tension and contractile power (Figure 2C, 2E) for the fibers analyzed for mechanical experiments. Previous cross-sectional studies of chronic resistance training history show that body builders and weightlifters have a larger fiber CSA with greater associated force and power compared to non-trained adults, yet when normalized for muscle size, differences are abolished (Shoepe et al., 2003), except in body builders whom also exhibited slight increases in specific tension (D'Antona et al., 2006). Contrary to these findings, Meijer et al., 2015 found that body builders had lower single fiber specific tension and power than non-trained control fibers, despite increases in CSA, absolute force, and absolute power (Meijer et al., 2015). In line with these findings, one study has suggested that when measuring contractile properties of large fibers, typically from populations such as body builders, the CSA may be overestimated (Monti et al., 2020). In permeabilized fibers, it is generally accepted that fibers swell around 20% of initial volume (Moss, 1979). However, Monti et al. suggest that larger fibers may swell disproportionately more than smaller fibers and thus tension, and possibly power, may be artificially reduced. In their study of 6 male body builders and 6 non-trained males, fibers from body builders had lower normalized force however when correcting for fiber swelling by normalizing to the average CSA from histological cross-sections, the differences were abolished. In the current study, the lack of differences in isometric tension were expected, especially considering the fiber CSA was not different.

Interestingly, maximum loaded shortening velocity was lower in RT compared to NT, opposite our hypotheses. However, this is consistent with our findings that MyBP-C

phosphorylation was also lower in RT compared to NT. MyBP-C can bind actin in its native state and provide a drag effect, slowing actin sliding velocity in cardiac filaments (Previs et al., 2016). Upon phosphorylation in skeletal muscle, loaded shortening velocity within the c-zone is increased and subsequently slowed when de-phosphorylated with lambda phosphatase (Robinett et al., 2019). It is possible, that reduced baseline phosphorylation of MyBP-C or RLC in RT individuals elicits velocity-specific deficits to contractile function at the single fiber. An important critique of relating protein phosphorylation in vivo to single fiber function in vitro is if this phosphorylation remains following mechanical tissue preparation as these modifications may be short-lived. In one participant, we assessed MyBP-C phosphorylation in flash frozen tissue compared to 48 hours post-mechanical preparation and found that phosphorylation persisted in this tissue sample (Supplementary 8), suggesting differences in this sarcomeric protein phosphorylation may contribute to this altered contractile phenotype. In a second participant, we assessed RLC phosphorylation from flash frozen and mechanical preparation for 48 hours up to 4 weeks and found very little phosphorylation of RLC remained in mechanically prepared tissue at any time point (Supplementary 8). Therefore, the effects of training seen on single muscle fibers in this current study are unlikely to be explained by RLC phosphorylation.

Fatiguing exercise improves single fiber velocity and power dependent on training and biological sex.

The current study presents a novel finding that fatiguing exercise in vivo alters single muscle fiber contractile performance in vitro, specifically velocity and power. These differences appear paradoxical, however the solutions were near optimal for both non-fatigued and fatigued fibers at neutral pH and low P_i ensuring that the contractile phenotype was not impacted by

altered intracellular metabolic conditions. Thus, the resultant altered contractile performance of these fibers is likely due to inherent differences in the fiber, most likely post-translational modifications to sarcomeric regulatory proteins. During fatiguing exercise, it is likely that oxidation of myosin contributes to altered contractile function in vivo as previous studies show H₂O₂ treatment of skeletal muscle fibers leads to paradoxical increases in Ca²⁺ sensitivity and specific force (Lamb & Posterino, 2002). However, our solutions contain 1mM dithiothreitol (DTT), an antioxidant that removes oxidation in vitro and it is unlikely that baseline or fatigue-induced changes to the redox state explain any observed differences between groups or fatigue. Two main regulatory proteins of interest are MyBP-C and RLC, which have been documented to alter contractile performance of single muscle fibers in a phosphorylation dependent manner as discussed above. We utilized a fatiguing exercise to task failure in order to induce phosphorylation of these key regulatory proteins, among others.

During skeletal muscle contraction in vivo, large Ca²⁺ transients increase the sarcoplasmic Ca²⁺ concentrations, ultimately activating the skeletal specific Ca²⁺/calmodulin dependent kinase, myosin light chain kinase (skMLCK), which phosphorylates serine residues 14 and 15 on RLC (Blumenthal & Stull, 1980). In vitro, RLC phosphorylation by incubation with skMLCK results in improved single fiber Ca²⁺ sensitivity (Persechini et al., 1985; Sweeney & Stull, 1986), rate of tension redevelopment (k_{tr}) (Metzger et al., 1989; Sweeney & Stull, 1990), and cross-bridge attachment kinetics (f_{app}) (Sweeney & Stull, 1990). While no differences have been shown with regards to unloaded shortening velocity via slack-test maneuver (Sweeney & Stull, 1990), it remains unknown how RLC phosphorylation impacts loaded shortening and contractile power in single muscle fibers. At the whole muscle level however, in situ work and power was increased following conditioning contractions that increased RLC phosphorylation of

mouse extensor digitorum (EDL) (Xeni et al., 2011), suggesting a role for altered contractile function during loaded shortening. It has yet to be explored the effects of RLC phosphorylation in vitro via skMLCK in human single fibers. Future studies would benefit from assessing fiber type dependent differences in single fiber function following in vitro phosphorylation as pre-clinical models suggest RLC in slow muscle is not as phosphorylatable and has little to no influence on muscle function (Crow & Kushmerick, 1982; Moore & Stull, 1984; Westwood et al., 1984), along with lower skMLCK expression in slow muscle (Zhi et al., 2005).

MyBP-C is a ~125-140kDa thick filament associated protein that exists within the inner two thirds of each half sarcomere, “c-zone”, each spaced approximately 40nm apart along the axis of the thick filament in a ratio of 1 MyBP-C : 3 myosin (Heling et al., 2020b; Robinett et al., 2019). MyBP-C is phosphorylated mainly by cyclic AMP dependent protein kinase (protein kinase A, PKA) and additionally by protein kinase C (PKC) (Ackermann & Kontrogianni-Konstantopoulos, 2011). While fsMyBP-C has no known phosphorylation sites, ssMyBP-C has 3 phosphorylatable serine residues in the proline-alanine rich region near the C1 domain and 1 in the M-motif (Barefield & Sadayappan, 2010). In mouse soleus muscle, a fatiguing tetanic stimulation protocol was sufficient to induce ssMyBP-C phosphorylation (Ackermann & Kontrogianni-Konstantopoulos, 2011) suggesting MyBP-C dynamically regulates skeletal muscle contraction during fatiguing exercise. However, it is less clear how fatiguing exercise may impact fast muscle despite both fsMyBP-C and ssMyBP-C being expressed. Our in vivo fatiguing protocol was utilized in order to do induce PKA-dependent phosphorylation of MyBP-C via beta-adrenergic signaling cascades in a heterogenous muscle. It is also likely that PKC signaling is increased during this fatiguing exercise, however we were limited in our ability to measure PKC activity on MyBP-C in the way we could with PKA.

Effects of Resistance Training and Fatigue on RLC and MyBP-C Phosphorylation.

We did not see an effect of fatigue on RLC phosphorylation in either NT or RT groups. As stated above, RLC phosphorylation is induced upon muscle activation, and we hypothesized that a fatiguing exercise to task failure would be a sufficient stimulus to increased RLC phosphorylation. Prior studies in humans tend to utilize a more brief conditioning contraction in order to induce RLC phosphorylation, such as 10s MVIC (Houston et al., 1985; Houston & Grange, 1991; Stuart et al., 1988). These studies have shown increases in RLC phosphorylation and associated twitch potentiation, a phenomenon largely attributed to RLC phosphorylation. It is possible that the time between the final contraction and tissue acquisition was too long in order to capture the anticipated rise in RLC phosphorylation. RLC phosphorylation in skeletal muscle remains elevated for a short duration before returning to resting levels due to both reduced skMLCK and increased myosin light chain phosphatase (MLCP) activity (Stull et al., 2011). Our previous unpublished work has shown reduced RLC phosphorylation via liquid chromatography tandem mass spectrometry following a similar fatiguing exercise protocol. However, it is unclear if MLCP activity remains elevated for long enough following a conditioning contraction to reduce phosphorylation levels below resting. In the current study, there was variation in the time from final contraction to tissue acquisition and the range was approximately 5-19 minutes. While it is technically challenging to perform muscle biopsies so quickly after exercise, future studies of RLC phosphorylation should consider a more time-sensitive approach.

Interestingly, we found that RT individuals had lower resting RLC phosphorylation than NT. To our knowledge, this is the first study to directly compare RLC phosphorylation between NT and RT individuals. However, previous work has demonstrated that resistance training

improves potentiation of isometric and dynamic force following conditioning contractions (Chiu et al., 2003; Hicks et al., 1991). The mechanism for greater potentiation is not fully understood but is likely attributed to an increase in fast-twitch MHC II fiber area. Older adults, who contain lower MHC II area than younger adults, tend to have a reduced capacity for post-activation potentiation that is enhanced following resistance training (Hicks et al., 1991; Petrella et al., 1989). Furthermore, older males have exhibited reduced RLC phosphorylation (Gelfi et al., 2006) and older females have been shown to exhibit reduced RLC phosphorylation compared to younger adults and older males (Miller et al., 2013), suggesting chronic adaptations to resting RLC phosphorylation levels that may have implications for muscle function. Here, our RT individuals had greater MHC II area than NT, thus drawing a conclusion dependent on fiber type abundance difficult. We found that both fast and slow RLC isoforms were lower in RT than NT, which suggests this may not be as fiber type dependent as previously thought. Similarly, we found that MyBP-C phosphorylation was lower in RT than NT. While there is literature to describe that resistance training alters the proteomic profile in human skeletal muscle (Du et al., 2024; O’Leary et al., 2024), it is unclear how the phosphoproteomic profile, specific to proteins of the contractile machinery, are altered. Furthermore, how or if resistance training changes the sensitivity to exercise in the context of intracellular signaling is not currently understood. From these data, it is possible that resistance training elicits chronic adaptations to resting phosphorylation in a way that allows for greater potentiation of contractile function during and following the onset of exercise. This would serve as a beneficial tool that helps limit or forestall fatigue *in vivo*.

In our phosphoproteomic analysis, we utilized an 18 plex design comparing the effects of RT and fatigue within a biological sex. Interestingly, we did not find many differentially

phosphorylated residues with fatigue, however RT males showed 15 residues with increased phosphorylation and 322 with decreased phosphorylation in comparison to 2 increased and 2 decreased in NT males, 2 increased and 1 decreased in NT females, and 0 in RT females (Supplementary 9). This broad approach suggests that the muscle phosphoproteome is changing following fatiguing exercise dependent on sex and training. Previous studies have shown that exercise alters the muscle phosphoproteome, specifically signaling pathways associated with muscle adaptations, in an intensity dependent manner (Hoffman et al., 2025). While our study did not identify many differences by fatigue, we did see large differences by training in both males and females. We found 751 and 270 differentially phosphorylated residues in RT compared to NT males and females, respectively (Supplementary 9). Interestingly, of these many residues, Ser15 in RLC and multiple Serine's on ssMyBP-C has lower phosphorylation in the RT males compared to NT males, in agreement with our western blot data. While RLC is known to be phosphorylated at Ser15, ssMyBP-C has many splice variants (Li et al., 2019) and it is difficult to identify residue specificity in this approach. Additionally, previous single cell proteomics have identified differences in the proteomic profile between fiber types (Momenzadeh et al., 2023), which may greatly influence the adaptability between individuals with differences in MHC isoform distribution and hybridized fiber numbers as in the current study. Future approaches should utilize a targeted proteomics approach to identify residue specificity, and identify the splice variants that exist across samples to create a more comprehensive understanding of the molecular changes with fatigue or training.

Limitations

While the current study provided a robust analysis of over 400 fibers from 18 participants, we are limited by the lack of MHC I containing fibers in the dataset. Human skeletal muscle is heterogenous with many muscles expressed multiple fiber types along with hybridized fibers. Slow fibers are traditionally fatigue resistant, making them an interesting population of study as they may reveal unique responses to fatigue that has exercise and training implications. Additionally, our single fiber analyses were performed in near optimal intracellular conditions of low P_i and neutral pH. This allowed us to identify potential mechanisms of altered contractile function unique to the sarcomeric proteins rather than altered intracellular metabolic conditions. However, during exercise and training, cellular function of the fiber depends on the intracellular conditions and future study would benefit from identifying if similar performance potentiation persists during fatiguing conditions. Our identification of protein modifications was limited to phosphorylation of RLC and MyBP-C. Oxidation (Lamb & Posterino, 2002), heat shock protein (HSP) production (Liu et al., 2006), and other post-translational modifications may alter contractile performance during exercise. Our current findings are unlikely to be due to oxidation as the solutions for mechanical experiments contained DTT, as discussed above, however it may provide a more comprehensive picture of the relationship between acute and chronic mediators of muscle function. Further, MyBP-C phosphorylation was measured as the ratio of PKA signal at the MyBP-C band to total MyBP-C protein on that gel. Therefore, we extrapolate that greater PKA:MyBP-C is indicative of greater MyBP-C phosphorylation. Lastly, the female menstrual cycle and circulating sex hormones such as 17β -Estradiol (E2) are known to impact muscle function (Chidi-Ogbolu & Baar, 2019). Although we did not measure circulating sex hormones,

all female participants were either scheduled during the early follicular phase or were taking hormonal contraceptive, in which cases E2 was presumed to be low.

Conclusion

This study is the first to directly test the effects of in vivo fatigue on in vitro contractile performance of single muscle fibers. We are also the first to directly compare resting RLC and MyBP-C phosphorylation between RT and NT males and females and if protein phosphorylation remains in tissue prepared for mechanical analysis compared to flash frozen. Overall, our study found that in vivo fatigue induces velocity specific increases in contractile performance of MHC II fibers. Specifically, RT individuals exhibited a more robust increase to loaded shortening velocity than NT providing an interesting outlook on fatigue resistance in RT compared to NT individuals. Additionally, RT individuals had slower loaded shortening velocity than NT and lower, but non-significant, maximum power. We did not capture fatigue-induced changes to RLC or MyBP-C in western blot or phosphoproteomics. However, the time-sensitivity of RLC phosphorylation may have limited our ability to test this hypothesis. For MyBP-C, this protein is phosphorylated by PKA and PKC, in which cases we were unable to detect residue specificity or PKC dependent phosphorylation. We found reduced RLC and MyBP-C phosphorylation in RT compared to NT individuals via western blot that was confirmed with phosphoproteomic analysis. Overall, our study provides valuable insight into the dynamic regulation of muscle function during fatigue and how chronic influencers such as RT and biological sex mediate this response.

4. Aim 2: To assess how chronological age mediates the effects of fatiguing exercise on single muscle fiber contractile function and regulatory protein modification.

4A. Introduction

Chronological aging of the neuromuscular system is characterized by reduced motor unit number (McNeil et al., 2005; Power et al., 2014), muscle fiber number and size (Lexell et al., 1988), and a shift in fiber type distribution from fast (MHC II) to slow (MHC I) (Hunter et al., 1999; Lexell et al., 1983). These morphological changes generally describe the reductions in physical function commonly seen in the elderly such as maximal strength and power (Callahan & Kent-Braun, 2011). The loss of muscle mass, along with increased intramuscular adipose content, mostly explain the loss of isometric muscle strength (Goodpaster et al., 2008), however older adults experience power deficits that are greater than their strength deficits compared to younger adults (Callahan & Kent-Braun, 2011). These deficits are velocity specific in that as the velocity of contraction increases, power disproportionately decreases in older compared to younger adults that is likely explained by changes within the muscle, rather than with neuromuscular activation (Wrucke et al., 2024). To identify the extent to which contractile deficits arise from changes to the muscle cell itself, single fiber mechanical assays provide a unique perspective into the inherent functional capacity of the muscle independent of extracellular influences such as neuromuscular activation, metabolic homeostasis, etc. Whether loss of contractile velocity in single fibers occurs with age remains equivocal as multiple studies have shown maximum unloaded shortening velocity (V_o) is reduced in both MHC I and MHC IIA fibers (D'Antona et al., 2003; Frontera et al., 2000; Larsson et al., 1997; Ochala et al., 2007; Yu et al., 2007), whereas a few suggest no difference (Frontera et al., 2008; Korhonen et al.,

2006; Trappe et al., 2003). Miller et al. demonstrates a slowing of cross-bridge kinetics evidenced by prolonged t_{on} in MHC IIA fibers from older adults (M. S. Miller et al., 2013a). Consistency across studies regarding physical activity level needs to be addressed because when matched for activity level, fiber size and specific tension is not different between younger and older fibers ((Trappe et al., 2003; Venturelli et al., 2015). It is possible that the reduction in habitual physical activity that generally occurs with older age may exacerbate reductions in muscle mass and function, even at the cellular level.

Muscle strength and power are key predictors of independence, quality of life, and all cause mortality in older adults (Fragala et al., 2015; Metter et al., 2004), however muscle fatigue can greatly exacerbate declines in physical function. The acute reduction in the force and power generating capacity following repeated or prolonged activation (Callahan et al., 2009), i.e. muscle fatigue, disproportionately impacts older adults, who already experience deficits in strength and power. Interestingly, older adults resist fatigue better than younger adults during isometric contractions, however, lose more power more quickly during high velocity concentric contractions (Callahan & Kent-Braun, 2011). Improved isometric fatigue resistance is thought to be attributed to low relative area of MHC II fibers (Callahan et al., 2016) and lower accumulation of inorganic phosphate (P_i) and proton (H^+), the main metabolic drivers of muscle fatigue (Debold et al., 2016). It is thought that the mechanisms behind this velocity dependence in muscle fatigue may arise due to contractile speed, in which case shortening velocity in single fibers may explain age-related differences.

Furthermore, fatiguing exercise is accompanied by increases in catecholamines, epinephrine and norepinephrine, which act on β -adrenergic receptors. Downstream of adrenergic signaling, cyclic adenosine monophosphate (cAMP) activates protein kinase A (PKA), known to

phosphorylate many proteins, including myosin binding protein C (MyBP-C), which is known to tune contractility in skeletal muscle (Robinett et al., 2019). MyBP-C regulates crossbridge formation by directly interacting with both thick and thin filaments and is phosphorylated by PKA, resulting in enhanced velocity and power (Robinett et al., 2019). Older adults seem to have a reduced sensitivity to β -adrenergic agonists (Ford et al., 1995), which may explain an inability to maintain velocity and power during dynamic fatiguing exercise. Additionally, myosin regulatory light chain (RLC) is phosphorylated following transient increases in sarcoplasmic Ca^{2+} concentrations during prolonged muscle activation (Gittings et al., 2011), resulting in enhanced myofilament Ca^{2+} sensitivity (Persechini et al., 1985; Sweeney & Stull, 1986) and myosin kinetics (Metzger et al., 1989; Sweeney & Stull, 1990) *in vitro*. *In vivo*, RLC phosphorylation following a sustained maximal voluntary contraction (MVC) potentiates force and power in humans (Chiu et al., 2003; Houston et al., 1985; Stuart et al., 1988), and is thought to be the mechanism behind post-activation potentiation (PAP). RLC content has been shown to be lower in older males (Gelfi et al., 2006), and phosphorylation is reduced in older females (M. S. Miller et al., 2013a) and in aged rats (Gregorich et al., 2016). Activation-dependent increases in RLC and MyBP-C phosphorylation may act to limit or forestall muscle fatigue *in vivo*, improving performance during repetitive and strenuous tasks. However, it is possible that a reduced capacity to phosphorylate these proteins *in vivo*, perhaps with aging, leads to poor fatigue resistance during dynamic contractions.

Therefore, the purpose of this study was to assess the contractile performance of single muscle fibers of the vastus lateralis (VL) *in vitro* before and after *in vivo* dynamic fatiguing knee extensor contractions to task failure in young and older males and females. We also sought to investigate age- and fatigue-induced differences to the phosphorylation status of key sarcomeric

regulatory proteins, myosin regulatory light chain (RLC) and myosin binding protein C (MyBP-C). We hypothesized that fatiguing exercise would improve contractile performance in single muscle fibers to a greater extent in young compared to older adults. Additionally, we hypothesized that RLC and MyBP-C phosphorylation would be reduced in older compared to younger adults, and fatiguing exercise would increase phosphorylation status, less so in older adults.

4B. Methods

Study Design: A total of 9 young (4 males; 5 females) and 12 older (5 males; 7 females) healthy adults performed an acute bout of isotonic fatiguing knee extensor contractions at 30% MVIC on their dominant limb. Muscle biopsies from the dominant (fatigued) and non-dominant (control/non-fatigued) limb were performed, and muscle samples were separated for assessment of in vitro cellular contractile performance and western blot to assess phosphorylation of MyBP-C and RLC.

Participants: A total of total of 9 young (4 males; 5 females) and 12 older (5 males; 7 females) healthy adults participated in the study. All participants completed informed consent and health history questionnaire, prior to inclusion in the study. To limit the potential for menstrual cycle-dependent variation in circulating estradiol, all female participants either reported use of hormonal contraceptive or were tested in the pre-follicular phase of the menstrual cycle, (within 5 days of menses onset). Participants reported no orthopedic limitations (severe osteoarthritis, prior joint replacement, etc.), endocrine disease (hypo/hyperthyroidism, Addison's Disease or Cushing's syndrome, etc.), uncontrolled hypertension (>140/90 mmHg), neuromuscular disorder,

significant heart, liver, kidney or respiratory disease, and/or diabetes. Participants were non-smokers. Finally, participants taking medications known to affect either muscle contractility or beta-adrenergic signaling of neuromuscular activation (including but not limited to beta blockers, calcium channel blockers, and muscle relaxers) were not included.

Physical Activity Monitoring: Habitual physical activity was monitored for approximately 7 days (including at least 1 weekend day) using an ActivPAL (PAL Technologies, UK) triaxial accelerometer affixed to the anterior aspect of the mid-thigh using a waterproof protective barrier (Tegaderm, 3M). Data was categorized according to ActivPAL Daily Summary Outcomes Exports as step count (steps/day) and time spent in 4 different activity categories based on step cadence: time in sedentary (0steps/min), light (<75steps/min), moderate (≥ 75 steps/min, <125steps/min), and vigorous (≥ 125 steps/min) activity.

Knee Extensor Strength, Muscle Morphology, and Fatigue Protocol: Participants became familiarized with the BioDex System 3™ Dynamometer (Biodex, USA) on a previous day by performing 3 MVIC and a single fatiguing exercise as described below. On this same day, vastus lateralis (VL) muscle thickness (MT) was measured transversely using B-mode ultrasonography (Philips iE33; Philips, Andover, MA) and a linear-array ultrasound probe transducer (L9-3, 3-9 MHz, 33-mm field of view; Philips, Andover, MA) as the distance between the superficial and deep aponeuroses. Participants were situated in the upright seated position with the hip and knee flexed at 90 degrees (180 degrees = full extension) with the knee joint and dynamometer axis of rotation aligned. Hands were placed on support handles at their side for additional support during exercise and to ensure no hip extension. Range of motion of the knee joint was set to 90 degrees.

Participants then performed 3 maximum voluntary isometric contractions (MVIC), with one-minute rest between contractions, for measurement of peak isometric torque and rate of torque development (RTD). Participants were then transferred to the bed for preparation of the muscle biopsy. Following administration of subcutaneous 1% lidocaine HCl injection at the planned site of biopsy and initial incision, the incision was closed with steri-strips (3M) and covered with Tegaderm (3M) to maintain a sterile field. Participants returned to the dynamometer for the isotonic fatiguing exercise protocol. Participants were instructed to “kick out as hard and fast as you can” at 30% of their MVIC along to a metronome at 40bpm with strong verbal encouragement as well as visual feedback of their torque trace in real time. Participants were considered fatigued when their range of motion became significantly reduced by more than 50% on subsequent contractions. Raw analog data was converted to digital using an A/D converter (CED, UK) and recorded using Spike2 software (CED, UK). Digital signals corresponding to position, torque, and velocity were exported and analyzed in a custom MATLAB code (MATLAB 2022a, MathWorks). Immediately following the last contraction, the volunteer was moved to the bed, incision opened, and the area was sterilized again before performing the biopsy. A biopsy was performed on the contralateral control limb immediately following the fatigued limb biopsy.

Muscle Biopsy and Tissue Processing: Percutaneous needle muscle biopsy of the vastus lateralis muscle was performed as described (Privett et al., 2024). Briefly, following sterilization of the skin, subcutaneous and intramuscular 1% lidocaine injections were delivered. Following the fatiguing exercise, a scalpel blade was used to make a 5mm incision on the vastus lateralis muscle. A 5mm Bergström needle was inserted to the belly of the muscle and manual suction

applied to acquire the tissue samples. Muscle samples were then blotted and removed of fat and connective tissue before transfer to either cold (4°C) dissecting solution (120mM NaMS, 5mM EGTA, 0.1mM CaCl₂, 6 mM MgCl₂, 0.25mM KH₂PO₄, 20mM BES, 1.8mM KOH, 1mM DTT, and 5mM ATP-Mg; pH = 7.0) for mechanical analysis or snap frozen in liquid nitrogen (LN₂) and stored at -80°C for isoelectric separation and immunoblot analysis. Tissue designated for mechanical experiments were dissected at 4°C into bundles of ~100 fibers, tied to glass rods at slightly stretched lengths, and placed in skinning solution (5mM EGTA, 2.5mM MgCl₂, 2.5mM ATP-Na₂H₂, 10mM imidazole, 170mM potassium propionate, EDTA-free protease inhibitor; pH = 7.0) for 24h at 4°C. Next, bundles were transferred into a series of storage solutions (identical to skinning solution but containing 1 mM sodium azide and excluding the protease inhibitor cocktail) with increasing concentrations of glycerol (10%, 25%, 50% v/v) for 2 hours each at 4°C. The 50% glycerol solution contained an EDTA-free protease inhibitor tablet (Thermo Scientific). Upon final storage in 50% glycerol solution, bundles were kept at -20°C for up to 4 weeks until mechanical analysis.

Single Fiber Mechanical Experiments: Upon day of experiments, one bundle was isolated, trimmed evenly in dissecting solution at 4°C and placed in an additional skinning solution (dissecting solution with 1% Triton-X100 v/v) for 20min at 4°C. Following skinning, the bundle was placed back in dissecting solution at 4°C and fibers were manually dissected at random. Each fiber to be used for mechanical experiments underwent an additional 20min of skinning (dissecting solution with 1% Triton-X100 v/v) at 4°C. Following preparation, each fiber was placed into a large well consisting of relaxing solution (identical to dissecting solution but with the addition of 15mM creatine phosphate (CP), 5mM P_i, 300 units ml⁻¹ creatine phosphokinase

(CPK)) and tied end to end to a force transducer and a length motor with extended troughs using the Moss clamp technique (Moss, 1979) on a custom apparatus (Aurora Scientific Inc., Aurora, ON, Canada) (Privett, et al., 2024). The glass-bottomed aluminum bath plate consists of 8 wells temperature controlled by a built-in thermo-electric cooler. The bath plate moves independently from the force transducer and length motor allowing for the transfer of the mounted fiber to different solutions. The bath plate and troughs are mounted to an inverted microscope (Leica Microsystems, Wetzlar, Germany) to track vertically. The fiber was first stretched to a sarcomere length (SL) of $2.65\mu\text{m}$ measured by a Fourier transformation of optical density viewed longitudinally (Aurora Scientific), cross sectional area (CSA) then measured assuming elliptical shape by taking the average of 3 measurements along the length of both the fiber top and side widths. Side widths are viewed through a right-angled prism mounted on the largest bath plate chamber. The fiber was then slacked to set zero force, re-stretched to a SL of $2.65\mu\text{m}$, upon which fiber length and passive tension was measured, then force was again set to zero to ensure any additional force to be attributed to active contraction, not passive stretch. The fiber was then placed into a second bath containing pre-activating solution (identical to relaxing solution but with EGTA 0.5 mM) for 30sec to provide optimal Ca^{2+} activation upon subsequent transfer into the third bath containing activating solution (identical to relaxing solution but at pCa 4.5). In activating solution, the fiber is allowed to contract maximally until peak force plateaus. Upon maximal activation (force plateau), an isotonic load clamp is performed before returning to relaxing solution. Using the initial fiber length (L_o) and maximum force (F_{max}), the fiber is shortened at progressively higher velocities to achieve 3 different target submaximal loads. This process is repeated until all 5 series of load clamps have been completed (15 load steps in total). The forces are plotted against their associated velocities to generate a force-velocity curve fit

with the Hill equation. The Hill fits derive the following parameters: maximum tension (T_{\max}), maximum velocity (V_{\max}), and maximum power (P_{\max}). Fibers were excluded for further analysis if tension dropped >10% from the first to last activation and/or if the SL patterns are disrupted or other evidence of damage is seen. All experiments are performed at 15°C. Upon completion of experiments, the fiber was collected and transferred to an individual tube containing sample preparation buffer (SPB; 2% SDS (v/v), 12.5% Tris/HCl pH 6.8 (v/v), 25% glycerol (w/v), 0.05% β -mercaptoethanol (BME; v/v), drop of 1.0 M bromophenol blue), spun for 30sec @8500RPM, heated for 2min at 65°C, and stored at -80°C for SDS-PAGE.

SDS-PAGE/MHC Isoform Identification: To assess MHC isoform in single muscle fibers, SDS-PAGE was performed. The resolving gel contained 7% acrylamide/Bis (50:1; w/v), 1.5M Tris/HCl (pH 8.8), 1.0 M glycine, 4% SDS, 30% glycerol and the stacking gel contained 4% acrylamide/Bis (50:1; w/v), 0.5M Tris/HCl (pH 6.8), 0.1M EDTA (pH 7.0), 4% SDS, 5% glycerol. Upon polymerization, upper and lower chamber running buffers consisting of 1X SDS and 0.5X SDS, respectively, were poured prior to protein loading. 20 μ l of solution containing a single fiber was aliquoted into each lane, with a sample homogenate (~2.5mg; 2-5 μ l) from the same volunteer in the center lane as a standard. Gels were run for 3.5 hours at 70V followed by 20 hours at 200V. Following completion of electrophoresis, the gels were stained using a Pierce Silver Stain Kit (BioRAD) and either immediately dried or stored in gel drying buffer (10% glycerol, 20% ethanol) at 4°C for later analysis. MHC isoforms assessed were MHC I, MH IIA, MHC IIX as well as hybridized MHC I/IIa and MHC IIA/IIX. A separate gel was run identical to above yet only including sample homogenates (~2.5mg; 2-5 μ l) to assess relative abundance of MHC I, IIA, and IIX in each individual and compare across groups.

Western Blot: For semi-quantitative analysis of MyBP-C phosphorylation, frozen biopsy samples are thawed and weighed, homogenized, and extracted in protein extraction buffer (600mM KCl, 150mM KH₂PO₄, 20mM EDTA, 5mM MgCl₂, 3.3mM ATP-Na₂H₂, EDTA-free protease inhibitor, pH 6.7) for 90min on ice. Protein concentration was quantified in the lysate using a Pierce BCA Protein Assay Kit (Thermo Fisher). The sample is then heated to 65°C, and 20µg protein is loaded into each well on 4-20% pre-cast SDS-PAGE in Mini-PROTEAN tetra system (BioRAD). Gels are run for 40min at 200V and transferred to a nitrocellulose membrane for 1 hour at 100V in a 1X Tris-glycine buffer with 20% methanol. Ponceau staining is done to confirm a successful transfer, then blocked in TBS Intercept buffer (LI-COR Biosciences, USA) prior to overnight rocking incubation at 4°C in primary antibody. The next day, a second incubation with near-infrared secondary antibodies is performed for 1 hour at room temperature. All immunoblots are imaged on a Bio-Rad ChemiDoc™ MP Imaging System (Bio-Rad Laboratories, US) and densitometry analysis performed in Image J.

For semi-quantitative analysis of RLC phosphorylation, frozen tissue samples were weighed prior to homogenization for 5 min using a glass homogenizer chilled periodically in liquid nitrogen. 40mL of sample preparation buffer (8M urea, 80 Tris, 488 Glycine, 0.1% Bromophenol blue, 100 DTT, protease inhibitor tablet (Pierce), 10ul/ml phosphatase inhibitor cocktails 2 and 3 (Sigma) with 50% Glycerol) was added for each milligram of tissue sample. Samples were then homogenized in solution for 5 min at 60°C. After centrifugation at 12000 rpm for 5 min, the supernatant was aliquoted and stored at -80°C for subsequent analysis. Phosphorylated and non-phosphorylated RLC was separated by charge using 1d isoelectric gel electrophoresis with urea-glycerol gels (stacking gel: 20 Tris-Glycine, 5% Acrylamide stock

(29.22% Acrylamide, 0.78% Bis-acrylamide), 20% Glycerol, 0.1% TEMED, 0.03% Ammonium persulfate; resolving gel: 20 Tris-Glycine, 10% Acrylamide, 40% Glycerol, 0.1% TEMED, 0.02% Ammonium persulfate), 10ul per lane, using 1X running buffer (.122M Glycine, 20 Trizma base, pH 8.6) at 400 V, 16 hours at 4°C. Gels were transferred to a nitrocellulose membrane for 1 hour at 100V in a 1X Tris-Glycine buffer with 20% methanol. Membranes were blocked in TBS intercept buffer (LI-COR Biosciences, USA), then rocked overnight at 4°C in primary antibody. The next day, a second incubation with near-infrared secondary antibodies is performed for 1 hour at room temperature. All immunoblots are imaged on a Bio-Rad ChemiDoc™ MP Imaging System (Bio-Rad Laboratories, US) and densitometry analysis performed in Image J.

Immunohistochemistry: Muscle bundles (~100 fibers) from the vastus lateralis muscle were blotted and embedded in O.C.T. (Tissue-Tek®, Sakura Finetek, USA) before placed in isopentane precooled with LN₂ and stored at -80°C. Samples were acclimated for 1hr at -20°C before cryo-sectioning at a thickness of 8µm on a Leica Cryostat (Leica CM 1850UV) and placed on glass slides. Samples were covered and dried overnight. The next day, samples were rehydrated for 10min in a PBS/1% BSA solution, followed by incubation in primary antibody overnight. Then, samples were washed twice for 5min each and incubated in secondary antibody for 1hr. Samples were then washed twice for 5min each before and after application of methanol for 10min. Lastly, one drop of SlowFade™ Diamond Antifade Mountant with DAPI (Invitrogen, Waltham, MA) was applied directly on the sample, followed by two drops of permount mounting medium (Electron Microscopy Sciences, Hatfield, PA) on the glass slide and cover slip placed on top. Samples were imaged on a Leica fluorescence microscope (Leica DM4000B) and Leica

camera (Leica DFC 360FX) at 10x magnification. Composite image generation and subsequent analyses were performed in ImageJ. Each fiber was carefully traced and area was measured. The mean area of MHC I and not MHC I (MHC II) was calculated for each individual. Area fraction was calculated as the percentage of total muscle area occupied by MHC I and MHC II. Fiber type distribution was determined as the total number MHC I or MHC II containing fibers as a proportion of total fiber number in the sample.

Antibodies: Antibodies used for western blot include Rabbit anti-Myosin Light Chain 2 (Abcam, ab92721, 1:5000), Rabbit anti-MYBPC1 (Abcam, ab124196, 1:2000), Rabbit anti-PKA (Cell Signaling Technologies, 9621, 1:300), IRDye® 800CW donkey anti-rabbit (LI-COR, 926-32213, 1:15000), IRDye® 680RD goat anti-rabbit (LI-COR, 926-68071, 1:15000). Antibodies used for histology include BA-D5 MIgG2b (DHSB, 1:100), SC-71 MIgG1 (DHSB, 1:100), 6H1 MIgGM (DHSB, 1:100), ab11575 IgG (Abcam, 1:100), Goat anti-mouse IgG2b AlexaFluor 647 (Invitrogen, 1:500), Goat anti-mouse IgG1 AlexaFluor 488 (Invitrogen, 1:500), Goat anti-mouse IgM AlexaFluor 568 (Invitrogen, 1:500), Goat anti-rabbit IgG AlexaFluor 488 (Abcam, ab150077, 1:500).

Statistical Analysis: Two-way ANOVA with fixed effects of Age and Sex was used to assess differences in anthropometrics, whole muscle function, and fatiguing exercise performance. A two-way Repeated Measures ANOVA with fixed effects of fatigue and age was performed for the comparison of RLC and MyBP-C phosphorylation. To assess differences in single fiber contractile properties between groups, fatigued vs. non-fatigued, and biological sex, a linear mixed effects model was performed within a fiber type and a random effect of Participant ID.

Participant ID allows for each individual participant to be weighted in accordance with the number of fibers they contributed to the total data set. To assess contractile function at baseline, a linear mixed model was performed in non-fatigued fibers with fixed effects of age and sex, and random effect of Participant ID, within a fiber type. To assess the effect of fatigue, a linear mixed model was performed within an age group, with fixed effects of condition (non-fatigue/fatigue) and sex, and random effect of Participant ID. In the event of a condition by sex interaction effect, independent samples t-test were run for the comparison between non-fatigued and fatigued fibers within a sex. All statistical analyses were performed in SPSS (IBM, SPSS Inc.).

4C. Results

Table 4: Anthropometric and Activity Data of Young and Older Participants

	n	Height (cm) *	Weight (kg) *	BMI (kg/m ²)	Step Count (steps/day) *	Light Activity (mins/day)	Moderate Activity (mins/day) *#	Vigorous Activity (mins/day)	
Young	Female	5	162.1 ± 6.1	55.0 ± 3.2	20.9 ± 0.6	7098±2176	25 ± 8	43 ± 15	0.5 ± 0.6
	Male	4	185.3 ± 13.0	84.0 ± 10.1*	24.5 ± 1.2	10013±5001	54 ± 27	72 ± 37	0.7 ± 0.6
Older	Female	7	164.1 ± 6.47	74.4 ± 11.7	27.6 ± 4.1	9107±2313	42 ± 10‡	71 ± 24	1.6 ± 3.9
	Male	5	188.59 ± 27.23	77.5 ± 13.3	23.0 ± 8.1	14937±8625	36 ± 4	115 ± 71	5.1 ± 5.7

Symbols indicate a significant main effect of * biological sex or # age, ‡ different than younger female (p<0.05).
Data are shown as mean ± SD.

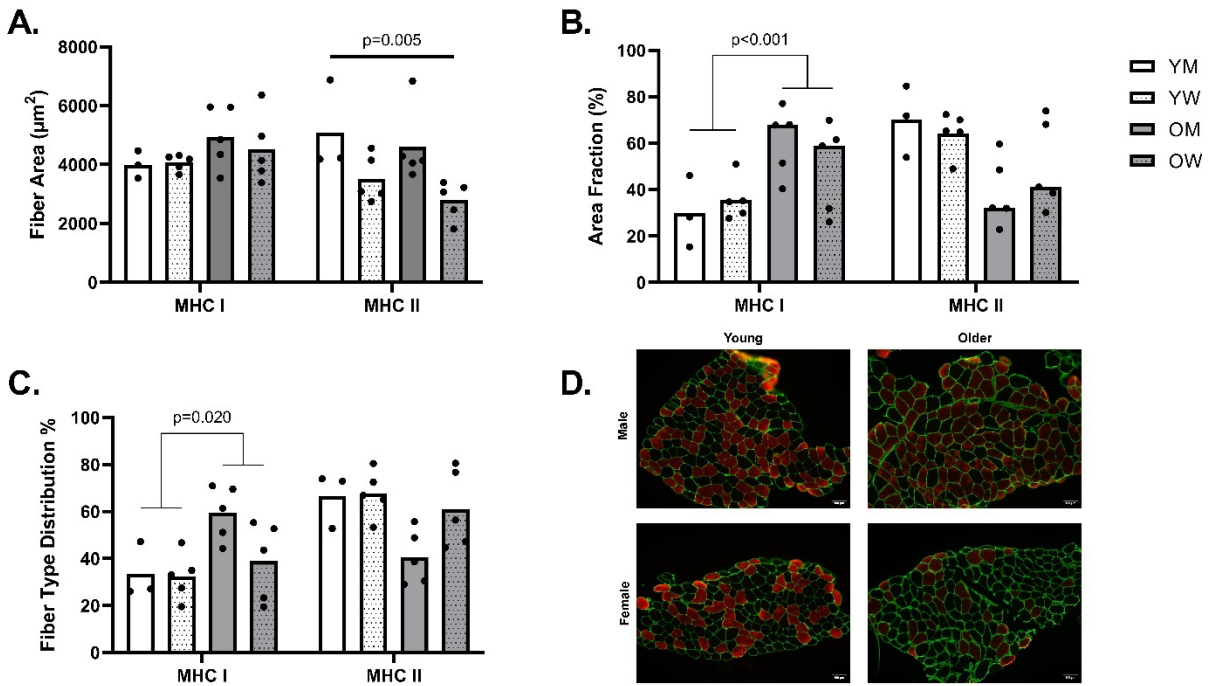


Figure 6. Histological analysis of fiber morphology and fiber type distribution in Younger (white) and Older (gray) males (open) and females (textured). A. Average fiber area of MHC I or MHC II. B. Area fraction of MHC I or MHC II expressed as a percent. C. Percentage of total fibers analyzed in a sample that expressed MHC I or not MHC I (MHC II). D. Representative image of Young (left) and Older (right) male (top) and female (bottom). Dots represent an individual's contribution to the group mean, which is represented as a bar. p-values denote significantly different by sex (A) or age (B,C).

Participant Characteristics, Fiber Type Distribution, and Morphology.

A total of 21 healthy adults participated in this study including 9 young (5 female and 4 male) and 12 older (7 female and 5 male). Males were taller (p=0.002) and weighed more (p=0.004) than females but were not different in BMI (p=0.789) (Table 4). There was no effect of age on height (p=0.683), weight (p=0.191), or BMI (p=0.207) (Table 4). As measured via ActivPAL accelerometry in 18/21 participants, males had a higher step count than females (p=0.044) and spent more minutes per day spent in moderate-vigorous physical activity (p=0.042) (Table 4). Older females spent more time in light activity than younger females (p=0.001), and older adults spent more time in moderate activity than younger adults (p=0.048) (Table 4).

Immunohistochemical analysis was performed in 18/21 participants to assess fiber type distribution and fiber area. The area fraction of MHC I fibers was greater in older compared with younger adults ($p=0.008$), and was not different by sex ($p=0.712$) (Figure 6B). Fiber type distribution was also assessed as number of MHC I or II fibers as a percentage of the total number of fibers analyzed in cross-section. In this analysis, fiber type distribution was greater in older compared with young adults ($p=0.020$), but not different by sex ($p=0.104$) (Figure 6C). In a separate sample stored in SDS sample buffer, tissue homogenate was separated via SDS-PAGE and densitometry was performed to assess relative abundance of MHC I, IIA, and IIX. This method showed greater relative abundance of MHC I in older adults compared with young ($p=0.022$), but no difference by sex ($p=0.508$). No difference in MHC IIA or MHC IIX abundance was found by age ($p=0.215$, $p=0.079$) or sex ($p=0.166$, $p=0.732$), however, an age by sex interaction effect ($p=0.042$) followed by independent samples t-test suggest younger males has greater MHC IIX than older males ($p=0.013$), not seen in females ($p=0.815$) (Supplementary 9A). In older adults, paired samples t-test revealed greater area of MHC I fibers than MHC II ($p=0.027$) but this was not seen in younger adults ($p=0.908$) (Figure 6A).

Comparing the two methods fiber type abundance (IHC vs SDS-PAGE), there was an association between area fraction via IHC and relative abundance via SDS-PAGE ($R^2 = 0.515$, $p<0.001$; Supplementary 10B). Relative abundance via SDS-PAGE was associated with fiber type distribution ($R^2 = 0.377$, $p=0.007$; Supplementary 10C). Average fiber area was not different for neither MHC I nor MHC II by age ($p=0.121$, $p=0.251$), but males had greater MHC II area than females ($p=0.005$) (Figure 6A).

Table 5: Fatigue Data and Whole-Muscle Performance In Young and Older Participants

		n	Time to Fatigue (sec)	Fatigue Ratio (P _f /P _i)	Peak Power (W) *#	Relative Peak Power (W/kg) *#	Peak Torque (Nm) *#	Relative Peak Torque (Nm/kg) *#
Young	Female	5	68±8.8	0.34±0.10	295±33	5.43±0.32	140±8	2.54±0.12
	Male	4	75±29	0.41±0.16	532±95	6.43±1.42	281±44‡	3.34±0.34
Older	Female	7	70±12	0.32±0.06	198±33	2.67±0.21	124±20	1.71±0.39
	Male	5	125±101	0.40±0.11	334±59	4.3±0.07	174±33	2.24±0.15

Symbols indicate a significant main effect of *biological sex or # age, ‡ different than older male (p<0.05).
Data are shown as mean ± SD.

Fatiguing Exercise and Whole Muscle Performance.

Due to data loss during transfer, whole muscle power and time to fatigue are reported in 20/21 participants. Young adults produced more isometric torque (p<0.001) and power (p<0.001) compared to older adults (Table 5). Males also produced more absolute torque (p<0.001) and power (p<0.001) than females (Table 5). Relative torque and relative power was greater in older compared to younger (p<0.001, p<0.001) and in males compared to females (p<0.001, p<0.001) (Table 5). Interestingly, neither the time to fatigue nor the fatigue ratio (representative of power loss) during the exercise protocol were different by age (p=0.165, p=0.149) or sex (p=0.239, p=0.831) (Table 5).

Table 6: CSA and MHC Isoform Distribution of Single Fibers Analyzed in Young and Older Participants

		n	CSA (mm ²) *	MHC Isoform Distribution			
				I	I/IIA	IIA	IIA/X
Young	Female	117	0.0045 ± 0.0013	24	5	57	31
	Male	85	0.0068 ± 0.0019	4	0	55	26
Older	Female	246	0.0046 ± 0.0017	96	13	83	54
	Male	173	0.0069 ± 0.0021	84	33	45	11

Data are shown as mean ± SD. * indicates main effects of biological sex (p<0.05).

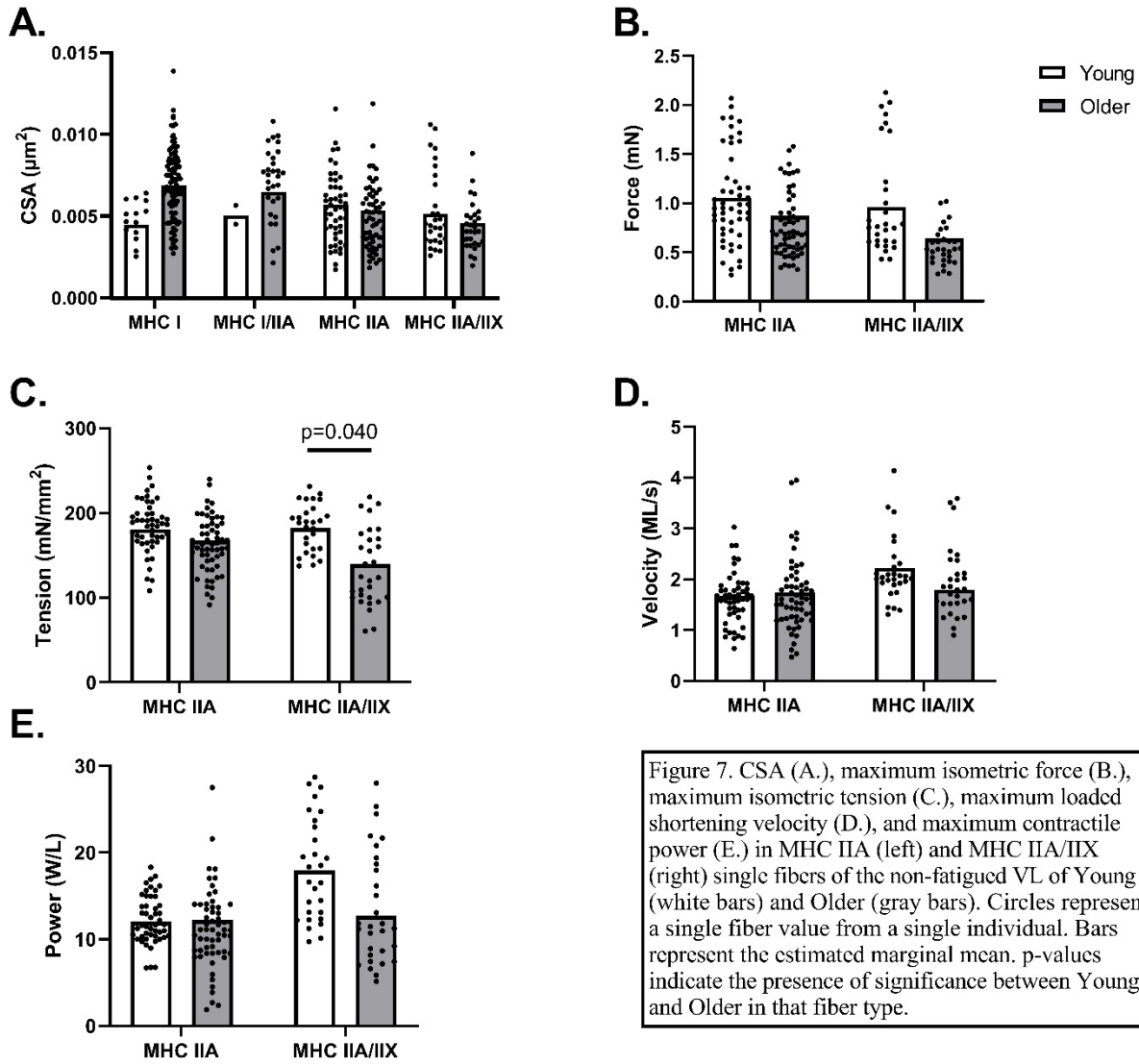


Figure 7. CSA (A.), maximum isometric force (B.), maximum isometric tension (C.), maximum loaded shortening velocity (D.), and maximum contractile power (E.) in MHC IIA (left) and MHC IIA/IIX (right) single fibers of the non-fatigued VL of Young (white bars) and Older (gray bars). Circles represent a single fiber value from a single individual. Bars represent the estimated marginal mean. p-values indicate the presence of significance between Young and Older in that fiber type.

Single fiber contractile performance in non-trained and resistance trained males and females.

In single fibers analyzed for mechanical experiments, there was low number of MHC I (n= 28) and MHC I/IIA (n=5) containing fibers in the young cohort compared with 180 MHC I and 46 MHC I/IIA in the older (Table 6). In all fibers analyzed, males had a larger fiber CSA than females (p<0.001) but no differences were seen by age (p=0.833). In older adults, MHC I fibers had greater CSA (p<0.001), lower force (p=0.005), and lower tension (p<0.001) than MHC II fibers. Due to the low and uneven distribution of MHC I and MHC I/IIA fibers within

the young cohort, age comparisons of single fiber size and function are limited to MHC IIA and MHC IIA/IIX fibers. In MHC IIA fibers, no differences were observed by age in CSA ($p=0.721$), F_{\max} ($p=0.166$), T_{\max} ($p=0.198$), V_{\max} ($p=0.953$), or P_{\max} ($p=0.574$) (Figure 7). CSA ($p<0.001$) and F_{\max} ($p<0.001$) were greater in fibers from males compared to females (Supplementary 10A,B). In MHC IIA/IIX fibers, CSA ($p=0.574$), F_{\max} ($p=0.138$), V_{\max} ($p=0.085$), and P_{\max} ($p=0.108$) were not different by age, yet T_{\max} ($p=0.040$) was lower in older adults compared to young (Figure 10). Fibers from females had lower CSA ($p=0.075$) and F_{\max} ($p=0.072$) along with greater velocity ($p=0.077$) than males, although not statistically significant (Supplementary 12A,B,D). No differences by sex were observed for T_{\max} ($p=0.442$) or P_{\max} ($p=0.334$) (Supplementary 12C,E).

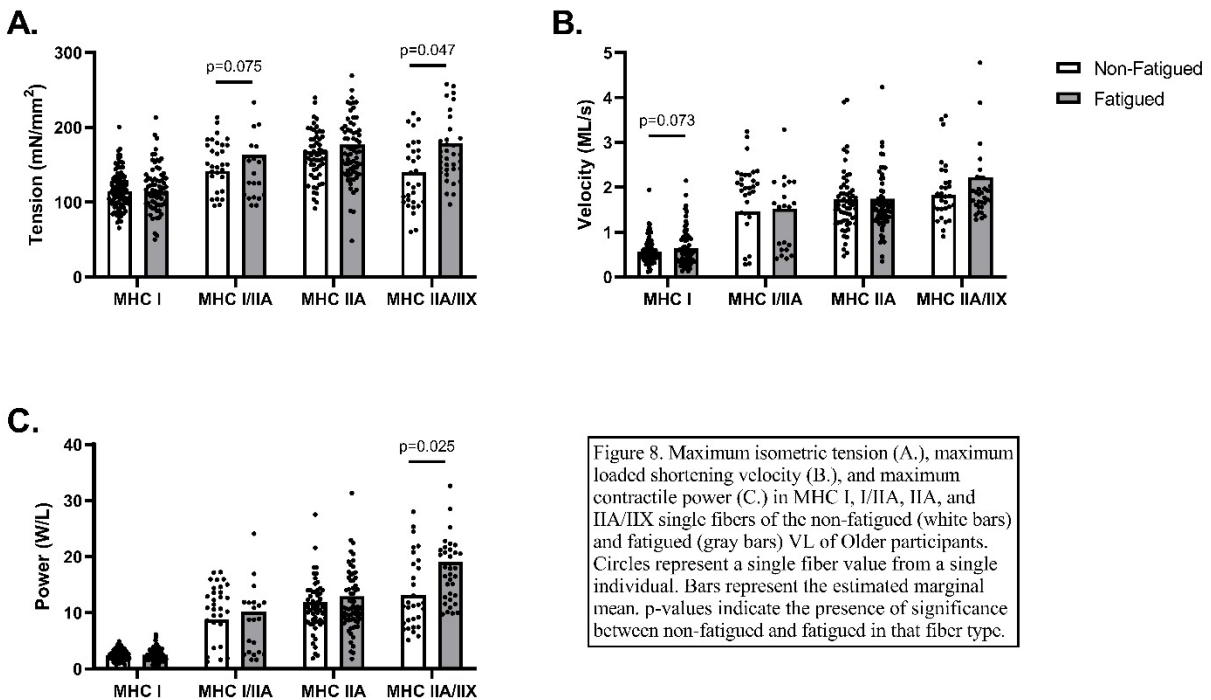


Figure 8. Maximum isometric tension (A.), maximum loaded shortening velocity (B.), and maximum contractile power (C.) in MHC I, I/IIA, IIA, and IIA/IIX single fibers of the non-fatigued (white bars) and fatigued (gray bars) VL of Older participants. Circles represent a single fiber value from a single individual. Bars represent the estimated marginal mean. p-values indicate the presence of significance between non-fatigued and fatigued in that fiber type.

Effects of in vivo fatigue on permeabilized single fiber contractile performance in vitro.

The data concerning the effects of fatigue on single fiber function in the young cohort have been previously reported in Chapter 3C. In the young participants, fibers from the fatigued limb had no significant effect on T_{\max} on either fiber type ($p=0.217$, $p=0.097$; Figure 3A). A fatigue by sex interaction effect in MHC IIA/IIX fibers necessitated repeating the statistical analysis within each sex and suggests no change in females ($p=0.338$; Supplementary 5A) but increased T_{\max} in males ($p=0.006$; Supplementary 5A). V_{\max} was greater in fatigued MHC IIA fibers ($p=0.008$), but not MHC IIA/IIX ($p=0.808$) compared with non-fatigued fibers (Figure 3B). P_{\max} was not different between non-fatigued and fatigued fibers in either fiber type ($p=0.226$, $p=0.109$; Figure 3C).

In the older cohort, MHC I, I/IIA, IIA, and IIA/IIX fibers were considered for analysis. In MHC I fibers, fatigue did not have an effect on T_{\max} ($p=0.852$), or P_{\max} ($p=0.515$), but showed a non-significant trend towards increased V_{\max} ($p=0.073$) (Figure 8). MHC I/IIA T_{\max} was not different by fatiguing condition ($p=0.075$), yet a fatigue by sex interaction ($p=0.049$) suggest females had reduced T_{\max} ($p=0.017$) not seen in males ($p=0.849$) (Figure 8A). Neither V_{\max} ($p=0.763$) nor P_{\max} ($p=0.396$) were different by fatigue in MHC I/IIA fibers (Figure 8B,C). In MHC IIA fibers, no differences were found by fatigue in T_{\max} ($p=0.113$), V_{\max} ($p=0.849$), or P_{\max} ($p=0.171$) (Figure 9). T_{\max} ($p=0.047$) and P_{\max} ($p=0.025$), but not V_{\max} ($p=0.195$) were greater in fatigued MHC IIA/IIX fibers compared with non-fatigued fibers (Figure 8).

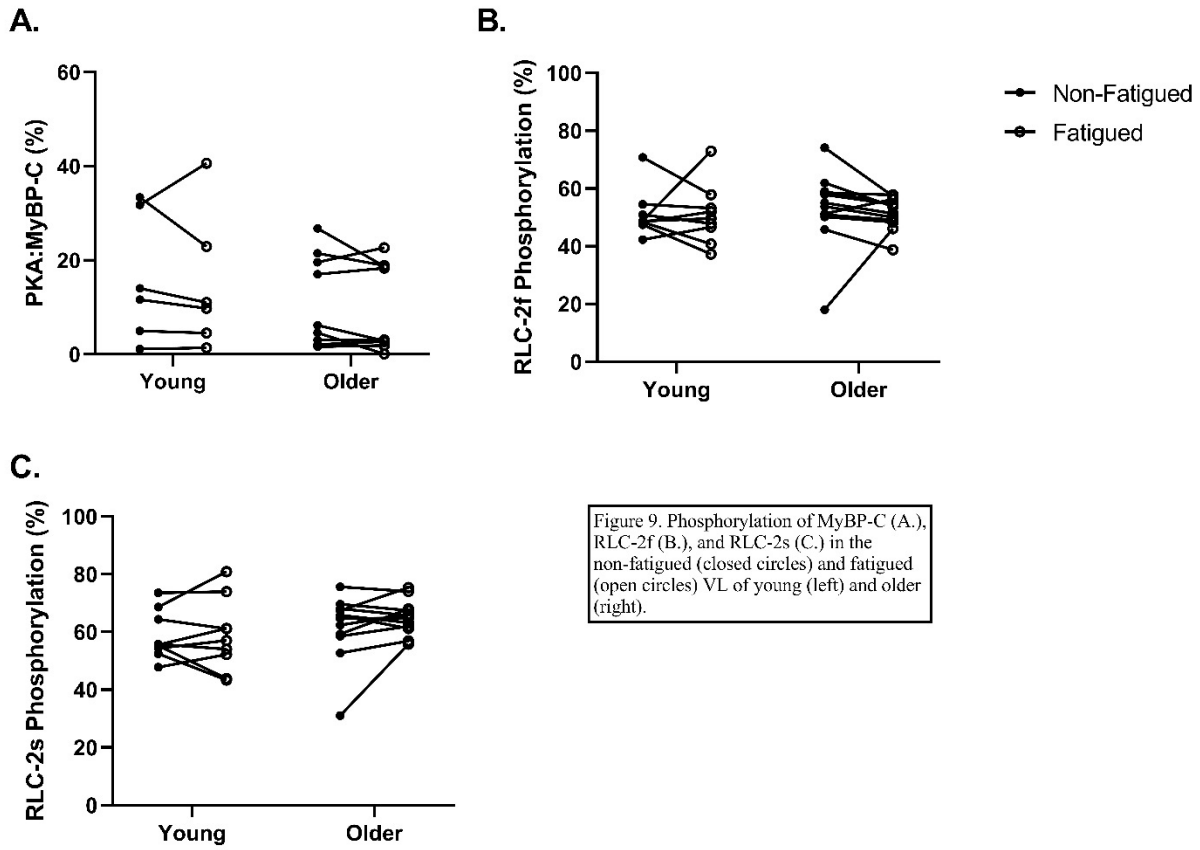


Figure 9. Phosphorylation of MyBP-C (A.), RLC-2f (B.), and RLC-2s (C.) in the non-fatigued (closed circles) and fatigued (open circles) VL of young (left) and older (right).

Western Blot Analysis of MyBP-C and RLC.

MyBP-C and RLC phosphorylation were compared between young and older adults and by fatigue condition via two-way ANOVA. RLC-2s and RLC-2f phosphorylation were not different by fatigue ($p=0.345$, $p=0.711$) or age ($p=0.243$, $p=0.732$) (Figure 9B,C). MyBP-C was also not different by fatigue ($p=0.321$) but was lower in older compared to young adults ($p=0.419$) (Figure 9A).

4D. Discussion

This study examined the chronic effect of age and the acute effect of muscle fatigue on single muscle fiber contractile function and phosphorylation of sarcomeric regulatory proteins,

MyBP-C and RLC from the vastus lateral muscle. In this study sample of 9 young (5F, 4M) and 12 older (5F, 4M), height and weight, but not BMI, were greater in males than females yet no differences were present between young and older adults (Table 4). Interestingly, while step count was not different by age, older adults spent more time in moderate physical activity compared to young adults (Table 4). The young adults were undergraduate students at the University of Oregon, reported no structured physical activity yet were recreationally active and reported walking to and from campus, classes, etc. The older adults were local Eugene, OR community members who reported being physically active with tasks such as walking, gardening, and some reported recreational cycling. These reports were thought to have recruited activity-matched individuals, however we underestimated the reported physical activity of our older adults. Despite these differences, younger adults still exhibited greater absolute and relative muscle torque and power. During the fatiguing exercise task, there was no difference in time to fatigue or fatigue ratio. It would be anticipated that older adults would fatigue quicker than younger adults as has been previously reported during high velocity dynamic contractions (Callahan et al., 2009; Callahan & Kent-Braun, 2011). However, these studies perform fatiguing exercise tasks at a fixed velocity (isokinetic) for a set period of time, whereas the present study performed knee extensions to task failure at a fixed load (isotonic) of 30% MVIC strength. Isotonic contractions may be more representative of tasks of daily living, however the notion that truly isotonic contractions exist in a “free-living environment” is heavily contested by Callahan et al., 2009. Nevertheless, it is possible that because the dynamometer lever arm will rotate about its axis upon a knee extension meeting the set 30% torque threshold and the angular velocity is modulated by the “effort” the participant places on the lever arm, participants that become fatigued may still be able to meet the demands of the torque requirement to move the lever arm,

yet will do so by significantly reducing the angular velocity, thus increasing their time to fatigue. However, because the task involved “kicking out as hard and as fast as you can” and relative decline in muscle power between age groups were not different, this suggests that the fatiguing task was similar for both young and older and met our research goal of significantly fatiguing the knee extensor muscles.

Single fiber morphology and fiber type distribution in young and older males and females.

The lack of sufficient MHC I-containing fibers (both MHC I and MHC I/IIA) in our current sample provides a limitation in our ability to test fiber-type dependent age-related differences in fiber morphology and function. Thus, our analyses for these measures are restricted to MHC IIA and MHC IIA/IIX fibers. As reported in Table 6, younger adults contributed 28 MHC I (~14%) and 5 MHC I/IIA (~2.5%) compared to 180 MHC I (~43%) and 46 MHC I/IIA (~11%) from older adults. Figure 7 and Supplementary Figure 9 highlight the abundance of MHC I fibers in the younger sample as analyzed by IHC and the relative abundance of MHC I in tissue homogenate separated by SDS-PAGE. Despite our low MHC I fiber count in the sample of fibers run for mechanical experiments, we see that younger participants still possess ~33% MHC I compared to MHC II fibers (Figure 7C, Supplementary 9A). This is in stark comparison to ~49% MHC I in older participants (Figure 7C, Supplementary 9A). However, as previously discussed in Chapter 3D, when isolating single muscle fibers from muscle bundles at random, the probability of isolating an MHC I is low. However, we have established a method to predict the MHC isoform upon initial isolation from the bundle based on the post-dissection fiber length, or the amount of recoil the fiber experiences following isolation (Privett, et al., 2024). These data were collected and published during the

collection of the data from the present study, however when we applied this method to 2 younger females, and the older adults, we were able to successfully isolate an even distribution of MHC I and MHC II fibers. 8/18 and 18/39 fibers from 2 younger females were MHC I-containing fibers, showing that our methodology in this younger cohort was successful. Therefore, we believe that the low MHC I fiber count in young participants is a result of difficulty to isolate these fibers at random, as opposed to an inherent property or low abundance of these fiber types. In both the total fiber data set and when limited to MHC IIA and MHC IIA/IIX, fiber CSA was not different by age but was larger in males than females (Table 6, Figure 8A). In older adults, CSA of MHC I fibers were larger than those of MHC II, which is consistent with previous literature (Lexell et al., 1988). This was confirmed in histological cross-sections as the average area of MHC I fibers was larger than MHC II fibers in the older participants, but not in the young (Figure 7A). It is surprising that CSA was not different by age, yet the relatively high activity level of the older adults may have preserved fiber size. Reduced fiber size is a hallmark of the aging muscle (Lexell et al., 1988), yet when matched for physical activity age-related differences in fiber size disappear (Trappe et al., 2003).

Single fiber contractile function is not different between young and older adults.

Previous studies have shown that when activity level is matched between young and older adults, inherent contractile function of single muscle fibers is generally not different (Frontera et al., 2008; Korhonen et al., 2006; Trappe et al., 2003). However, the low sample size of MHC II containing fibers in these studies limit the interpretation. As aging is associated with the preferential atrophy of MHC II fibers (Hunter et al., 1999; Lexell et al., 1988) it is imperative that the MHC II fibers are studied as they are the most “at risk” fiber type and are correlated with

physical performance in older adults (Frontera et al., 2008). In the present study, tension, velocity, and power of both MHC IIA and MHC IIA/IIX show lower means in older compared with young adults (Figure 10). However, only differences in tension in MHC IIA/IIX fibers were statistically significant. The preservation of MHC II function in this cohort may be explained by the increased physical activity level. In comparison to the resistance trained cohort presented in Chapter 3, the older adults exhibited similar activity levels. It is interesting that for the older adults, in comparison to the young cohort (the NT group in Chapter 3), despite greater activity levels, the differences in velocity and power were non-significant, whereas they were stark in the RT group. It is likely that the greater activity level in older adults preserved muscle fiber size, which preserved contractile function. In contrast, through resistance training the muscle fiber size was enhanced possibly increasing lattice spacing, reducing the contractile performance as seen previously (D'Antona et al., 2006).

Regulatory proteins such as MyBP-C and RLC may influence contractile performance throughout the lifespan. As previously discussed in Chapter 3D, alterations to RLC phosphorylation *in vivo* are unlikely to influence single fiber mechanics in our preparation. However, MyBP-C phosphorylation may better explain differences in contractile function. Single fiber studies and *in vitro* motility assays suggest that phosphorylation of MyBP-C via PKA elicits increases in shortening velocity and actin sliding velocity, respectively (Previs et al., 2016; Robinett et al., 2019). MyBP-C has 2 skeletal isoforms, slow skeletal (ssMyBP-C) and fast skeletal (fsMyBP-C). ssMyBP-C is expressed in both slow and fast muscle, so age-differences in contractile function of fast fibers in the present study may be due in part to ssMyBP-C phosphorylation. fsMyBP-C does not have any known phosphorylation sites, however ssMyBP-C has 3 sites near the C1 domain and 1 in the M-motif (Barefield & Sadayappan, 2010). In

addition to PKA, these serine residues can be phosphorylated by PKC downstream of Ca^{2+} signaling (Heling et al., 2020b). Therefore, it is possible that the ratio of PKA to MyBP-C as measured here does not fully reveal the phosphorylation status of MyBP-C. In soleus muscle of rats, aging was associated with reduced cytosolic PKC (Ishizuka et al., 1993), which may contribute to reduced MyBP-C phosphorylation although this was not measured in the study. The present study found that older adults did not have different PKA:MyBP-C than younger adults, which does not describe the difference in tension between young and older adults. Although non-significant, the mean differences in velocity and power may be explained by lower MyBP-C phosphorylation in some of the older adults, but drawing these conclusions in the present study is unwarranted.

Fatiguing exercise improves single fiber contractile function in an age-dependent manner.

We found that fatiguing exercise improved contractile velocity and power in single muscle fibers of younger males and females, but not older adults. The effect of fatigue in the younger cohort was previously discussed in Chapter 3D. Briefly, we posited that there may exist multiple mechanisms to improve contractile function during repeated or prolonged contractions that may help limit or forestall fatigue in vivo. Of such mechanisms are oxidation, which we do not attribute these findings to as our mechanical preparation includes the use of 1mM dithiothreitol (DTT), an antioxidant that removes oxidation in vitro. Thus, phosphorylation of key regulatory proteins remain a likely candidate, despite not capturing fatigue-induced changes to PKA:MyBP-C. In older adults, the lack of change to contractile velocity or power, with the exception of power in MHC IIA/IIX fibers, is consistent with age-related fatigability. It is possible that the reduced power generating capacity during muscle shortening throughout a

fatigue protocol may arise in part due to the inability to potentiate muscle performance in the face of H^+ and P_i , rather than an heightened susceptibility to these metabolites. These in vitro experiments of permeabilized fibers remove the possibility for alterations to Ryanodine receptor (RyR) function and sarcoplasmic reticulum (SR) Ca^{2+} release, H^+ and P_i , or substrate availability to explain contractile functional differences. Thus, the resultant changes, or lack thereof, may be mediated by regulatory protein modification. Additionally, aging has been associated with reduced resting levels of epinephrine secretion in humans (Esler et al., 1995). In this study, older men had a significantly lower epinephrine release response following isometric exercise compared to young men (Esler et al., 1995). This potential mechanism would suggest lower MyBP-C phosphorylation the older adults of our study, however we did not find significant differences. Although, the variation in MyBP-C phosphorylation could be explained by life-long activity level, although we are not equipped to answer this question with the current data set. Further, it has been shown that both P_i and H^+ accumulate less in older compared to young adults following intermittent MVIC exercise (Lanza et al., 2007). Considering P_i is a requirement for protein phosphorylation, it is possible that a reduced epinephrine secretion, and by extension reduced β -adrenergic signaling, combined with reduced P_i accumulation within the muscle leads to reduced phosphorylation of regulatory proteins such as MyBP-C via PKA. However, it is not clear whether reductions in free-flowing P_i remain lower following dynamic exercise in older adults compared with young as well as a reduced β -adrenergic response, therefore this possibility in the context of fatiguing exercise, while interesting, should be taken with caution.

The lack of cellular contractile phenotypic response to acute fatigue in the older adults suggests the role for altered sex hormone status. Older males and females experience significantly reduced testosterone (T) and estrogen (E2) in old age (>65yr), respectively. This

decline in T and E2 has been associated with loss in muscle mass and function (Sipilä et al., 2013). Older females typically experience greater musculoskeletal maladaptation to aging such as greater rates of osteoporosis and sarcopenia and as such E2 decline post-menopause should be taken into consideration. In the current study, T and E2 levels were not directly measured in young or older participants however we did attempt to control for the menstrual cycle phase by targeting the early follicular phase of the menstrual cycle in young females, or recruited females that were taking oral contraceptive. This was assumed to target days when E2 levels are relatively low in these females. However, chronic exposure to E2 during the menstrual cycle is likely more important compared to acute fluctuations in regards to regulation muscle function (Taylor et al., 2024). Nevertheless, chronic deficiency of E2 in female rats (Lai et al., 2016) and adult females post-menopause (Miller et al., 2013) has been associated with reduced RLC phosphorylation. While we have demonstrated that RLC phosphorylation likely is not playing a role in cellular contractile mechanics in our preparation, it is possible that variation in RLC phosphorylation at baseline and throughout fatiguing exercise impacts fatigability and the amount of activity experienced by the muscle. However, we did not see an effect of age or sex in the time to fatigue or fatigue ratio, nor did we see significant differences in RLC phosphorylation between groups suggesting this potential mechanism via chronic E2 deficiency may not fully explain the results.

Limitations

This study is limited in its ability to test fiber-type dependent changes to contractile function with age. However, previous studies have investigated these outcome measures in MHC I fibers and suggest that in activity matched older adults, there are no reported difference in

tension, velocity, or power. However, our cohort was more active than the young adults, and likely with exercise that is low load in nature such as walking and cycling. Therefore, the fiber-type comparisons would have greatly benefited this study as slow-twitch fibers are often preserved in older adults. We have shown that our method for predicting MHC isoform is successful and should be applied to future participants in order to increase the number of MHC I in young adults. Additionally, our lack in ability to detect phosphorylation changes to MyBP-C and RLC limits our interpretation of potential mechanisms. Future studies should aim at identifying these mechanisms *in vitro* by incubation in PKA or phosphatase to selectively phosphorylate and dephosphorylate downstream targets. Another option is to identify the role of MyBP-C in aging or fatigue, by performing these isotonic load clamps inside and outside the “c-zone” where MyBP-C does and does not reside, respectively.

Conclusion

Overall, this study found that in a group of active older adults compared to recreationally active younger adults, muscle fiber size and contractile performance was not different in MHC II fibers. These data provide additional insight into the effects of physical activity on preservation of muscle function and build upon previous studies suggesting similar results in MHC I fibers by including a large number of MHC II fibers. In response to fatiguing exercise, older adults did not have altered single muscle fiber contractile performance, in contrast to increased velocity and power in younger adults. We propose, in conjunction with prior literature, that differences in intracellular signaling downstream of β -adrenergic stress in response to exercise may contribute to the results presented here.

5. Aim 3: To investigate the role of estrogen in mediating post-activation potentiation independent of age.

5A. Introduction

The loss of estrogen with age has been associated with declines in physical function and increased risk for certain health outcomes. The age-related loss in muscle mass and function, i.e. sarcopenia, tends to affect females more than males which severely increases falls risk, injury, and loss of mobility (Kirchengast & Huber, 2009). Postmenopausal females exhibit lower muscle size, strength and power than younger females (Callahan & Kent-Braun, 2011), and reduced cellular hypertrophy following resistance training (Bamman et al., 2003a). In young menstruating females, circulating E2 can fluctuate up to 5-fold during each menstrual cycle, reaching values >500 pg/mL (Elliott-Sale et al., 2021). Following menopause, E2 levels drop significantly to <10pg/mL while estrone (E1), produced by adipocytes rather than the ovaries, becomes dominant (Coelingh Bennink, 2004). In females aged 50-57 years, those that undergo estrogen replacement therapy have greater muscle cross-sectional area (CSA) and strength (Taaffe et al., 2005).

Less is known about how estrogen deficiency in younger females affects muscle structure and function. For premenopausal females, the use of hormonal contraceptives (HC) is common and provides an added layer of complexity regarding the effects of circulating estrogen on muscle-specific outcomes. HC's contain synthetic variations of estrogen (ethinyl estradiol, EE) and/or progesterone (progestin) to suppress ovulation and prevent pregnancy. Combination pills taken orally often contain both EE and progestin, however other options, often termed "mini pills", contain only progestin. Another class of HC's include subdermal implants, Implanon™

and Nexplanon®, that contain only progestin and release this hormone for an extended period, usually 3-5 years. Hormonal intrauterine devices (IUD) are inserted into the uterus and release progestins as well, however these progestins act directly on the uterus and do not have a notable effect on circulating estrogen (Jin et al., 2022). Combined oral contraceptives that contain both EE and progestin act to suppress endogenous E2 and progesterone production while providing a supplement of both synthetic estrogen and progesterone. Two independent systematic reviews of the current literature suggest that exercise performance may be trivially reduced during early follicular phase, when E2 is relatively low, (McNulty et al., 2020), or when taking oral combined EE and progestin contraceptive (Elliott-Sale et al., 2020). However, much of the literature has highlighted oral contraceptive use, whereas progestin only contraceptives such as subdermal implants may provide a unique insight into estrogen suppression in young females.

The ability to potentiate twitch force following voluntary muscle activation, termed post-activation potentiation (PAP), may provide better fatigue resistance or falls prevention, which overall can limit risk of injury. PAP has been shown to be primarily caused by increased RLC phosphorylation following the rise in intracellular Ca^{2+} during muscle contraction. Estrogen has been shown to play a significant role in RLC phosphorylation and subsequent twitch potentiation in pre-clinical models. OVX mice exhibited reduced RLC phosphorylation that was recovered with addition of exogenous estradiol (Lai et al., 2016). In C2C12 cells, increasing exogenous estradiol concentrations linearly increases RLC phosphorylation (Lai et al., 2016). Furthermore, post tetanic potentiation is reduced with OVX and again restored with estradiol administration, but interestingly not different between sham control administered with vehicle vs estrogen (Lai et al., 2016). However, the increase in maximal rate of force development during twitch potentiation is lower in OVX than OVX + estrogen, but sham animals with exogenous estrogen

also exhibited increased maximal rate of force development compared to vehicle administration (Lai et al., 2016). ER α -knockout mice have also exhibited reduced post tetanic potentiation and significant reductions in RLC phosphorylation (Collins et al., 2018). These studies have provided a mechanistic link between estrogen deficiency and twitch potentiation. It is unclear, however, if estrogen deficiency in postmenopausal females or estrogen suppression in younger females would lead to similar results. Therefore, the propose of this study was to utilize a novel study design of estrogen suppression in humans by comparing eumenorrheic young females (EU) during the mid-luteal phase of the menstrual cycle (high E2), younger females taking progestin only HC (low E2), and postmenopausal females (low E2) to identify the role of reduced circulating E2 independent of age on RLC phosphorylation and twitch potentiation. We hypothesized that estrogen would be lower in the HC group compared to EU and that RLC phosphorylation and twitch potentiation would be lower in HC and postmenopausal females compared to EU.

5B. Methods

Study Design: A total of 16 healthy adults participated in the study including 5 young eumenorrheic females, 6 young females on hormonal contraceptive, and 5 older postmenopausal females. Young eumenorrheic females tracked two menstrual cycles to time their laboratory visit for the mid-luteal phase where estrogen and progesterone are relatively high concentrations, while hormonal contraceptive and older postmenopausal females came to the laboratory with no additional time restrictions. All study visits occurred in the morning to avoid any diurnal shifts in muscle function. Participants donated a blood sample for analysis of sex hormones (estrogen and progesterone), then performed a maximum voluntary isometric contraction (MVIC)

preceded and followed by an electrically evoked muscle twitch at 10% MVIC and two muscle biopsies of the vastus lateralis (VL), one of the experimental limb and the other of the contralateral control limb. Muscle samples were assessed for RLC phosphorylation and prepared for histology.

Participants: A total of 16 healthy adults participated in the study including 5 young eumenorrheic females, 6 young females on hormonal contraceptive, and 5 older postmenopausal females. All participants completed informed consent and health history questionnaire, prior to inclusion in the study. Admission to the eumenorrheic group required that participants experienced regular menstrual cycles as defined by a cycle that lasts 21-35 days in duration with no more than 3 missed cycles per year (Elliott-Sale et al., 2021) and have not been taking hormonal contraceptives for at least 12 months. Admission to the hormonal contraceptive group required the use of progesterone-only contraceptives excluding intrauterine devices (IUD) for at least 3 months. One participant in the hormonal contraceptive group reported the use of combined estrogen and progesterone combination pill and will be highlighted in the data below. Participants reported no orthopedic limitations (severe osteoarthritis, prior joint replacement, etc.), endocrine disease (hypo/hyperthyroidism, Addison's Disease or Cushing's syndrome, etc.), uncontrolled hypertension (>140/90 mmHg), neuromuscular disorder, significant heart, liver, kidney or respiratory disease, and/or diabetes. Participants were non-smokers. Finally, participants taking medications known to affect either muscle contractility or beta-adrenergic signaling of neuromuscular activation (including but not limited to beta blockers, calcium channel blockers, and muscle relaxers) were not included.

Menstrual Cycle Tracking: All female participants in the eumenorrheic group were provided with ovulation test strips (Pregmate®) and instructed to track 2 menstrual cycles. Participants reported to the research team when their first menstrual cycle (“lead-in cycle”) began (first day of menses onset), took the urine-based test strip daily starting on day 5 of their cycle until a positive luteinizing hormone (LH) surge (ovulation expected 1-2 days following) was detected and confirmed via photograph by the research team, then reported when their next menstrual cycle began (first day of menses onset). This test was used to confirm a cycle length between 21-35 days and used for better precision in their study visit day. Participants then began tracking a second cycle (“experimental cycle”) and upon positive LH surge, were then scheduled for their study visit 6-9 days following with exact days following determined at the research team’s discretion based on lead-in cycle length.

Physical Activity Monitoring: Habitual physical activity was monitored for approximately 7 days (including at least 1 weekend day) using an ActivPAL (PAL Technologies, UK) triaxial accelerometer affixed to the anterior aspect of the mid-thigh using a waterproof protective barrier (Tegaderm, 3M). Data was categorized according to ActivPAL Daily Summary Outcomes Exports as step count (steps/day) and time spent in 4 different activity categories based on step cadence: time in sedentary (0steps/min), light (<75steps/min), moderate (≥ 75 steps/min, <125steps/min), and vigorous (≥ 125 steps/min) activity.

Habituation Session and Ultrasonography: A habituation session was performed, termed “Day 1” and was scheduled in the morning hours. Participants in the eumenorrheic group came to the lab during menstruation, where estrogen was presumed to be low. On the first study day,

participants arrived to the laboratory to assess muscle area via 2-D Ultrasonography (Philips EPIQ series Diagnostic Ultrasound System; Philips, Andover, MA) with a Philips eL18-4 transducer (Philips, Andover, MA). Five panoramic images were captured at the quadriceps muscle group for compositional and morphological measures along with one longitudinal image spanning the length of the vastus lateralis. Each panoramic image was taken in a lateral-to-medial sweep at 5 locations along the length of the thigh. Due to reliability and repeatability issues with images most distal and most proximal, we utilized two images at the mid-belly of the thigh for our analyses of VL muscle area. First, a scale was applied to the image and then using the polygon tool, the VL was outlined using the superficial and deep aponeuroses as boundary markers. Muscle area and echogenicity, the average pixel intensity of the measured area, was taken for each measure. Images were analyzed using ImageJ software.

Participants also underwent a habituation session in order to understand the twitch potentiation and muscle strength measures protocol. Utilizing a Grass® S48 Stimulator (Natus, USA), muscle twitches were performed with the use of surface stimulation electrodes on the quadriceps muscle group. More specifically, one electrode was placed lateral to the midline of the thigh and 2 inches distal to the inguinal crease, and the other placed medial to the midline of the thigh and one inch proximal to the patella. The participants were then seated on a BioDex System 3™ Dynamometer (Biodex, USA) in the upright seated position with the hip and knee flexed at 90 degrees (180 degrees = full extension) with the knee joint and dynamometer axis of rotation aligned. Hands were placed on support handles at their side for additional support during contractions to ensure no hip extension. The participants then performed 3 maximum voluntary isometric contractions (MVIC) each separated by 60s to assess muscle strength and contractile kinetics. The average of 3 peak toques during the MVIC's were used as maximum strength.

Following strength measures, a single twitch stimulus was delivered via 400 μ s square pulse. Voltage started at 0mV and then increased on subsequent stimulations until a resultant isometric torque of 10% MVIC was achieved. The participants were then instructed to perform a 10s MVIC followed by a single twitch exactly 5s after.

Experimental Study Session: On the second study visit, “Day 2”, participants came to the laboratory in the morning having fasted overnight and refrained from caffeine upon waking up. First, a venous blood draw was performed in the antecubital vein for the collection of serum and plasma. Total blood volume was approximately 32mL. Serum samples were collected in tubes with micronized silica and inverted 5 times, left to sit at room temperature for 30min while plasma samples collected in tubes with EDTA and were inverted 8-10 times and placed on ice for 30min. Both samples were centrifuged at 1100RCF for 10min at 4°C, then supernatant was extracted and stored in cryogenic vials at -80°C until later analysis.

Following blood draw, participants were moved to our BioDex System 3™ Dynamometer (Biodex, USA) and performed 3 MVIC as described above. Then, participants were reclined in the exercise chair where preparation of the biopsy site occurred, as described below. Briefly, skin was sterilized, and 1% or 2% lidocaine was delivered subcutaneously and intramuscularly. Participants were sat up again at the same hip and knee joint angles as before. The twitch potentiation protocol was performed as described above including increasing the stimulation voltage until 10% MVIC was reached, performing a 10s MVIC followed by a single electrically evoked twitch exactly 5s after. Participants were then reclined and a muscle biopsy was taken from the experimental VL followed by the control VL as described below.

Dynamometry Data Analysis: Raw analog data was converted to digital using an A/D converter (CED, UK) and recorded using Spike2 software (CED, UK). Digital signals corresponding to torque and time were exported at 500Hz sampling rate and analyzed in a custom MATLAB code (MATLAB 2022a, MathWorks). Maximum torque was calculated as the average of the 3 MVIC contraction peak torques. Rate of torque development was calculated as the greatest positive value of the first derivative of the torque-time curve. Relative rate of torque development was expressed as MVIC/s, utilizing the peak torque during that contraction. Twitch potentiation was measured as the percentage increase in torque from baseline. Twitch rate of torque development and relative rate of torque development were calculated the same as those of the MVIC.

Muscle Biopsy and Tissue Processing: Percutaneous needle muscle biopsy of the vastus lateralis muscle was performed as described (Privett et al., 2024). Briefly, following sterilization of the skin, subcutaneous and intramuscular 1% or 2% lidocaine injections were delivered. Following the final twitch, a scalpel blade was used to make a 5mm incision on the vastus lateralis muscle. A 5mm Bergström needle was inserted to the belly of the muscle and manual suction applied to acquire the tissue samples. This was repeated on the contralateral control limb. Muscle samples were blotted and removed of fat and connective tissue before either flash frozen in liquid nitrogen (LN₂) and stored at -80°C for immunoblot analysis, bundles (~100 fibers) embedded in O.C.T. (Tissue-Tek®, Sakura Finetek, USA) and placed in isopentane precooled with LN₂ and stored at -80°C for immunohistochemistry, or ~2.5mg muscle sample blotted and stored in sample preparation buffer (SPB; 2% SDS (v/v), 12.5% Tris/HCl pH 6.8 (v/v), 25% glycerol (w/v), 0.05% β-mercaptoethanol (BME; v/v), drop of 1.0 M bromophenol blue), spun for 30sec @8500RPM, heated for 2min at 65°C, and stored at -80°C for SDS-PAGE.

Western Blot: For semi-quantitative analysis of RLC phosphorylation, frozen tissue samples were weighed prior to homogenization for 5 min using a glass homogenizer chilled periodically in liquid nitrogen. 40mL of sample preparation buffer (8M urea, 80 Tris, 488 Glycine, 0.1% Bromophenol blue, 100 DTT, protease inhibitor tablet (Pierce), 10ul/ml phosphatase inhibitor cocktails 2 and 3 (Sigma) with 50% Glycerol) was added for each milligram of tissue sample. Samples were then homogenized in solution for 5 min at 60°C. After centrifugation at 12000 rpm for 5 min, the supernatant was aliquoted and stored at -80°C for subsequent analysis.

Phosphorylated and non-phosphorylated RLC was separated by charge using 1d isoelectric gel electrophoresis with urea-glycerol gels (stacking gel: 20 Tris-Glycine, 5% Acrylamide stock (29.22% Acrylamide, 0.78% Bis-acrylamide), 20% Glycerol, 0.1% TEMED, 0.03% Ammonium persulfate; resolving gel: 20 Tris-Glycine, 10% Acrylamide, 40% Glycerol, 0.1% TEMED, 0.02% Ammonium persulfate), 10ul per lane, using 1X running buffer (.122M Glycine, 20 Trizma base, pH 8.6) at 400 V, 16 hours at 4°C. Gels were transferred to a nitrocellulose membrane for 1 hour at 100V in a 1X Tris-Glycine buffer with 20% methanol. Membranes were blocked in TBS intercept buffer (LI-COR Biosciences, USA), then rocked overnight at 4°C in primary antibody. The next day, a second incubation with near-infrared secondary antibodies is performed for 1 hour at room temperature. All immunoblots are imaged on a Bio-Rad ChemiDoc™ MP Imaging System (Bio-Rad Laboratories, US) and densitometry analysis performed in Image J.

SDS-PAGE/MHC Isoform Identification: To assess MHC isoform distribution, SDS-PAGE was performed. The resolving gel contained 7% acrylamide/Bis (50:1; w/v), 1.5M Tris/HCl (pH 8.8),

1.0 M glycine, 4% SDS, 30% glycerol and the stacking gel contained 4% acrylamide/Bis (50:1; w/v), 0.5M Tris/HCl (pH 6.8), 0.1M EDTA (pH 7.0), 4% SDS, 5% glycerol. Upon polymerization, upper and lower chamber running buffers consisting of 1X SDS and 0.5X SDS, respectively, were poured prior to protein loading. 2 μ l of solution containing a sample homogenate (~2.5mg + 200 μ l SPB). Gels were run for 3.5 hours at 70V followed by 20 hours at 200V. Following completion of electrophoresis, the gels were stained using a Pierce Silver Stain Kit (BioRAD) and either immediately dried or stored in gel drying buffer (10% glycerol, 20% ethanol) at 4°C for later analysis. Gels were imaged on a Bio-Rad ChemiDoc™ MP Imaging System (Bio-Rad Laboratories, US) and densitometry analysis performed in Image J. MHC isoforms assessed were MHC I, MHC IIA, and MHC IIX.

Immunohistochemistry: Muscle bundles (~100 fibers) from the vastus lateralis muscle were blotted and embedded in O.C.T. (Tissue-Tek®, Sakura Finetek, USA) before placed in isopentane precooled with LN₂ and stored at -80°C. Samples were acclimated for 1hr at -20°C before cryo-sectioning at a thickness of 8 μ m on a Leica Cryostat (Leica CM 1850UV) and placed on glass slides. Samples were covered and dried overnight. The next day, samples were rehydrated for 10min in a PBS/1% BSA solution, followed by incubation in primary antibody overnight. Then, samples were washed twice for 5min each and incubated in secondary antibody for 1hr. Samples were then washed twice for 5min each before and after application of methanol for 10min. Lastly, one drop of SlowFade™ Diamond Antifade Mountant with DAPI (Invitrogen, Waltham, MA) was applied directly on the sample, followed by two drops of permount mounting medium (Electron Microscopy Sciences, Hatfield, PA) on the glass slide and cover slip placed on top. Samples were imaged on a Leica fluorescence microscope (Leica DM4000B) and Leica

camera (Leica DFC 360FX) at 10x magnification. Composite image generation and subsequent analyses were performed in ImageJ. Each fiber was carefully traced and area was measured. The mean area of MHC I and not MHC I (MHC II) was calculated for each individual. Area fraction was calculated as the percentage of total muscle area occupied by MHC I and MHC II. Fiber type distribution was determined as the total number MHC I or MHC II containing fibers as a proportion of total fiber number in the sample.

Antibodies: Antibodies used for western blot include Rabbit anti-Myosin Light Chain 2 (Abcam, ab92721, 1:5000), IRDye® 800CW donkey anti-rabbit (LI-COR, 926-32213, 1:15000).

Antibodies used for histology include BA-D5 MIgG2b (DHSB, 1:100), SC-71 MIgG1 (DHSB, 1:100), 6H1 MIgGM (DHSB, 1:100), ab11575 IgG (Abcam, 1:100), Goat anti-mouse IgG2b AlexaFluor 647 (Invitrogen, 1:500), Goat anti-mouse IgG1 AlexaFluor 488 (Invitrogen, 1:500), Goat anti-mouse IgM AlexaFluor 568 (Invitrogen, 1:500), Goat anti-rabbit IgG AlexaFluor 488 (Abcam, ab150077, 1:500).

Statistical Analysis: A one-way ANOVA was used to assess differences in body composition, muscle size, muscle performance, activity level, blood hormone concentrations, and muscle fiber area and distribution. Where applicable, Bonferroni corrected t-tests were performed. A RM-ANOVA was used to assess differences in twitch torque and RLC phosphorylation before and after 10s MVIC. All statistical analyses were performed in SPSS (IBM, SPSS Inc.). Simple linear regression analysis was performed to identify the association between circulating estrogen and measures of muscle function, potentiation, and RLC phosphorylation.

5C. Results

Table 7: Anthropometric and Activity Data of EU, HC, and OF Participants.

	n	Height (cm)	Weight (kg)	BMI (kg/m ²)	Step Count (steps/day)	Light Activity (mins/day)	Moderate Activity (mins/day)	Vigorous Activity (mins/day)
EU	5	163.5 ± 4.6	63.9 ± 6.1	24.0 ± 3.17	9882 ± 1129	31.6 ± 15.0	75.4 ± 11.6	5.4 ± 6.2
HC	6	162.0 ± 7.1	56.3 ± 10.3	21.1 ± 2.6 [#]	8255 ± 2158	33.2 ± 4.2	63.3 ± 14.9	1.76 ± 1.6
OF	5	164.2 ± 8.2	72.0 ± 13.0	26.7 ± 4.0	8950 ± 3250	40.8 ± 9.3	66.6 ± 26.05	1.2 ± 2.3

*indicate a significant main effect of group ($p < 0.05$), # different than OF ($p < 0.05$). Data are shown as mean ± SD.

Anthropometrics, Activity Level, and Whole Muscle Performance

The age of the EU group was 19.4 ± 2.6 , 20.3 ± 0.8 for the HC group, and 73.2 ± 4.0 for the OF group. There was no difference in height ($p = 0.957$) or weight ($p = 0.073$) between the three groups, however BMI was lower in the HC group compared to OF ($p = 0.041$) but not EU ($p = 0.483$) (Table 7). Step count ($p = 0.597$), and time in light ($p = 0.401$), moderate ($p = 0.616$), or vigorous ($p = 0.253$) activity was not different between the groups (Table 7). One participant in HC group has not yet completed their activity monitoring session and is therefore omitted from analysis of activity. There was no main effect of study group on maximum strength ($p = 0.167$) or absolute ($p = 0.221$) and relative ($p = 0.833$) RTD (Table 8). Muscle CSA ($p = 0.317$) and echogenicity ($p = 0.219$) were not different by group, and strength normalized for muscle CSA was also not different ($p = 0.644$). During the 10s MVIC, or conditioning contraction, peak torque was lower compared with during the initial 3 MVICs ($p < 0.001$) (Table 8). Peak RTD ($p < 0.001$) and relative RTD ($p < 0.001$) were also lower during the 10s MVIC compared with the initial 3 MVICs (table 8). However, strength ($p = 0.200$), RTD ($p = 0.118$), or relative RTD ($p = 0.577$) were not different by group during the 10s MVIC (Table 8).

Table 8: Whole-Muscle Performance and Twitch Characteristics in EU, HC, and OF Participants

	n	MVIC (Nm)	RTD (Nm/sec)	Relative RTD (MVIC/sec)	Baseline Twitch Torque (N/m)	10s MVIC (Nm)	10s RTD (Nm/sec)	10s Relative RTD (MVIC/sec)
Eu	5	174.1 ± 22.7	852.3 ± 305.6	4.8 ± 2.1	16.7 ± 1.9	158.3 ± 9.8	733.7 ± 109.3	4.1 ± 1.3
HC	6	168.9 ± 63.4	628.7 ± 130.8	5.4 ± 1.1	16.4 ± 6.5	154.3 ± 62.3	725.8 ± 324.9	4.2 ± 1.3
OF	5	124.6 ± 20.1	915.1 ± 307.8	5.0 ± 1.0	11.6 ± 1.3	114.0 ± 22.7	439.8 ± 109.3	3.5 ± 0.9

Symbols indicate a significant main effect of group ($p < 0.05$). Data are shown as mean ± SD.

Table 9: Blood 17β -Estradiol (E2) and Progesterone (P4) Concentrations in EU, HC, and OF Participants

	n	Serum		Plasma	
		E2* (pg/mL)	P4 (pg/mL)	E2 (pg/mL)	P4 (pg/mL)
Eu	5	72.4 ± 46.7	13.7 ± 11.7 [#]	66.9 ± 46.3	13.9 ± 11.0 [#]
HC	6	15.0 ± 6.7	1.6 ± 1.3	12.6 ± 5.8	1.0 ± 0.5
OF	5	20.2 ± 36.2	0.5 ± 0.6	20.8 ± 38.6	0.3 ± 0.3

*indicate a significant main effect of group ($p < 0.05$), # different than other groups ($p < 0.05$).
Data are shown as mean ± SD.

Serum and Plasma 17β -Estradiol and Progesterone

Each female in the EU group tracked 2 consecutive menstrual cycles and was targeted to volunteer on study Day 2 during the mid-luteal phase, when E2 and P4 are high. The average lead in cycle length was 26.8 days with a range of 24-31 days. For the experimental cycle, the average length was 28.2 days with a range of 24-37 days.

One HC participant has not yet had their blood analyzed via ELISA and therefore is not included in these analyses. There was a main effect of group on serum E2 ($p = 0.040$), and Bonferroni corrected independent samples t-tests suggest near significantly greater in EU

compared to HC ($p=0.064$), but not OF ($p=0.101$). (Table 9). Plasma E2 was not significantly different by group ($p=0.063$) (Table 9). Serum progesterone was significantly greater in EU compared to HC ($p=0.045$) and OF ($p=0.028$) (Table 9). Plasma progesterone was significantly greater in EU compared to HC ($p=0.022$) and OF ($p=0.016$) (Table 9).

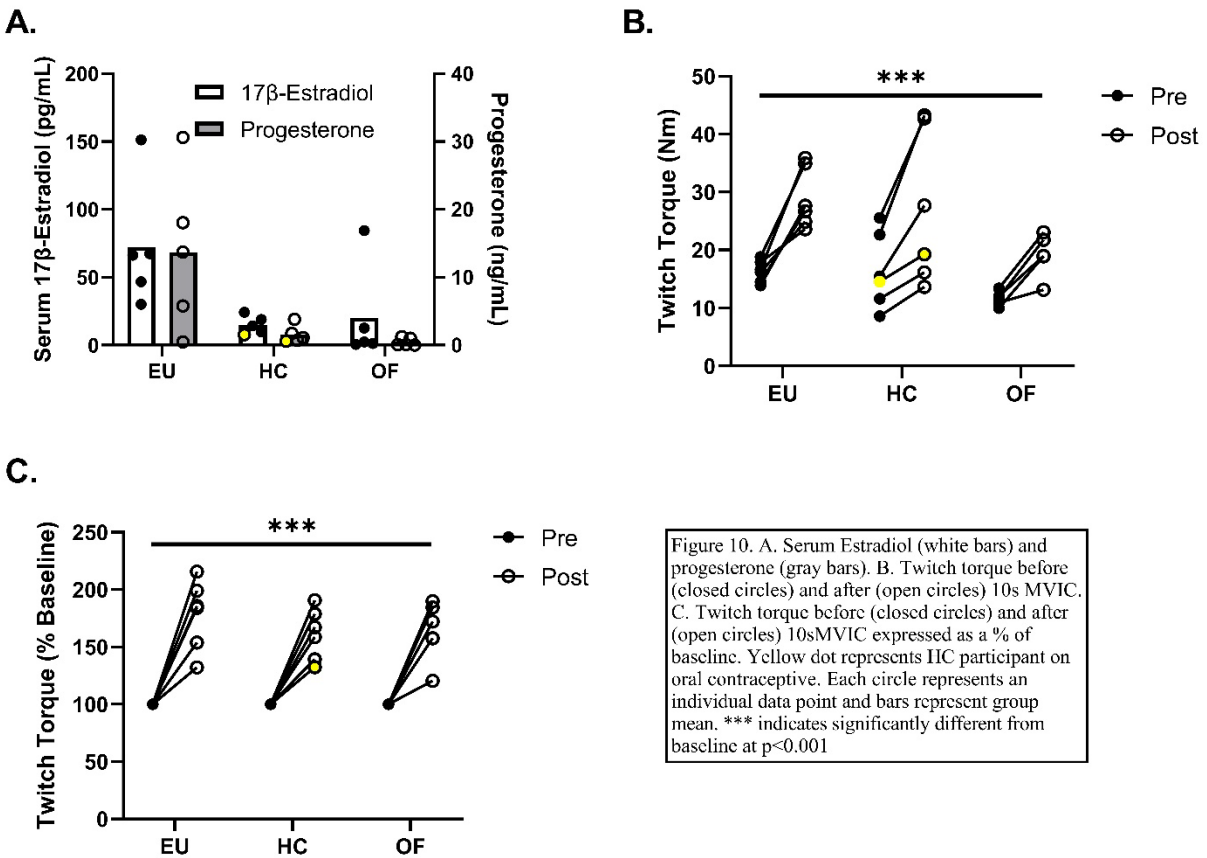


Figure 10. A. Serum Estradiol (white bars) and progesterone (gray bars). B. Twitch torque before (closed circles) and after (open circles) 10s MVIC. C. Twitch torque before (closed circles) and after (open circles) 10sMVIC expressed as a % of baseline. Yellow dot represents IIC participant on oral contraceptive. Each circle represents an individual data point and bars represent group mean. *** indicates significantly different from baseline at $p<0.001$

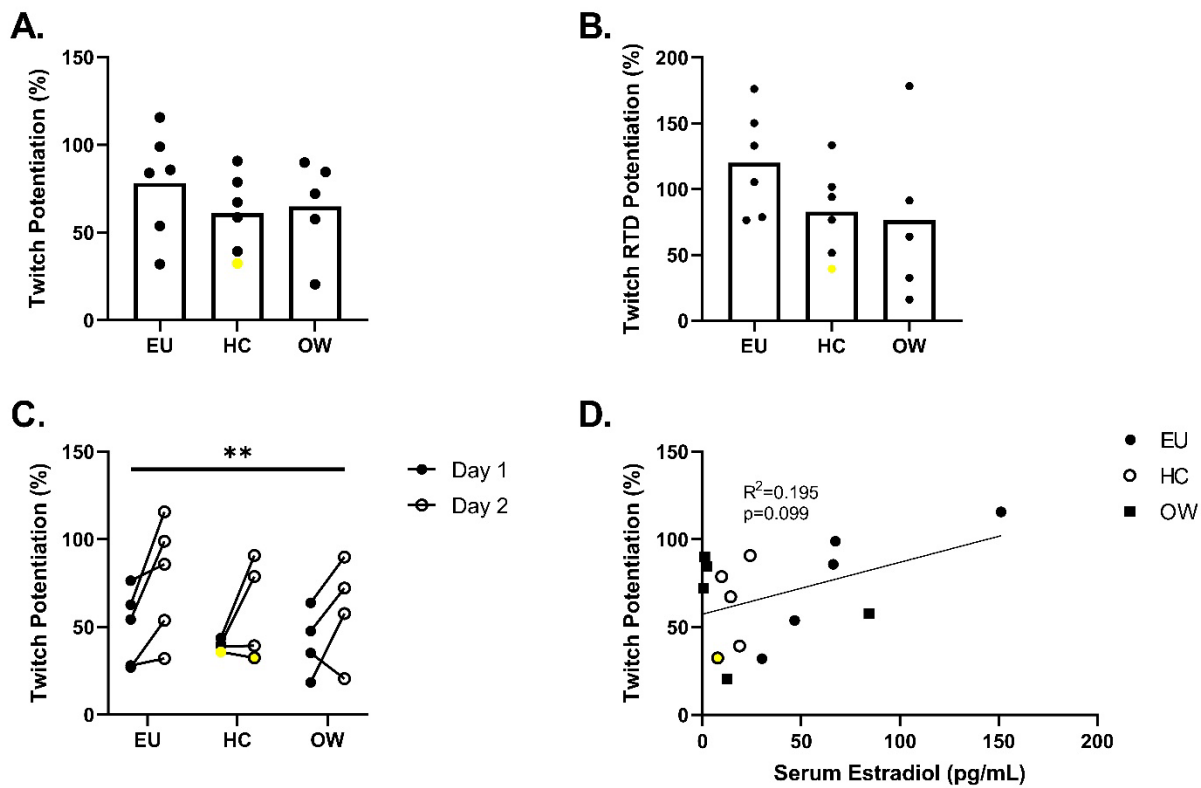


Figure 11. Twitch potentiation (A) and Twitch RTD potentiation (B) in EU, HC, and OF. Twitch potentiation on Day 1 (closed circles) vs Day 2 (open circles) in EU, HC, and OF (C). Relationship between Serum E2 and Twitch Potentiation (D). Yellow dot indicates HC participant on oral contraceptive. Each circle represents an individual data point and bars represent the group mean. ***indicates significantly different by Day at $p < 0.001$.

Twitch Characteristics, Potentiation, and RLC Phosphorylation

Twitch torque at 10% MVIC was not different between groups at baseline ($p=0.137$) or following conditioning contraction ($p=0.206$) (Table 8, Figure 10B). There was considerable variability in the HC group compared with the EU and OF group as evidenced by a significant test for equal variance (Levene's test) at $p=0.011$. Therefore, a Welch's test was used to assess differences in baseline twitch torque and found a main effect of group ($p=0.004$) (Figure 10B). Games-Howell post-hoc comparisons suggest that EU had greater baseline twitch torque than OF

($p=0.004$) but not HC ($p=0.995$) (Figure 10B). HC did not have significantly different twitch torque compared to OF ($p=0.267$) (Figure 10B). Similar results were found for twitch RTD, therefore these statistics were repeated and found no difference by group ($p=0.670$). The conditioning contraction significantly increased twitch torque as assessed by RM-ANOVA and Greenhouse-Geisser correction ($p<0.001$) but this was not dependent on group ($p=0.369$) (Figure 10B,C). When twitch potentiation was expressed as a percent change from baseline was assessed via one way ANOVA, there was no significant difference between the groups ($p=6.33$) (Figure 11A). Twitch RTD was also greater following conditioning contraction ($p<0.001$) and a near significant interaction effect ($p=0.075$) (Figure 11B). Twitch potentiation was also conducted on Day 1 and compared to Day 2 via RM-ANOVA. Potentiation on Day 2 was greater than on Day 1 ($p=0.007$) (Figure 11C).

Simple linear regression showed a non-significant relationship between E2 and twitch potentiation ($R^2=0.195$, $p=0.099$) (Figure 11D). Fiber area was not associated with twitch potentiation in either MHC I or MHC II ($p=0.814$, $p=0.530$) (Supplementary 13B,C)). Biopsy samples were collected in 11/16 participants but only 9/16 participants had matched samples. RLC phosphorylation was assessed in 8/9 participants that had matched samples due to lack of band separation on the gel. In those samples, there was no difference in RLC-2s or RLC-2f phosphorylation by group ($p=0.471$, $p=0.214$) or with potentiation ($p=0.110$, $p=0.140$) (Figure 12).

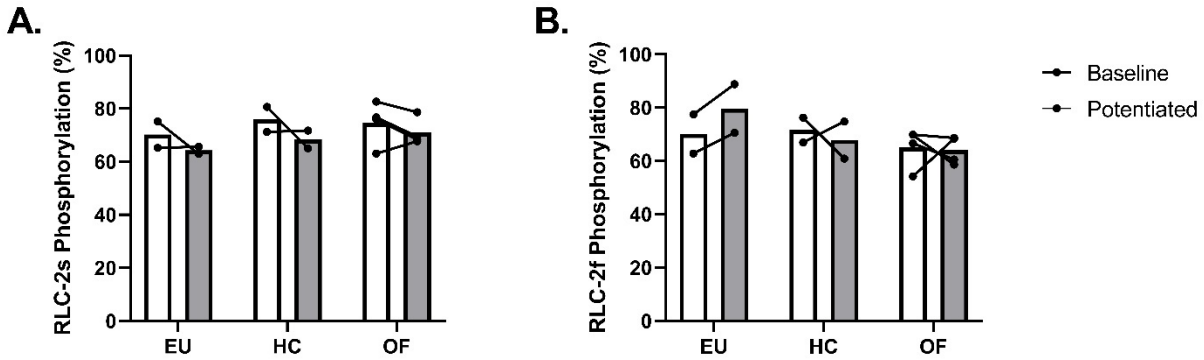


Figure 12: RLC-2s (A) and RLC-2f (B) phosphorylation before (white bars) and after (gray bars) 10sMVIC. Circles represent a single individual and bars represent the group mean.

5D. Discussion

This study utilized a novel study design to investigate the effects of low circulating E2, independent of age, on whole muscle function and twitch potentiation in females. Overall, we found that our protocol was successful in establishing a relatively low and high E2 group in young healthy females. Furthermore, circulating E2 levels in the HC group were not different than OF which allows the ability to isolate the effects of E2 from age in this population.

Mechanisms Influencing Twitch Potentiation

There was significant variation in twitch potentiation and twitch RTD potentiation within groups, and no statistically significant differences between groups. In all participants, the conditioning contraction via 10s MVIC successfully induced potentiation of twitch force as has been well documented in the prior literature (Grange & Houston, 1991; Houston et al., 1985, 1987; Houston & Grange, 1991; Stuart et al., 1988). While previous studies have shown age is associated with reduced twitch potentiation (Hicks et al., 1991), the current study did not identify differences between OF and either of the young female groups. Prior activity level, specifically

resistance training has been shown to improve twitch potentiation in the elderly (Hicks et al., 1991). Additionally, post-activation performance enhancement (PAPE), a similar phenomenon during dynamic performance measures, has been shown to be most effective in young adults that are resistance trained compared to recreationally active (Chiu et al., 2003). The current study included individuals who ranged from recreationally to moderately active and there were no differences between groups in activity level as measured via ActivPAL. However, resistance training background was not controlled for and it is possible this may influence the results. Strength, muscle CSA, and specific torque were not different between the groups, indicating that training backgrounds not captured were unlikely to influence our results. In the biopsy samples collected, there were no differences in average fiber area between groups, and fiber area was not associated with twitch torque potentiation. It has been hypothesized previously that older adults have a reduced potentiation of twitch torque due to increase fatigability during the conditioning contraction. However, previous literature suggest older adults exhibit improved isometric fatigue resistance (Callahan et al., 2009; Callahan & Kent-Braun, 2011).

RLC is the primary mechanism that contributes to twitch potentiation and has been shown to be reduced in older females (M. S. Miller et al., 2013a). Proteomic analysis aged rats suggest lower RLC phosphorylation at Serine14/15 (Gregorich et al., 2016) and reduced RLC content in older males (Gelfi et al., 2006). In the current study, RLC phosphorylation was not different between groups, however the limited sample size limits our conclusions. In Chapter 4, young and older adults did not show differences in RLC phosphorylation and there was no effect of sex or interaction between age and sex. Chapter 3, however, did show reduced phosphorylation in RT participants compared to NT.

Prior literature has established a relationship between estrogen and RLC phosphorylation, Ca^{2+} handling, and twitch potentiation. OVX mice have demonstrated reduced calcium sensitivity (Wattanapernpool & Reiser, 1999), RLC phosphorylation (Lai et al., 2016), and twitch potentiation (Lai et al., 2016). In culture, treatment of C2C12 cells with estrogen increased RLC phosphorylation in a dose-dependent manner (Lai et al., 2016). However, one study argues that a more representative model of menopause, chemically induced ovarian failure (VCD), does not replicate the findings of OVX (Mashouri et al., 2024). Specifically, they did not find changes to in vitro contractile performance of single muscle fibers such as rate of tension redevelopment (ktr), calcium sensitivity, or specific force (Mashouri et al., 2024). However, data from Chapter 3 in this dissertation suggest that RLC, assumed to be the mechanism behind hypothesized reductions in single fiber performance, does not remain following permeabilization and mechanical preparation. While there has yet to be a direct mechanistic link for how estrogen interacts with RLC phosphorylation, it is likely influencing CaMK and its ability to interact with skMLCK. RLC is phosphorylated via skMLCK following Ca^{2+} binding to calmodulin (CaM) and activating CaMK. E2 can bind to membrane-bound G-protein receptors (GPER) upregulating signaling pathways associated with mass regulation such as phosphatidylinositol-3-kinase (PI3K), protein kinase B (AKT), mammalian target of rapamycin (mTOR), p70s6k, 4E-BP1, FOXO3, MuRF1, and atrogin-1 that are restored with estradiol treatment (Cho et al., 2021; Pellegrino et al., 2022).

Updated Analysis Following Post-Study Methodological Considerations

In the EU group, one individual had an experimental cycle length of greater than 35 days, which fits the criteria for exclusion. Additionally, we attempted to bring all volunteers to

the laboratory between 6-9 days following positive LH test, yet one individual had a luteal phase, as defined by time between positive LH test and onset on next cycle, of 9 days. This participant was brought into the lab 7 days after the positive LH test. This participant's E2 levels were the lowest in the EU group at 30.1ng/mL in serum and 21.4ng/mL in plasma. Prior literature suggests that during the mid-luteal phase, E2 levels should range between ~60-200pg/mL (Elliott-Sale et al., 2021). P4 is also high during this phase with values >5ng/mL and this participant had P4 of 13.7ng/mL in serum and 14.4ng/mL in plasma. We likely did not capture the mid luteal phase for this participant as evidenced by low E2 and having the study day later than 3/4th of the luteal phase in total. Additionally, the participant that had an experimental cycle length of 37 days also had E2 lower than >60pg/mL at 46.7pg/mL in serum and 46.9pg/mL in plasma with P4 levels of 0.49ng/mL in serum and 0.45ng/mL in plasma. These two participants had the two lowest E2 values with the two lowest twitch torque potentiation and twitch RTD potentiation in the EU group.

In the HC group, one participant was taking a combined ethynyl-estradiol (EE) and progestin oral contraceptive (OC), highlighted in yellow in Figure 10 and Figure 11. This participant was brought to the lab for the experimental study day in the last two weeks of active pill phase, before placebo phase. E2 levels were 7.7pg/mL in serum and 6.7pg/mL in plasma, with P4 of 0.57ng/mL in serum and 0.53ng/mL in plasma. Although it seems as though OC reduces endogenous production of E2, EE has been shown to be more potent and could influence the results. However, the role of synthetic EE on muscle function has not been well documented and it is unclear whether suppression of E2 is sufficient for this study design or if progestin only contraceptives are more effective. Nevertheless, this participant exhibited adequately low E2 and low twitch torque and twitch RTD potentiation.

In the OF group, one participant had extremely elevated E2 in both serum (84.4pg/mL) and plasma (89.5pg/mL) that was confirmed in duplicate on two separate ELISA analyses. This participant reported no current use or history of hormone replacement therapy, and no medications or supplements that would interfere with our ability to detect E2 via ELISA. To our knowledge, hemolysis of blood during venipuncture or in processing did not occur and was stored at -80°C until use.

Given that the sample size is relatively low and that the study is in the early phase of completion, the following updated analyses are retrospective and serve as an investigative discussion (rather than forming deep conclusions) of the current findings taking consideration of the two participants who were outside the criteria for inclusion to the study. Supplementary Figure 14 shows twitch torque potentiation (A), twitch RTD potentiation (B), and the association between E2 and twitch torque potentiation (C). However, in panels A and B the two EU participants were excluded as they did not fit the criteria for acceptance to the EU group post-blood and cycle analysis. ANOVA suggests a trend towards significant main effect of group at $p=0.092$ for twitch torque potentiation and $p=0.090$ for twitch RTD potentiation. Panel C includes all younger participants that volunteered for the study and aims to capture the variability in E2 in both the EU and HC group where we expected to find the most variability. A linear regression analysis suggests a significant association between E2 and twitch torque potentiation ($R^2=0.471$, $p=0.028$). It is to be clear that these retrospective analyses, although promising, are to be taken with extreme caution. However, when clear cut-offs are applied to the current data set based on prior literature suggesting acceptable ranges of E2 and cycle length (Elliott-Sale et al., 2021) these data are more in line with our initial hypotheses and suggest a relationship between E2 and twitch potentiation in younger females.

17 β -Estradiol May Impact Twitch Potentiation in Young Females

The participants in the current study performed the twitch potentiation protocol two separate times, on their first study visit day termed “Day 1” and their second study visit day termed “Day 2”. For nearly all participants, the amount of twitch potentiation increased on Day 1 compared to Day 2, despite maximum strength and twitch torque (as a percent of maximum strength) not differing ($p=0.527$, $p=0.367$). For the EU group, all volunteers arrived to the lab for Day 1 in the early follicular phase (during menstruation), when E2 is presumed to be low. It was hypothesized, as an extension of the central hypothesis, that low E2 would be associated with low twitch potentiation. However, we did not collect blood samples on this Day 1 measure as it served as a habituation session. This becomes complex as we saw increases in potentiation on Day 2 in both the HC and OF groups, whose E2 values should remain relatively constant day to day. One potential explanation for this result may be the timing of muscle contractions on Day 1 vs Day 2. On Day 2, the participants come to the lab and perform 3 MVIC’s to assess peak strength and set their 10% MVIC target twitch torque. Following this, they are reclined on the Biodex and lidocaine is injected to the area where the biopsy is to be taken. Following lidocaine administration, they are inclined to the seated position and twitches are then delivered to find the current required to elicit 10% MVIC. The time between the 3 MVIC’s and onset of twitch delivery is approximately 30min. On Day 1, less care was taken as to the timing between the 3 MVIC’s and twitch delivery, with estimated time between to be >5 min. Therefore, it is possible that the 3 MVIC on Day 1 potentiated twitch torque during the process of setting the current. Despite the twitch torque being set to 10% MVIC, the current required to elicit that amount of torque, if potentiated, would be lower. Additionally, the muscle that was recruited by this

stimulation would have already been at least partially potentiated effectively providing a ceiling effect on the amount of potentiation possible. Twitch potentiation is a transient phenomenon and decreases over time, especially within 5 minutes, but likely remains elevated long enough for this to have an effect. Despite these findings, if isolating Day 1, the EU group still had greater twitch potentiation than the HC. It is difficult to draw strong conclusions from Day 1 as the timing was not controlled strongly as it was in Day 2, and we did not measure circulating E2. However, it remains an interesting finding and is worthy of further investigation.

Limitations

This study is not without limitations, and the biggest limitation of the current data set is the low sample size. It was expected that that the EU group would have high variability in E2 as has been previously documented (D'Souza et al., 2023). While this project is not entirely complete, and additional participants are required for a comprehensive analysis, these data are promising and track with our initial hypotheses. The time to biopsy was ~5 minutes on average, excluding one participant that took >17min to acquire tissue. Nevertheless, this was a great improvement from Chapters 3 and 4 and improves our confidence in capturing changes to RLC phosphorylation. However, the time course for RLC phosphorylation and dephosphorylation is rapid, although the exact duration of elevated phosphorylation is unknown. It is assumed that 6 minutes is generally too long to capture significant differences in RLC phosphorylation by group following conditioning contraction, especially given the variability in timing between participants. More specifically, 7/11 biopsy samples were acquired within 5 minutes, while 2 were <10min, and 2 >10min.

Another limitation is the ability to accurately predict mid-luteal phase in EU participants with shorter menstrual cycles or shorter luteal phase lengths. Although our study design provides a rigorous approach to tracking multiple menstrual cycles for accurate timing of Day 2, between-cycle and between-participant variation makes it difficult to discern the exact amount of days following LH surge. Our protocol states that participants will return to the lab 6-9 days following, but in once instance the luteal phase for a EU participant was 9 days in total, likely making the 6-9 day window too long. As the study progresses, considerations should be taken to adjust the return date to a more participant- and phase-specific timeline to target the middle of this phase. However, it can be argued that participants should be excluded from the study if their luteal phase does not fit within the guidelines previously suggested (Elliott-Sale et al., 2021), although this has the potential to exclude a significant portion of the female population who are often overlooked in clinical research.

Lastly, the largest limitation to the current study is the use of surface stimulation electrodes on the muscle belly as opposed to nerve stimulation. The feasibility, repeatability, and pain associated with nerve stimulation are typically worse in the femoral nerve compared with peroneal nerve. The angle of the hip makes it difficult to reliably place the electrode over the femoral nerve, and needle stimulation is difficult to repeat as contraction of the quadriceps also induces hip flexion which may act to move the needle providing difficulty in repeatability and increased pain for the participant. We decided to use surface stimulation to target a twitch torque of 10% MVIC as this has previously been shown to be near the maximal twitch torque in young and older adults (McNeil & Rice, 2007). The ideal method to standardize the twitch torque across all participants would be to elicit the maximum twitch torque, however with more adipose tissue and larger muscle mass, maximal twitch torque was not able to be achieved in all

participants due to limitations in the maximum current delivered by the stimulator. Further, it would be beneficial to include EMG in order to observe a relative proportion of muscle that is activated in comparison to either tetanic stimulation, MVIC, or superimposed twitch.

Conclusions

Overall, this study demonstrated the ability to create three female groups based on E2 status utilizing menstrual cycle tracking to predict the mid-luteal phase, hormonal contraceptive to ensure chronically low (suppressed) E2 independent of age, and post-menopausal females to ensure chronically E2 deficiency. We hypothesized that E2 suppression would result in lower RLC phosphorylation and twitch torque potentiation in females, matched for activity level. We were limited in our ability to test the hypotheses surrounding RLC due to low biopsy sample acquisition, however despite statistically insignificant, our current data track with our hypotheses surrounding twitch potentiation. There was a lack of difference between groups, however two EU individuals were likely not tested during the mid-luteal phase, and when taken into consideration, a main effect of group is nearing statistical significance. Our most robust finding is that in the young females, E2 is positively associated with twitch potentiation which supports our hypothesis. As this study progresses, consideration should be taken for E2 values that are outside the literature ranges for mid-luteal cycle phase, older females, or females on HC. Finally, this study begins to demonstrate a relationship between E2 and twitch potentiation that has been well-established in the pre-clinical literature. To our knowledge, this study is the first of its kind to assess estrogen suppression independent of age and how estrogen impacts twitch potentiation in humans.

6. Final Discussion and Conclusions

These set of studies aimed to investigate how chronic stressors such as resistance training, age, and estrogen suppression interact with acute stressors of brief and prolonged muscle activation to alter skeletal muscle function at the cellular and whole tissue level. The first study (Aims 1 & 2) utilized a dynamic knee extension exercise protocol to task failure as a tool to fatigue the muscle and measure changes to the phosphorylation of key regulatory proteins, RLC and MyBP-C, and assess the contractile function of permeabilized single muscle fibers under near-optimal intracellular conditions. We chose to fatigue the muscle *in vivo* and assess single fibers *in vitro* under near-optimal conditions, rather than studying the fibers under fatigue-mimicking conditions, as a way to investigate changes inherent to myofilament function outside the influence of what is known to cause fatigue (H^+ and P_i). The primary findings were that fatiguing exercise paradoxically improved single fiber contractile velocity and power in young NT and RT (Aim 1), but not older (Aim 2) males and females. We did not identify differences in phosphorylation of RLC or MyBP-C with fatigue, however LCMS unveiled numerous differentially phosphorylated residues in RT males only.

We chose to utilize a dynamic fatiguing protocol for two central reasons. First, the age-related declines in physical function are velocity-specific in that isometric torque may be preserved in older adults yet power during dynamic contractions is greatly reduced, especially at high velocities (Callahan et al., 2009; Callahan & Kent-Braun, 2011). Muscle power is a stronger predictor of mortality than muscle strength (Araújo et al., 2025; Metter et al., 2004) in the elderly and is therefore an important outcome measure for improving or maintaining physical function and quality of life in older adults. The velocity dependence of greater fatigability in older adults (Callahan et al., 2009) necessitated that we employ a fatiguing exercise that most closely mimics

the heightened fatigability previously documented in the literature as well as investigating an outcome measure that is clinically relevant. We did not find any differences in the amount of power lost during the fatiguing exercise by group, which at first seems to suggest this protocol did not elicit the anticipated fatigue phenotype. However, this study design had participants perform knee extensions to task failure, rather than for a set amount of time or number of contractions. This ensured that every participant, regardless of duration of exercise, achieved the same level of fatigue so that any differences identified with respect to single fiber function would not be attributable to differences in fatigability per-se, but rather in that muscles response to the exercise task itself. This goal was achieved by denoting task failure as the inability to perform the contractions through 50% or more of the ROM and/or complete the contractions at the set pace of 1 contraction every 1.5 seconds. Second, isotonic contractions have been thought to better mimic real-world tasks as opposed to isokinetic. While it is argued that loads are rarely purely isotonic in tasks of a “free-living environment” (Callahan et al., 2009), during repetitive contractions such as walking, running, or squatting (Gash et al., 2025) the loads experienced are relatively constant. That is not to diminish the utility of isokinetic contractions as these allow researchers to control the velocity component and assess how force and power respond. In the current study, however, our goal was to mimic a real-world task and build upon previous literature that has established the force-velocity relationship with age.

It is important to note the possibility that differences in voluntary activation and motivation to complete the task between groups may have influenced the results of these studies, largely with respect to Aims 1 and 2. During fatiguing exercise, it has been shown that isokinetic force declines significantly more during voluntary activation compared with electrically stimulated muscle contractions (Callahan et al., 2009). This may suggest extrinsic factors such as

central fatigue or motivation contribute to fatigability. However much these factors contribute to fatigability during a voluntary dynamic knee extensor task, it is unlikely to explain differences in force decline between young and older adults (Callahan et al., 2009). In the recovery phase following low force (20% MVIC) isometric contractions, time to task failure was longer and voluntary activation was lower in older adults compared to younger adults suggesting that central fatigue plays a role in age-related differences in fatigability (Yoon et al., 2008). This was not seen at 80% MVIC, however, and authors suggest that contraction intensity and duration may be modulated in order to induce varying levels of fatigue in target populations. In Aims 1 & 2, the load was set at 30% MVIC, however this was performed at maximal voluntary effort during isotonic contractions. Furthermore, volunteers may be more or less “motivated” to complete the task as fatigue sets in during the exercise. Motivation via positive feedback has been shown to improve function during reaching task, more so for older adults (Huang et al., 2018). During our studies, we used strong verbal encouragement, ensuring that each participant provided maximal effort during all contractions. As we did not utilize EMG to measure amount of muscle activation, or superimposed twitch stimulation to assess central activation ratio before or after dynamic exercise, it is possible that central fatigue may play a role in mediating time to fatigue during our study. These values, however, were not different between groups which suggest our task was effective at inducing similar levels of fatigue in all participants.

The interpretation of these study findings depend highly on the assumption that changes to the phosphoproteome with fatigue (or between groups) influence the contractile phenotype of single muscle fibers in our preparation. It was reported in Chapter 3 that MyBP-C phosphorylation likely remains in the fibers following mechanical preparation, but RLC does not. In order to more definitively propose this to be true, a repeat analysis of parallel processing

of tissue samples from additional participants is necessary. Regardless, future study should be aimed at elucidating the specific mechanisms that contribute to this altered contractile phenotype. Our lab has previously tested the effects of PKA and LP incubation on passive modulus of single muscle fibers and was unable to recapitulate the fatigued phenotype. However, it was unclear if PKA incubation was indeed phosphorylating the target protein, in that case the giant elastic protein titin. Pilot data from our laboratory has found that PKA incubation lead to a higher PKA:MyBP-C ratio in one middle-aged male, but reduced phosphorylation from both the non-fatigued and fatigued samples in one young RT female. Additionally, in the middle-aged male, LP incubation lead to increased PKA:MyBP-C as well, and neither of these pilot data were collected in tandem with sham control. Previous studies have utilized PKA and LP to phosphorylate and dephosphorylate MyBP-C, respectively (Robinett et al., 2019) however this was performed in rat skeletal muscle. Thus, careful control of PKA and LP incubation in human muscle samples from our lab should be first confirmed to induce phosphorylation of target proteins and then these analyses should be repeated in order to identify which mechanisms contribute to the enhanced contractile velocity and power in single fibers from the fatigued limb.

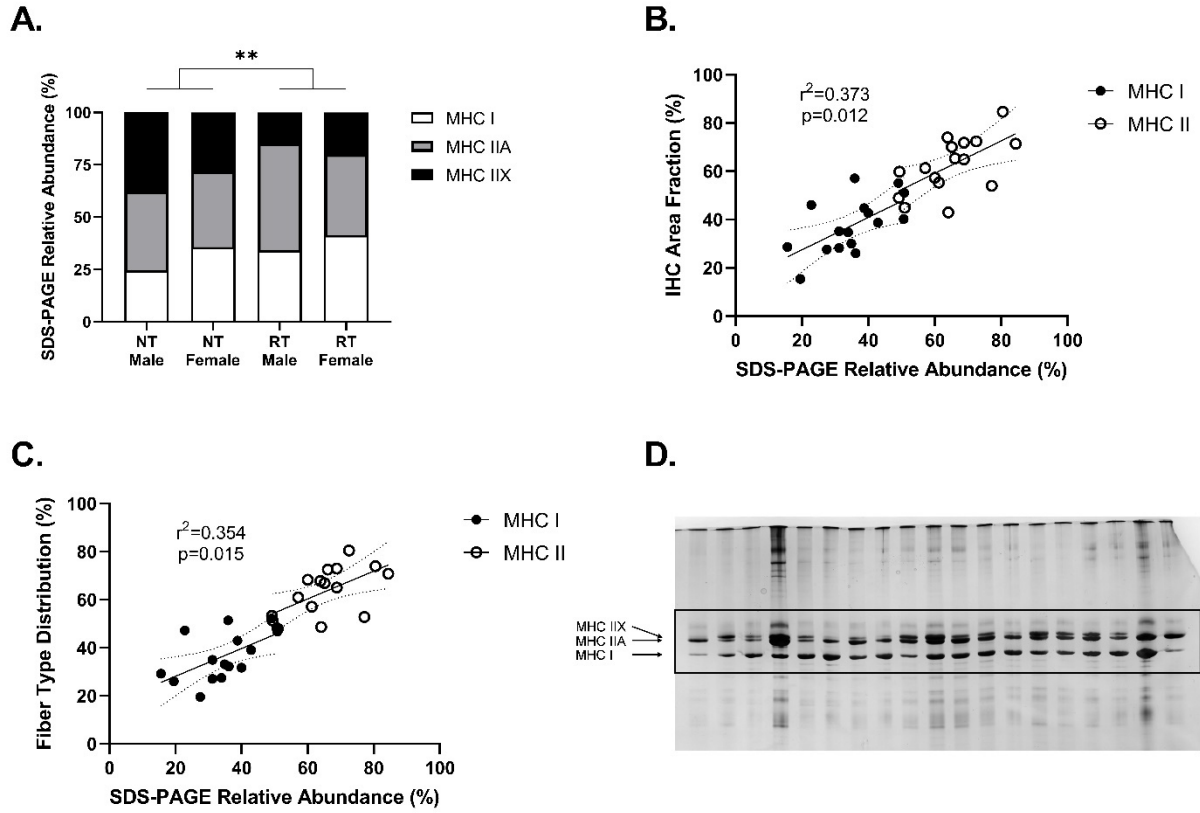
Aims 1 & 2 did attempt to control for menstrual cycle variation in muscle function by limiting young female lab visits to either the early follicular phase of the menstrual cycle if eumenorrheic, or allowed young females to visit the lab at any time if on hormonal contraceptive. Recent study into menstrual cycle variation on exercise performance have not uncovered significant improvements or deficits associated with a specific phase in eumenorrheic females (Taylor et al., 2024). However, it is possible that the exposure to circulating 17β -estradiol during the late follicular and luteal phase may be sufficient to provide the “protective” benefits reported in the literature. Aim 3 may help to inform this situation as we measured

muscle twitch potentiation on two separate study days in EU and HC groups. For the EU group, Day 1 was targeted for the early follicular phase when E2 is presumed to be low, however we did not measure serum or plasma E2 at this visit. The HC group is also assumed to have constant circulating E2, but again was not measured on this day. On Day 1, despite the presumed low E2, the EU group still had greater twitch potentiation than the HC group, which is one index of muscle function. What this may suggest is that regardless of the day-to-day estrogen status, the significant exposure to E2 throughout a menstrual cycle may be sufficient to provide this benefit. However, one participant in the HC group was not on a progestin only contraceptive but rather a combined EE and progestin oral pill. Our pilot data, and prior literature (Rodriguez et al., 2024), suggest that E2 may spike to significantly high levels during the placebo (withdrawal) phase of the pill pack. This participant did not show twitch potentiation values greater than the remainder of the HC group, and in fact was the lowest value in the entire data set of young females from either group. Overall, this complicates the interpretation for how estrogen may be regulating muscle function. Although, less described in the literature is progesterone. It is unclear what effects progesterone may have on muscle functional outcomes, however in Aim 3 the EU group had significantly greater progesterone than the HC and OF group. The mid-luteal phase is the one time in the menstrual cycle where estrogen and progesterone are relatively high at the same time, which makes the isolation of estrogen vs progesterone difficult. As this study continues, it may be worth consideration, although the same notion that short term spikes in a given hormone may be sufficient to produce an certain effect will likely be at play here as well.

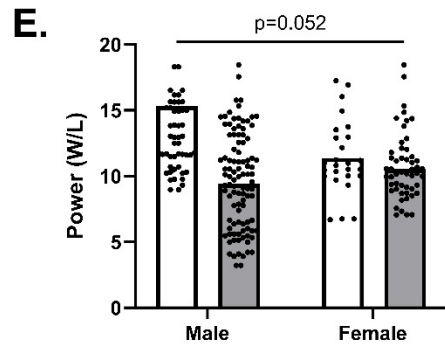
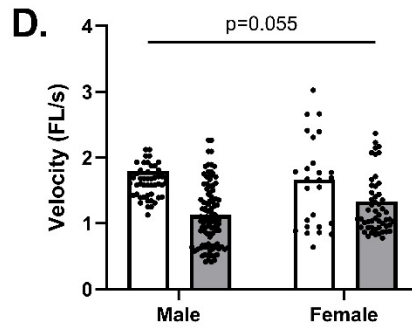
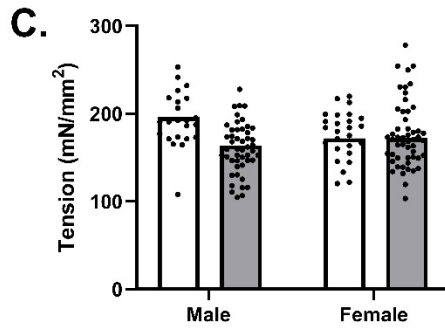
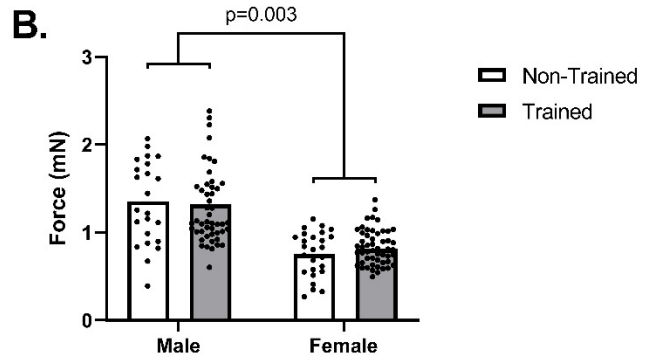
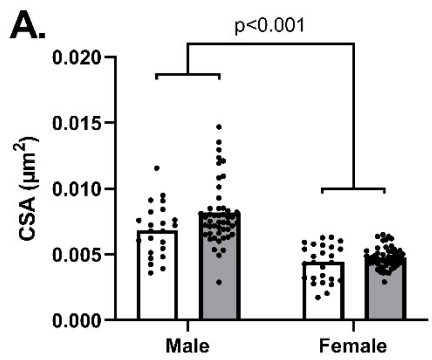
Overall, there exists a lack of support in the literature for the muscle specific mechanisms that may explain the greater fatigability in during high velocity contractions in older adults. This study aimed to address this gap and found that in younger adults, contractile velocity and power

was potentiated following fatiguing exercise but that this was not seen in the older adults. It is possible that the greater velocity and power decline seen with repeated contractions in the elderly may be attributed to a lack of ability to counteract fatigue through myofilament performance enhancement, rather than a greater susceptibility to the intracellular metabolic conditions that cause fatigue in vivo. Additionally, the study of highly trained young individuals allows a unique insight into how muscles perform at their best, and what mechanisms may be contributing to the inherent muscle performance benefits that are not solely explained by size. This study found that the fatigue-induced performance enhancements in single fibers were relatively more robust and that the muscle phosphoproteome changed significantly in RT males compared to other groups offering a training and sex-dependent perspective. Ultimately, if we can identify the intracellular mechanisms that explain how muscle positively adapts to chronic stimuli, coupled with those that explain negative adaptations, then we may be able to inform therapeutic and rehabilitative approaches with the goal of restoring or maintaining physical function in at-risk populations.

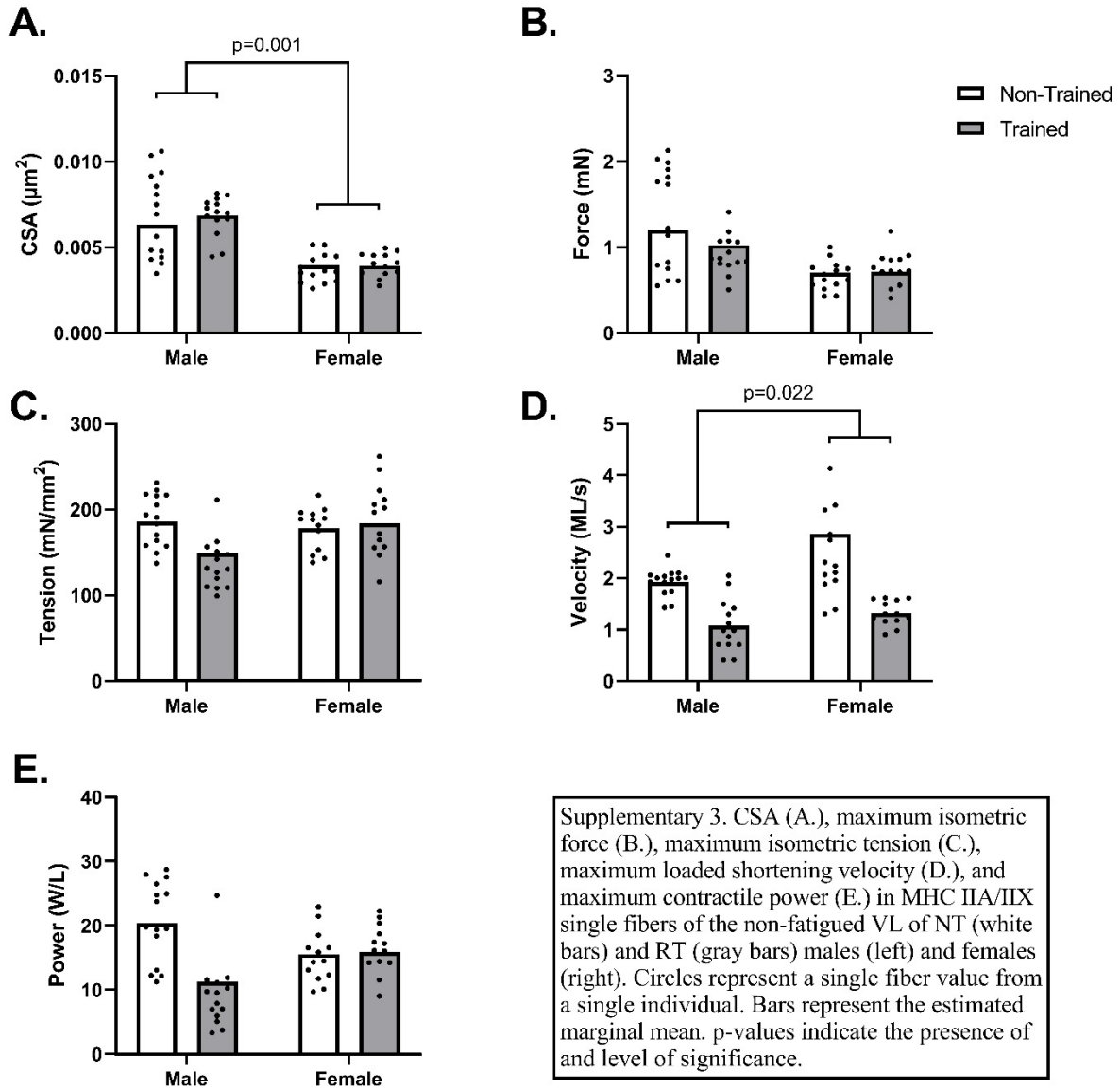
Supplementary Figures

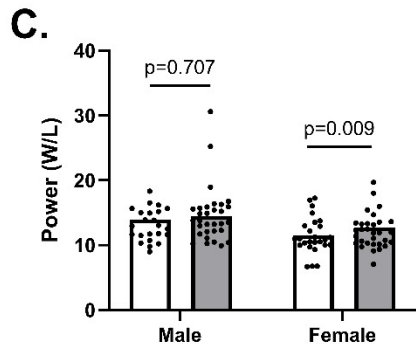
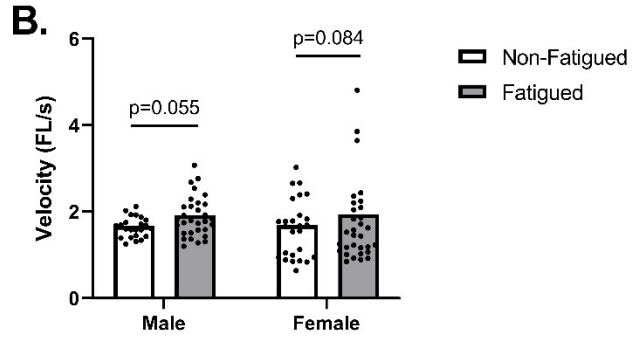
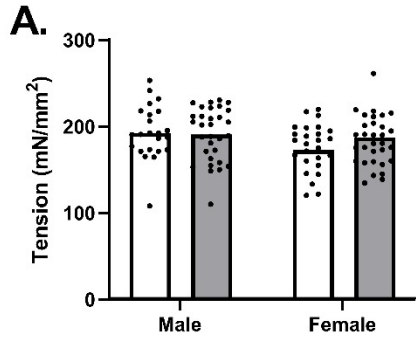


Supplementary 1. Comparison of different methods to assess fiber type in histology and SDS-PAGE. A. Relative abundance of MHC I, MHC IIA, and MHC IIX in NT and RT males and females. B. Association between Relative Abundance and Area Fraction of MHC I and MHC II fibers. C. Association between Relative Abundance and Fiber type distribution of MIIC I and MIIC II fibers. D. Representative image of MIIC homogenate samples via SDS-PAGE. ** indicates difference in MHC IIX abundance at $p < 0.01$

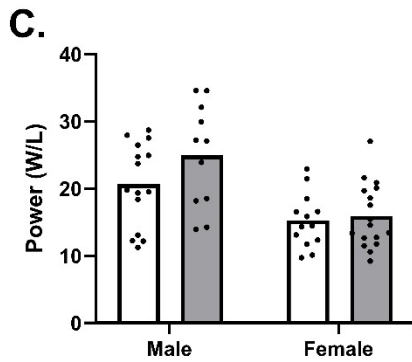
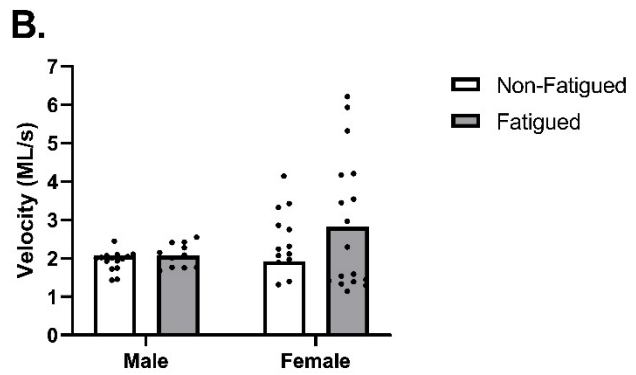
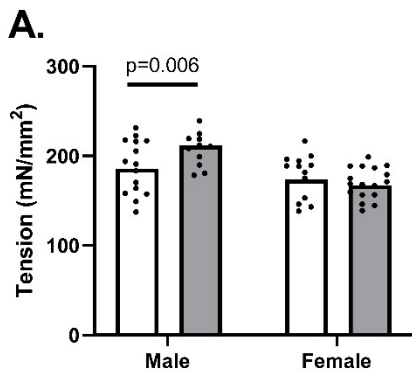


Supplementary 2. CSA (A.), maximum isometric force (B.), maximum isometric tension (C.), maximum loaded shortening velocity (D.), and maximum contractile power (E.) in MHC IIA single fibers of the non-fatigued VL of NT (white bars) and RT (gray bars) males (left) and females (right). Circles represent a single fiber value from a single individual. Bars represent the estimated marginal mean. p-values indicate the presence of and level of significance.

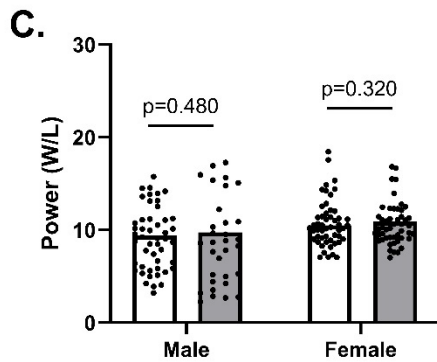
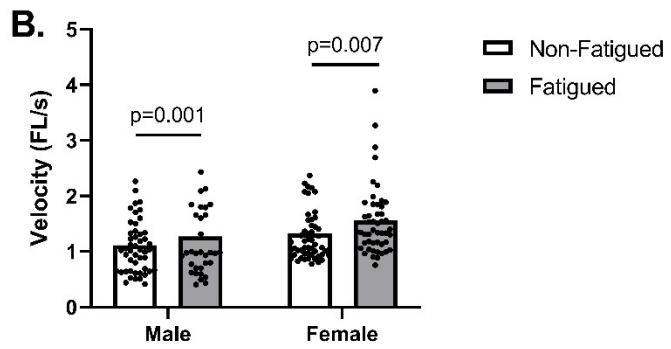
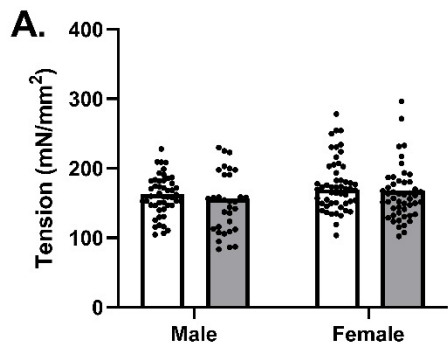




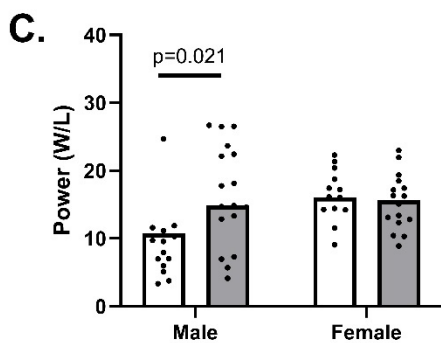
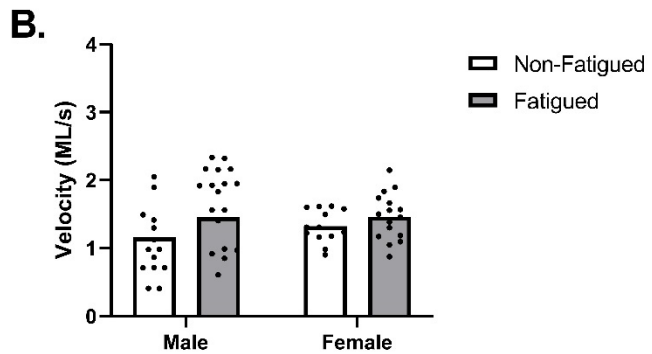
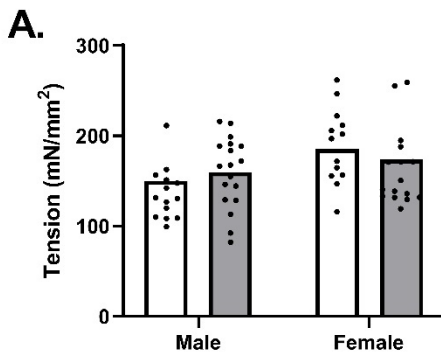
Supplementary 4. Maximum isometric tension (A.), maximum loaded shortening velocity (B.), and maximum contractile power (C.) in MHC IIA single fibers of the non-fatigued (white bars) and fatigued (gray bars) VL of NT males (left) and females (right). Circles represent a single fiber value from a single individual. Bars represent the estimated marginal mean. p-values indicate the presence of significance between non-fatigued and fatigued in that fiber type.



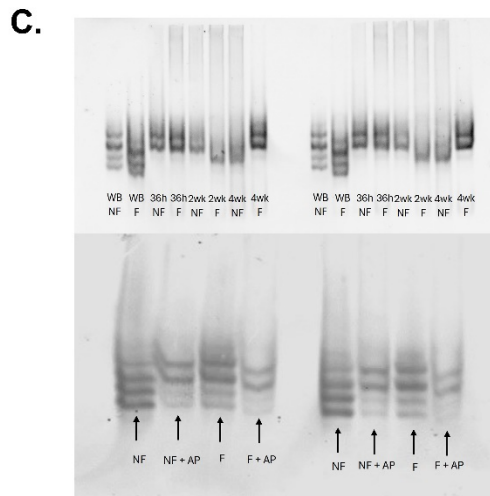
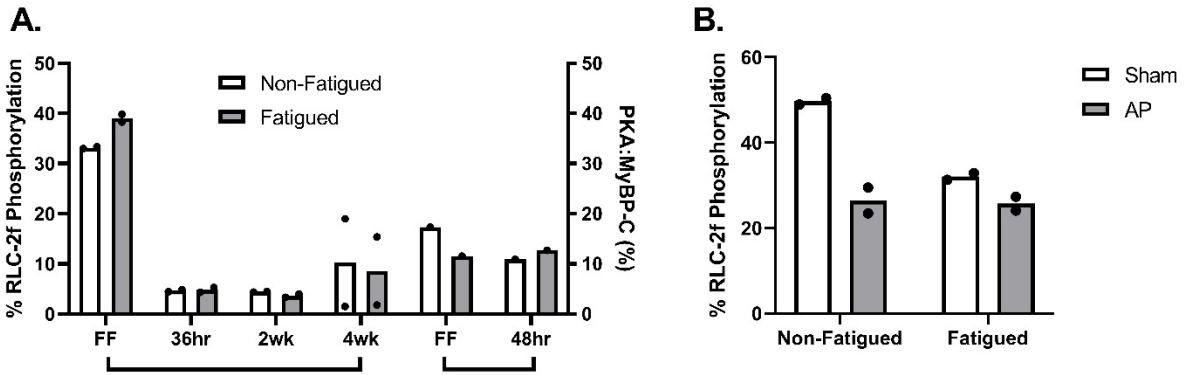
Supplementary 5. Maximum isometric tension (A.), maximum loaded shortening velocity (B.), and maximum contractile power (C.) in MHC IIA/IIX single fibers of the non-fatigued (white bars) and fatigued (gray bars) VL of NT males (left) and females (right). Circles represent a single fiber value from a single individual. Bars represent the estimated marginal mean. p-values indicate the presence of significance between non-fatigued and fatigued in that fiber type.



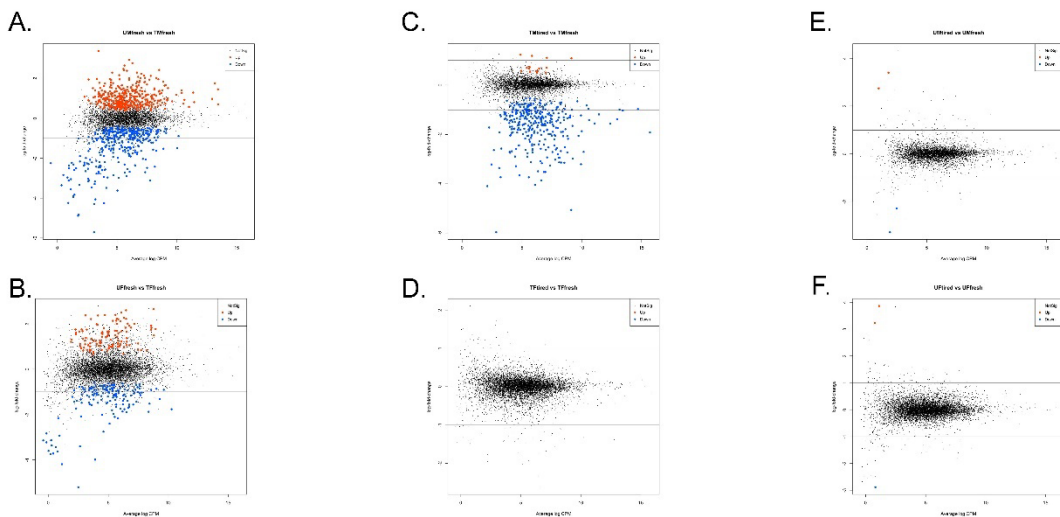
Supplementary 6. Maximum isometric tension (A.), maximum loaded shortening velocity (B.), and maximum contractile power (C.) in MHC IIA single fibers of the non-fatigued (white bars) and fatigued (gray bars) VL of RT males (left) and females (right). Circles represent a single fiber value from a single individual. Bars represent the estimated marginal mean. p-values indicate the presence of significance between non-fatigued and fatigued in that fiber type.



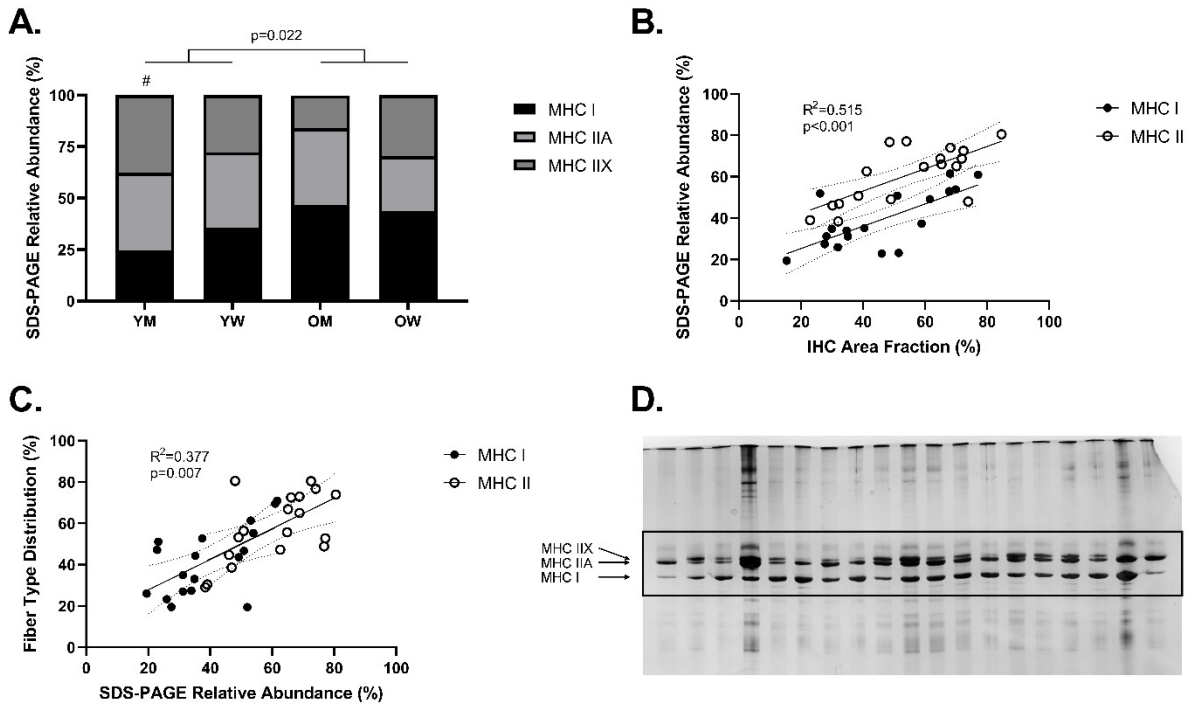
Supplementary 7. Maximum isometric tension (A.), maximum loaded shortening velocity (B.), and maximum contractile power (C.) in MHC IIA/IIX single fibers of the non-fatigued (white bars) and fatigued (gray bars) VL of RT males (left) and females (right). Circles represent a single fiber value from a single individual. Bars represent the estimated marginal mean. p-values indicate the presence of significance between non-fatigued and fatigued in that fiber type.



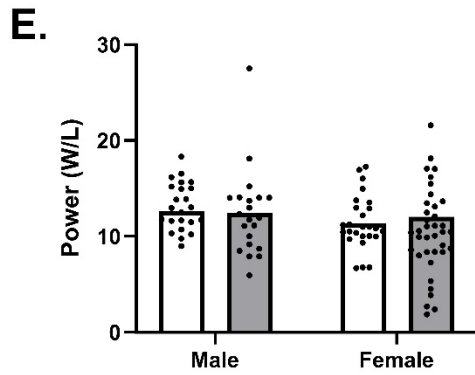
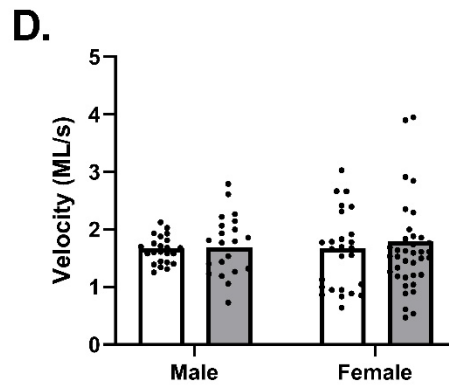
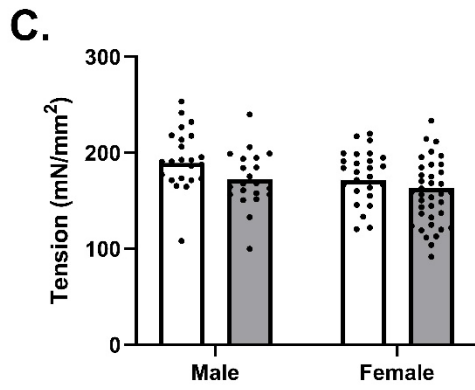
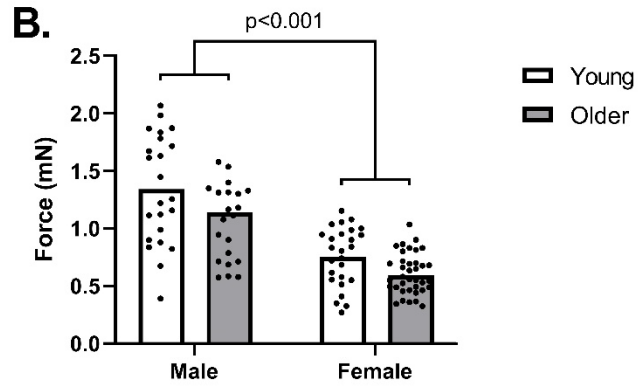
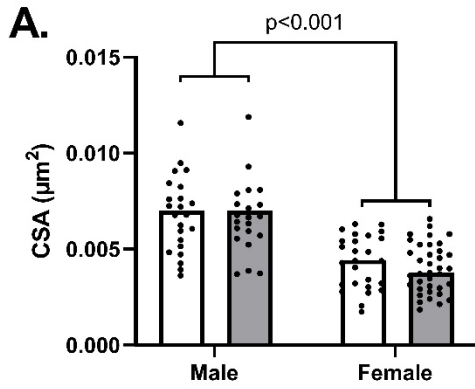
Supplementary 8. A. Phosphorylation of RLC-2f (left) and MyBP-C (right) in flash frozen (FF) and mechanically prepared tissue. B. RLC-2f phosphorylation following sham (white bars) or alkaline phosphatase (AP, gray bars) incubation to confirm phosphorylated bands. C. Western blot images of experiment A (top) and B (bottom) for RLC-2f.



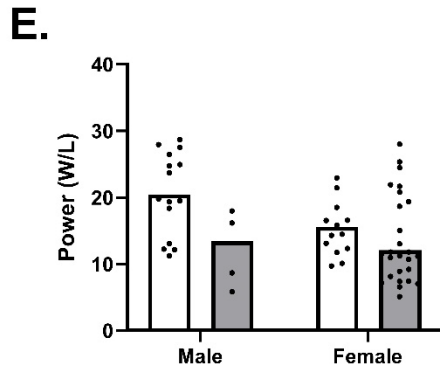
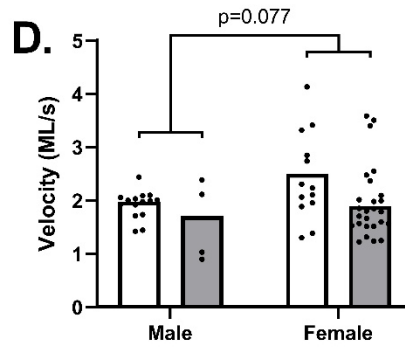
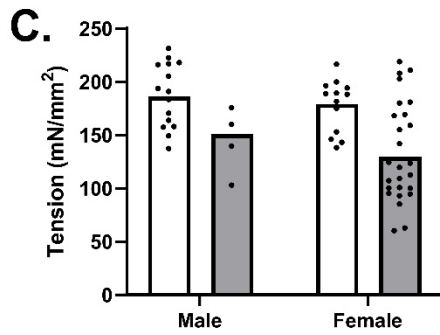
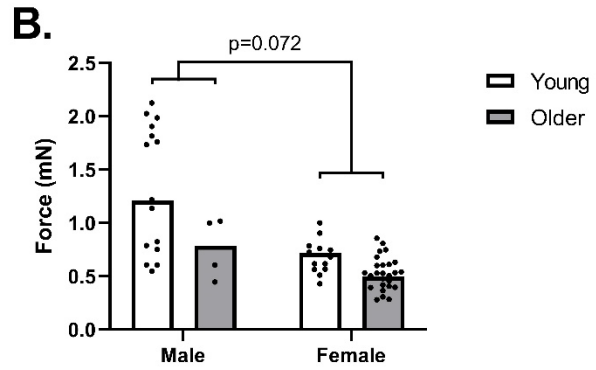
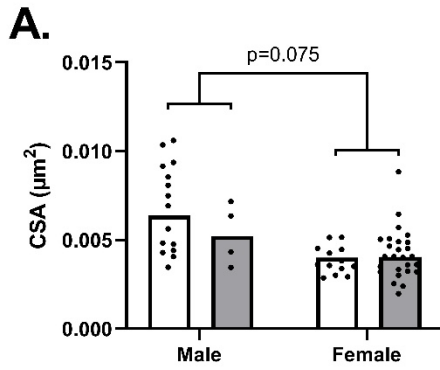
Supplementary Figure 9. Phosphoproteomic analysis of differentially phosphorylated residues from NT and RT NF and F samples. A. NT males vs RT males. B. NT females vs RT females. C. NF vs F in RT males. D. NF vs F in RT females. E. NF vs F in NT males. F. NF vs F in NT females. Each dot represents an individual residue and its fold change from RT male (A), RT female (B), NF (C,D,E,F). Red dots are significantly increased phosphorylation, blue dots are significantly decreased phosphorylation, and black dots are non-significant.



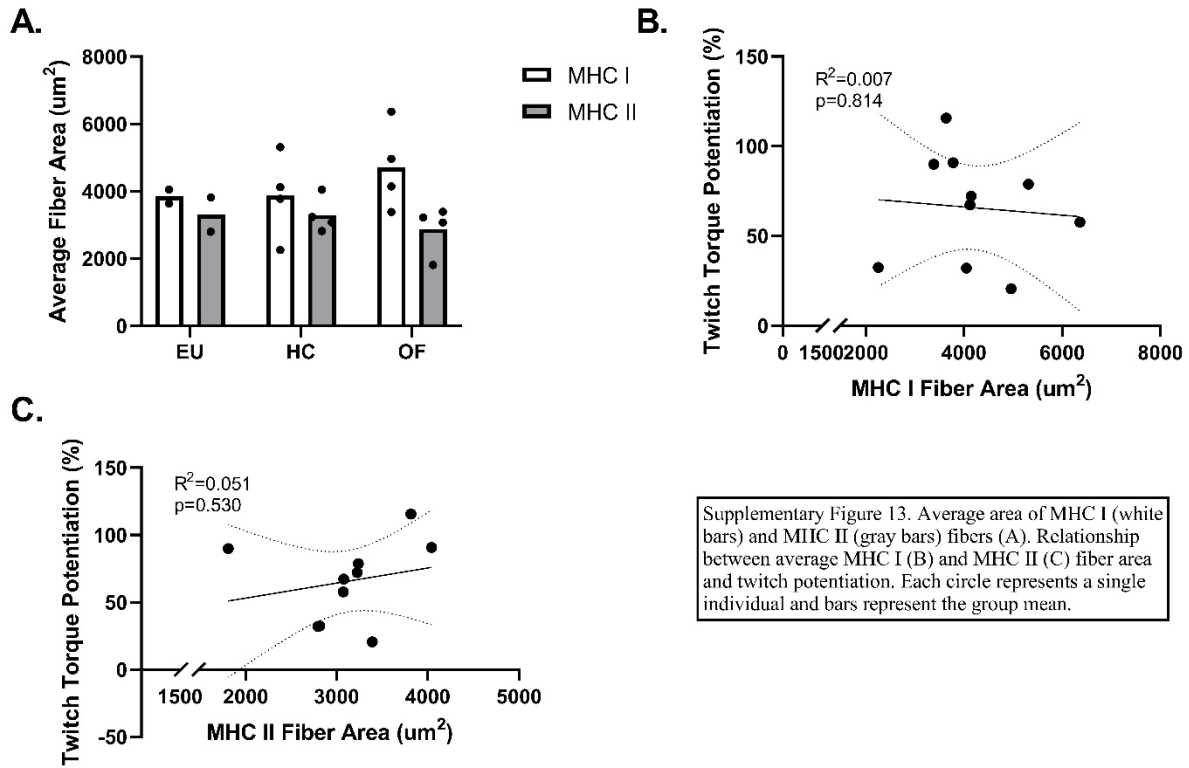
Supplementary 10. Comparison of different methods to assess fiber type in histology and SDS-PAGE. A. Relative abundance of MHC I, MHC IIA, and MHC IIX in Young and Older males and females. B. Association between Relative Abundance and Area Fraction of MHC I and MHC II fibers. C. Association between Relative Abundance and Fiber Type Distribution of MHC I and MHC II fibers. D. Representative image of MHC homogenate samples via SDS-PAGE. p-value indicates significantly different by age (A), # MHC IIX abundance different from Older male (A)



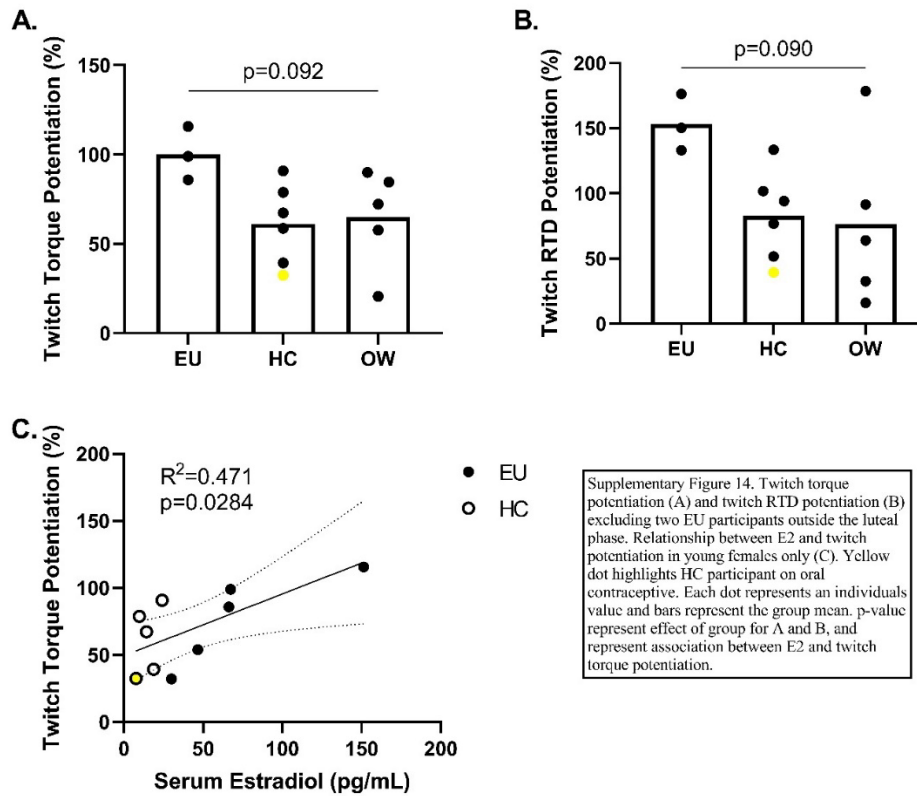
Supplementary 11. CSA (A.), maximum isometric force (B.), maximum isometric tension (C.), maximum loaded shortening velocity (D.), and maximum contractile power (E.) in MHC IIA single fibers of the non-fatigued VL of Young (white bars) and Older (gray bars) males (left) and females (right). Circles represent a single fiber value from a single individual. Bars represent the estimated marginal mean. p-values indicate the presence of significance between Male and Female in that fiber type.



Supplementary 12. CSA (A.), maximum isometric force (B.), maximum isometric tension (C.), maximum loaded shortening velocity (D.), and maximum contractile power (E.) in MHC IIA single fibers of the non-fatigued VL of Young (white bars) and Older (gray bars) males (left) and females (right). Circles represent a single fiber value from a single individual. Bars represent the estimated marginal mean. p-values indicate the presence of significance between Male and Female in that fiber type.



Supplementary Figure 13. Average area of MHC I (white bars) and MHC II (gray bars) fibers (A). Relationship between average MHC I (B) and MHC II (C) fiber area and twitch potentiation. Each circle represents a single individual and bars represent the group mean.



Supplementary Figure 14. Twitch torque potentiation (A) and twitch RTD potentiation (B) excluding two EU participants outside the luteal phase. Relationship between E2 and twitch potentiation in young females only (C). Yellow dot highlights HC participant on oral contraceptive. Each dot represents an individual value and bars represent the group mean. p-value represent effect of group for A and B, and represent association between E2 and twitch torque potentiation.

References

- Ackermann, M. A., Kerr, J. P., King, B., W. Ward, C., & Kontrogianni-Konstantopoulos, A. (2015). The Phosphorylation Profile of Myosin Binding Protein-C Slow is Dynamically Regulated in Slow-Twitch Muscles in Health and Disease. *Scientific Reports*, 5(1), 12637. <https://doi.org/10.1038/srep12637>
- Ackermann, M. A., & Kontrogianni-Konstantopoulos, A. (2011). Myosin binding protein-C slow is a novel substrate for protein kinase A (PKA) and C (PKC) in skeletal muscle. *Journal of Proteome Research*, 10(10), 4547–4555. <https://doi.org/10.1021/pr200355w>
- Akazawa, N., Kishi, M., Hino, T., Tsuji, R., Tamura, K., Hioka, A., & Moriyama, H. (2022). Relationship between muscle mass and fraction of intramuscular adipose tissue of the quadriceps in older inpatients. *PLOS ONE*, 17(2), e0263973. <https://doi.org/10.1371/journal.pone.0263973>
- Anderson, T., Wasserman, E. B., & Shultz, S. J. (2019). Anterior Cruciate Ligament Injury Risk by Season Period and Competition Segment: An Analysis of National Collegiate Athletic Association Injury Surveillance Data. *Journal of Athletic Training*, 54(7), 787–795. <https://doi.org/10.4085/1062-6050-501-17>
- Araújo, C. G. S., Kunutsor, S. K., Eijsvogels, T. M. H., Myers, J., Laukkanen, J. A., Hamar, D., Niebauer, J., Bhattacharjee, A., de Souza e Silva, C. G., Franca, J. F., & Castro, C. L. B. (2025). Muscle Power Versus Strength as a Predictor of Mortality in Middle-Aged and Older Men and Women. *Mayo Clinic Proceedings*. <https://doi.org/10.1016/j.mayocp.2025.02.015>

- Bamman, M. M., Hill, V. J., Adams, G. R., Haddad, F., Wetzstein, C. J., Gower, B. A., Ahmed, A., & Hunter, G. R. (2003a). Gender Differences in Resistance-Training-Induced Myofiber Hypertrophy Among Older Adults. *The Journals of Gerontology: Series A*, 58(2), B108–B116. <https://doi.org/10.1093/gerona/58.2.B108>
- Bamman, M. M., Hill, V. J., Adams, G. R., Haddad, F., Wetzstein, C. J., Gower, B. A., Ahmed, A., & Hunter, G. R. (2003b). Gender differences in resistance-training-induced myofiber hypertrophy among older adults. *The Journals of Gerontology. Series A, Biological Sciences and Medical Sciences*, 58(2), 108–116. <https://doi.org/10.1093/gerona/58.2.b108>
- Barefield, D., & Sadayappan, S. (2010). Phosphorylation and function of cardiac myosin binding protein-C in health and disease. *Journal of Molecular and Cellular Cardiology*, 48(5), 866–875. <https://doi.org/10.1016/j.yjmcc.2009.11.014>
- Bartolomei, S., Grillone, G., Di Michele, R., & Cortesi, M. (2021). A Comparison between Male and Female Athletes in Relative Strength and Power Performances. *Journal of Functional Morphology and Kinesiology*, 6(1), 17. <https://doi.org/10.3390/jfmk6010017>
- Blumenthal, D. K., & Stull, J. T. (1980). Activation of skeletal muscle myosin light chain kinase by calcium(2+) and calmodulin. *Biochemistry*, 19(24), 5608–5614. <https://doi.org/10.1021/bi00565a023>
- Bourne, M. N., Webster, K. E., & Hewett, T. E. (2019). Is Fatigue a Risk Factor for Anterior Cruciate Ligament Rupture? *Sports Medicine (Auckland, N.Z.)*, 49(11), 1629–1635. <https://doi.org/10.1007/s40279-019-01134-5>

- Bowman, B. F., Peterson, J. A., & Stull, J. T. (1992). Pre-steady-state kinetics of the activation of rabbit skeletal muscle myosin light chain kinase by Ca²⁺/calmodulin. *The Journal of Biological Chemistry*, *267*(8), 5346–5354.
- Bunch, T. A., Kanassatega, R.-S., Lepak, V. C., & Colson, B. A. (2019). Human cardiac myosin-binding protein C restricts actin structural dynamics in a cooperative and phosphorylation-sensitive manner. *The Journal of Biological Chemistry*, *294*(44), 16228–16240. <https://doi.org/10.1074/jbc.RA119.009543>
- Butler, T. M., Siegman, M. J., Mooers, S. U., & Barsotti, R. J. (1983). Myosin light chain phosphorylation does not modulate cross-bridge cycling rate in mouse skeletal muscle. *Science (New York, N.Y.)*, *220*(4602), 1167–1169. <https://doi.org/10.1126/science.6857239>
- Cabelka, C. A., Baumann, C. W., Collins, B. C., Nash, N., Le, G., Lindsay, A., Spangenburg, E. E., & Lowe, D. A. (2019). Effects of ovarian hormones and estrogen receptor α on physical activity and skeletal muscle fatigue in female mice. *Experimental Gerontology*, *115*, 155–164. <https://doi.org/10.1016/j.exger.2018.11.003>
- Callahan, D. M., Foulis, S. A., & Kent-Braun, J. A. (2009). Age-related fatigue resistance in the knee extensor muscles is specific to contraction mode. *Muscle & Nerve*, *39*(5), 692–702. <https://doi.org/10.1002/mus.21278>
- Callahan, D. M., & Kent-Braun, J. A. (2011). Effect of old age on human skeletal muscle force-velocity and fatigue properties. *Journal of Applied Physiology*, *111*(5), 1345–1352. <https://doi.org/10.1152/jappphysiol.00367.2011>

- Callahan, D. M., Umberger, B. R., & Kent, J. A. (2016). Mechanisms of in vivo muscle fatigue in humans: Investigating age-related fatigue resistance with a computational model. *The Journal of Physiology*, 594(12), 3407–3421. <https://doi.org/10.1113/JP271400>
- Campbell, K. S. (2006). Tension recovery in permeabilized rat soleus muscle fibers after rapid shortening and restretch. *Biophysical Journal*, 90(4), 1288–1294. <https://doi.org/10.1529/biophysj.105.067504>
- Carrier, L., Mearini, G., Stathopoulou, K., & Cuello, F. (2015). Cardiac myosin-binding protein C (MYBPC3) in cardiac pathophysiology. *Gene*, 573(2), 188–197. <https://doi.org/10.1016/j.gene.2015.09.008>
- Chidi-Ogbolu, N., & Baar, K. (2019). Effect of Estrogen on Musculoskeletal Performance and Injury Risk. *Frontiers in Physiology*, 9, 1834. <https://doi.org/10.3389/fphys.2018.01834>
- Chiu, L. Z. F., Fry, A. C., Weiss, L. W., Schilling, B. K., Brown, L. E., & Smith, S. L. (2003). Postactivation potentiation response in athletic and recreationally trained individuals. *Journal of Strength and Conditioning Research*, 17(4), 671–677. [https://doi.org/10.1519/1533-4287\(2003\)017<0671:ppriaa>2.0.co;2](https://doi.org/10.1519/1533-4287(2003)017<0671:ppriaa>2.0.co;2)
- Cho, E.-J., Choi, Y., Kim, J., Bae, J. H., Cho, J., Park, D.-H., Kang, J.-H., Yoon, J. H., Park, E., Seo, D. Y., Lee, S., & Kwak, H.-B. (2021). Exercise Training Attenuates Ovariectomy-Induced Alterations in Skeletal Muscle Remodeling, Apoptotic Signaling, and Atrophy Signaling in Rat Skeletal Muscle. *International Neurourology Journal*, 25(Suppl 2), S47–S54. <https://doi.org/10.5213/inj.2142334.167>

- Claflin, D. R., Larkin, L. M., Cederna, P. S., Horowitz, J. F., Alexander, N. B., Cole, N. M., Galecki, A. T., Chen, S., Nyquist, L. V., Carlson, B. M., Faulkner, J. A., & Ashton-Miller, J. A. (2011). Effects of high- and low-velocity resistance training on the contractile properties of skeletal muscle fibers from young and older humans. *Journal of Applied Physiology*, *111*(4), 1021–1030.
<https://doi.org/10.1152/jappphysiol.01119.2010>
- Coelingh Bennink, H. J. T. (2004). Are all estrogens the same? *Maturitas*, *47*(4), 269–275.
<https://doi.org/10.1016/j.maturitas.2003.11.009>
- Collins, B. C., Mader, T. L., Cabelka, C. A., Iñigo, M. R., Spangenburg, E. E., & Lowe, D. A. (2018). Deletion of estrogen receptor α in skeletal muscle results in impaired contractility in female mice. *Journal of Applied Physiology (Bethesda, Md.: 1985)*, *124*(4), 980–992. <https://doi.org/10.1152/jappphysiol.00864.2017>
- Colson, B. A. (2019). What a drag!: Skeletal myosin binding protein-C affects sarcomeric shortening. *The Journal of General Physiology*, *151*(5), 614–618.
<https://doi.org/10.1085/jgp.201912326>
- Colson, B. A., Petersen, K. J., Collins, B. C., Lowe, D. A., & Thomas, D. D. (2015). The myosin super-relaxed state is disrupted by estradiol deficiency. *Biochemical and Biophysical Research Communications*, *456*(1), 151–155.
<https://doi.org/10.1016/j.bbrc.2014.11.050>
- Cooke, R., Franks, K., Luciani, G. B., & Pate, E. (1988). The inhibition of rabbit skeletal muscle contraction by hydrogen ions and phosphate. *The Journal of Physiology*, *395*, 77–97. <https://doi.org/10.1113/jphysiol.1988.sp016909>

- Cooke, R., & Pate, E. (1985). The effects of ADP and phosphate on the contraction of muscle fibers. *Biophysical Journal*, 48(5), 789–798. [https://doi.org/10.1016/S0006-3495\(85\)83837-6](https://doi.org/10.1016/S0006-3495(85)83837-6)
- Crow, M. T., & Kushmerick, M. J. (1982). Myosin light chain phosphorylation is associated with a decrease in the energy cost for contraction in fast twitch mouse muscle. *The Journal of Biological Chemistry*, 257(5), 2121–2124.
- D’Antona, G., Lanfranconi, F., Pellegrino, M. A., Brocca, L., Adami, R., Rossi, R., Moro, G., Miotti, D., Canepari, M., & Bottinelli, R. (2006). Skeletal muscle hypertrophy and structure and function of skeletal muscle fibres in male body builders. *The Journal of Physiology*, 570(Pt 3), 611–627. <https://doi.org/10.1113/jphysiol.2005.101642>
- D’Antona, G., Pellegrino, M. A., Adami, R., Rossi, R., Carlizzi, C. N., Canepari, M., Saltin, B., & Bottinelli, R. (2003). The effect of ageing and immobilization on structure and function of human skeletal muscle fibres. *The Journal of Physiology*, 552(Pt 2), 499–511. <https://doi.org/10.1113/jphysiol.2003.046276>
- Dasa, M. S., Kristoffersen, M., Ersvær, E., Bovim, L. P., Bjørkhaug, L., Moe-Nilssen, R., Sagen, J. V., & Haukenes, I. (2021). The Female Menstrual Cycles Effect on Strength and Power Parameters in High-Level Female Team Athletes. *Frontiers in Physiology*, 12, 600668. <https://doi.org/10.3389/fphys.2021.600668>
- de la Motte, S. J., Lisman, P., Gribbin, T. C., Murphy, K., & Deuster, P. A. (2019). Systematic Review of the Association Between Physical Fitness and Musculoskeletal Injury Risk: Part 3-Flexibility, Power, Speed, Balance, and Agility. *Journal of Strength and*

Conditioning Research, 33(6), 1723–1735.

<https://doi.org/10.1519/JSC.0000000000002382>

Debold, E. P. (2012). Recent Insights into the Molecular Basis of Muscular Fatigue.

Medicine & Science in Sports & Exercise, 44(8), 1440.

<https://doi.org/10.1249/MSS.0b013e31824cfd26>

Debold, E. P., Beck, S. E., & Warshaw, D. M. (2008). Effect of low pH on single skeletal

muscle myosin mechanics and kinetics. *American Journal of Physiology. Cell*

Physiology, 295(1), C173–C179. <https://doi.org/10.1152/ajpcell.00172.2008>

Debold, E. P., Dave, H., & Fitts, R. H. (2004). Fiber type and temperature dependence of

inorganic phosphate: Implications for fatigue. *American Journal of Physiology. Cell*

Physiology, 287(3), C673–681. <https://doi.org/10.1152/ajpcell.00044.2004>

Debold, E. P., Fitts, R. H., Sundberg, C. W., & Nosek, T. M. (2016). Muscle Fatigue from the

Perspective of a Single Crossbridge. *Medicine and Science in Sports and Exercise*,

48(11), 2270–2280. <https://doi.org/10.1249/MSS.0000000000001047>

Debold, E. P., Walcott, S., Woodward, M., & Turner, M. A. (2013). Direct observation of

phosphate inhibiting the force-generating capacity of a miniensemble of Myosin

molecules. *Biophysical Journal*, 105(10), 2374–2384.

<https://doi.org/10.1016/j.bpj.2013.09.046>

Deitch, J. R., Starkey, C., Walters, S. L., & Moseley, J. B. (2006). Injury Risk in Professional

Basketball Players: A Comparison of Women's National Basketball Association and

National Basketball Association Athletes. *The American Journal of Sports Medicine*,

34(7), 1077–1083. <https://doi.org/10.1177/0363546505285383>

- D'Souza, A. C., Wageh, M., Williams, J. S., Colenso-Semple, L. M., McCarthy, D. G., McKay, A. K. A., Elliott-Sale, K. J., Burke, L. M., Parise, G., MacDonald, M. J., Tarnopolsky, M. A., & Phillips, S. M. (2023). Menstrual cycle hormones and oral contraceptives: A multimethod systems physiology-based review of their impact on key aspects of female physiology. *Journal of Applied Physiology (Bethesda, Md.: 1985)*, *135*(6), 1284–1299. <https://doi.org/10.1152/jappphysiol.00346.2023>
- Du, J., Yun, H., Wang, H., Bai, X., Su, Y., Ge, X., Wang, Y., Gu, B., Zhao, L., Yu, J.-G., & Song, Y. (2024). Proteomic Profiling of Muscular Adaptations to Short-Term Concentric Versus Eccentric Exercise Training in Humans. *Molecular & Cellular Proteomics : MCP*, *23*(4), 100748. <https://doi.org/10.1016/j.mcpro.2024.100748>
- Elliott-Sale, K. J., McNulty, K. L., Ansdell, P., Goodall, S., Hicks, K. M., Thomas, K., Swinton, P. A., & Dolan, E. (2020). The Effects of Oral Contraceptives on Exercise Performance in Women: A Systematic Review and Meta-analysis. *Sports Medicine*, *50*(10), 1785–1812. <https://doi.org/10.1007/s40279-020-01317-5>
- Elliott-Sale, K. J., Minahan, C. L., De Jonge, X. A. K. J., Ackerman, K. E., Sipilä, S., Constantini, N. W., Lebrun, C. M., & Hackney, A. C. (2021). Methodological Considerations for Studies in Sport and Exercise Science with Women as Participants: A Working Guide for Standards of Practice for Research on Women. *Sports Medicine*, *51*(5), 843–861. <https://doi.org/10.1007/s40279-021-01435-8>
- Enns, D. L., & Tiidus, P. M. (2010). The Influence of Estrogen on Skeletal Muscle: Sex Matters. *Sports Medicine*, *40*(1), 41–58. <https://doi.org/10.2165/11319760-000000000-00000>

- Erskine, R. M., Fletcher, G., & Folland, J. P. (2014). The contribution of muscle hypertrophy to strength changes following resistance training. *European Journal of Applied Physiology*, 114(6), 1239–1249. <https://doi.org/10.1007/s00421-014-2855-4>
- Esler, M., Kaye, D., Thompson, J., Jennings, G., Cox, H., Turner, A., Lambert, G., & Seals, D. (1995). Effects of aging on epinephrine secretion and regional release of epinephrine from the human heart. *The Journal of Clinical Endocrinology and Metabolism*, 80(2), 435–442. <https://doi.org/10.1210/jcem.80.2.7852502>
- Farrar, R. P., Monnin, K. A., Fordyce, D. E., & Walters, T. J. (1997). Uncoupling of changes in skeletal muscle beta-adrenergic receptor density and aerobic capacity during the aging process. *Aging (Milan, Italy)*, 9(1–2), 153–158. <https://doi.org/10.1007/BF03340141>
- Ford, G. A., Dachman, W. D., Blaschke, T. F., & Hoffman, B. B. (1995). Effect of aging on beta 2-adrenergic receptor-stimulated flux of K⁺, PO₄, FFA, and glycerol in human forearms. *Journal of Applied Physiology*, 78(1), 172–178. <https://doi.org/10.1152/jappl.1995.78.1.172>
- Fragala, M. S., Kenny, A. M., & Kuchel, G. A. (2015). Muscle Quality in Aging: A Multi-Dimensional Approach to Muscle Functioning with Applications for Treatment. *Sports Medicine*, 45(5), 641–658. <https://doi.org/10.1007/s40279-015-0305-z>
- Frontera, W. R., Reid, K. F., Phillips, E. M., Krivickas, L. S., Hughes, V. A., Roubenoff, R., & Fielding, R. A. (2008). Muscle fiber size and function in elderly humans: A longitudinal study. *Journal of Applied Physiology (Bethesda, Md.: 1985)*, 105(2), 637–642. <https://doi.org/10.1152/jappphysiol.90332.2008>

- Frontera, W. R., Suh, D., Krivickas, L. S., Hughes, V. A., Goldstein, R., & Roubenoff, R. (2000). Skeletal muscle fiber quality in older men and women. *American Journal of Physiology. Cell Physiology*, 279(3), C611-618.
<https://doi.org/10.1152/ajpcell.2000.279.3.C611>
- Fry, A. C. (2004). The Role of Resistance Exercise Intensity on Muscle Fibre Adaptations. *Sports Medicine*, 34(10), 663–679. <https://doi.org/10.2165/00007256-200434100-00004>
- Gash, M. C., Kandle, P. F., Murray, I. V., & Varacallo, M. A. (2025). Physiology, Muscle Contraction. In *StatPearls*. StatPearls Publishing.
<http://www.ncbi.nlm.nih.gov/books/NBK537140/>
- Gelfi, C., Viganò, A., Ripamonti, M., Pontoglio, A., Begum, S., Pellegrino, M. A., Grassi, B., Bottinelli, R., Wait, R., & Cerretelli, P. (2006). The human muscle proteome in aging. *Journal of Proteome Research*, 5(6), 1344–1353. <https://doi.org/10.1021/pr050414x>
- Gittings, W., Huang, J., Smith, I. C., Quadrilatero, J., & Vandenberg, R. (2011). The effect of skeletal myosin light chain kinase gene ablation on the fatigability of mouse fast muscle. *Journal of Muscle Research and Cell Motility*, 31(5–6), 337–348.
<https://doi.org/10.1007/s10974-011-9239-8>
- Goodpaster, B. H., Chomentowski, P., Ward, B. K., Rossi, A., Glynn, N. W., Delmonico, M. J., Kritchevsky, S. B., Pahor, M., & Newman, A. B. (2008). Effects of physical activity on strength and skeletal muscle fat infiltration in older adults: A randomized controlled trial. *Journal of Applied Physiology*, 105(5), 1498–1503.
<https://doi.org/10.1152/jappphysiol.90425.2008>

- Grange, R. W., & Houston, M. E. (1991). Simultaneous potentiation and fatigue in quadriceps after a 60-second maximal voluntary isometric contraction. *Journal of Applied Physiology (Bethesda, Md.: 1985)*, 70(2), 726–731.
<https://doi.org/10.1152/jappl.1991.70.2.726>
- Greenberg, M. J., Mealy, T. R., Jones, M., Szczesna-Cordary, D., & Moore, J. R. (2010). The direct molecular effects of fatigue and myosin regulatory light chain phosphorylation on the actomyosin contractile apparatus. *American Journal of Physiology. Regulatory, Integrative and Comparative Physiology*, 298(4), R989-996.
<https://doi.org/10.1152/ajpregu.00566.2009>
- Gregorich, Z. R., Peng, Y., Cai, W., Jin, Y., Wei, L., Chen, A. J., McKiernan, S. H., Aiken, J. M., Moss, R. L., Diffie, G. M., & Ge, Y. (2016). Top-Down Targeted Proteomics Reveals Decrease in Myosin Regulatory Light-Chain Phosphorylation That Contributes to Sarcopenic Muscle Dysfunction. *Journal of Proteome Research*, 15(8), 2706–2716.
<https://doi.org/10.1021/acs.jproteome.6b00244>
- Hansen, M., & Kjaer, M. (2014). Influence of sex and estrogen on musculotendinous protein turnover at rest and after exercise. *Exercise and Sport Sciences Reviews*, 42(4), 183–192. <https://doi.org/10.1249/JES.0000000000000026>
- Heldring, N., Pike, A., Andersson, S., Matthews, J., Cheng, G., Hartman, J., Tujague, M., Ström, A., Treuter, E., Warner, M., & Gustafsson, J.-A. (2007). Estrogen receptors: How do they signal and what are their targets. *Physiological Reviews*, 87(3), 905–931. <https://doi.org/10.1152/physrev.00026.2006>

- Heling, L. W. H. J., Geeves, M. A., & Kad, N. M. (2020a). MyBP-C: One protein to govern them all. *Journal of Muscle Research and Cell Motility*, *41*(1), 91–101.
<https://doi.org/10.1007/s10974-019-09567-1>
- Heling, L. W. H. J., Geeves, M. A., & Kad, N. M. (2020b). MyBP-C: One protein to govern them all. *Journal of Muscle Research and Cell Motility*, *41*(1), 91–101.
<https://doi.org/10.1007/s10974-019-09567-1>
- Hicks, A. L., Cupido, C. M., Martin, J., & Dent, J. (1991). Twitch potentiation during fatiguing exercise in the elderly: The effects of training. *European Journal of Applied Physiology and Occupational Physiology*, *63*(3–4), 278–281.
<https://doi.org/10.1007/BF00233862>
- Hoffman, N. J., Whitfield, J., Xiao, D., Radford, B. E., Suni, V., Blazev, R., Yang, P., Parker, B. L., & Hawley, J. A. (2025). Phosphoproteomics Uncovers Exercise Intensity-Specific Skeletal Muscle Signaling Networks Underlying High-Intensity Interval Training in Healthy Male Participants. *Sports Medicine*. <https://doi.org/10.1007/s40279-025-02217-2>
- Höök, P., Sriramoju, V., & Larsson, L. (2001). Effects of aging on actin sliding speed on myosin from single skeletal muscle cells of mice, rats, and humans. *American Journal of Physiology. Cell Physiology*, *280*(4), C782-788.
<https://doi.org/10.1152/ajpcell.2001.280.4.C782>
- Houston, M. E., & Grange, R. W. (1991). Torque potentiation and myosin light-chain phosphorylation in human muscle following a fatiguing contraction. *Canadian*

Journal of Physiology and Pharmacology, 69(2), 269–273.

<https://doi.org/10.1139/y91-041>

Houston, M. E., Green, H. J., & Stull, J. T. (1985). Myosin light chain phosphorylation and isometric twitch potentiation in intact human muscle. *Pflugers Archiv: European Journal of Physiology*, 403(4), 348–352. <https://doi.org/10.1007/BF00589245>

Houston, M. E., Lingley, M. D., Stuart, D. S., & Grange, R. W. (1987). Myosin light chain phosphorylation in intact human muscle. *FEBS Letters*, 219(2), 469–471.

[https://doi.org/10.1016/0014-5793\(87\)80274-0](https://doi.org/10.1016/0014-5793(87)80274-0)

Huang, J., Hegele, M., & Billino, J. (2018). Motivational Modulation of Age-Related Effects on Reaching Adaptation. *Frontiers in Psychology*, 9.

<https://doi.org/10.3389/fpsyg.2018.02285>

Hunter, S. K. (2014). Sex differences in human fatigability: Mechanisms and insight to physiological responses. *Acta Physiologica (Oxford, England)*, 210(4), 768–789.

<https://doi.org/10.1111/apha.12234>

Hunter, S. K., Thompson, M. W., Ruell, P. A., Harmer, A. R., Thom, J. M., Gwinn, T. H., & Adams, R. D. (1999). Human skeletal sarcoplasmic reticulum Ca²⁺ uptake and muscle function with aging and strength training. *Journal of Applied Physiology (Bethesda, Md.: 1985)*, 86(6), 1858–1865.

<https://doi.org/10.1152/jappl.1999.86.6.1858>

Hvid, L., Aagaard, P., Justesen, L., Bayer, M. L., Andersen, J. L., Ørtenblad, N., Kjaer, M., & Suetta, C. (2010). Effects of aging on muscle mechanical function and muscle fiber morphology during short-term immobilization and subsequent retraining. *Journal of*

Applied Physiology (Bethesda, Md.: 1985), 109(6), 1628–1634.

<https://doi.org/10.1152/jappphysiol.00637.2010>

Ishizuka, T., Yamamoto, M., Kajita, K., Yasuda, K., Miura, K., Hernandez, H., & Farese, R. V. (1993). Differential effect of aging on protein kinase C activity in rat adipocytes and soleus muscle. *Metabolism: Clinical and Experimental*, 42(4), 420–425.

[https://doi.org/10.1016/0026-0495\(93\)90097-8](https://doi.org/10.1016/0026-0495(93)90097-8)

Janse de Jonge, X. A., Boot, C. R., Thom, J. M., Ruell, P. A., & Thompson, M. W. (2001). The influence of menstrual cycle phase on skeletal muscle contractile characteristics in humans. *The Journal of Physiology*, 530(Pt 1), 161–166.

<https://doi.org/10.1111/j.1469-7793.2001.0161m.x>

Janssen, I., Heymsfield, S. B., & Ross, R. (2002). Low Relative Skeletal Muscle Mass (Sarcopenia) in Older Persons Is Associated with Functional Impairment and Physical Disability. *Journal of the American Geriatrics Society*, 50(5), 889–896.

<https://doi.org/10.1046/j.1532-5415.2002.50216.x>

Jin, X.-X., Sun, L., Lai, X.-L., Li, J., Liang, M.-L., & Ma, X. (2022). Effect of Mirena placement on reproductive hormone levels at different time intervals after artificial abortion. *World Journal of Clinical Cases*, 10(2), 511–517.

<https://doi.org/10.12998/wjcc.v10.i2.511>

Kirchengast, S., & Huber, J. (2009). Gender and age differences in lean soft tissue mass and sarcopenia among healthy elderly. *Anthropologischer Anzeiger*, 67(2), 139–151.

- Kitajima, Y., & Ono, Y. (2016). Estrogens maintain skeletal muscle and satellite cell functions. *The Journal of Endocrinology*, 229(3), 267–275.
<https://doi.org/10.1530/JOE-15-0476>
- Klug, G. A., Houston, M. E., Stull, J. T., & Pette, D. (1986). Decrease in myosin light chain kinase activity of rabbit fast muscle by chronic stimulation. *FEBS Letters*, 200(2), 352–354. [https://doi.org/10.1016/0014-5793\(86\)81167-x](https://doi.org/10.1016/0014-5793(86)81167-x)
- Knuth, S. T., Dave, H., Peters, J. R., & Fitts, R. H. (2006). Low cell pH depresses peak power in rat skeletal muscle fibres at both 30 degrees C and 15 degrees C: Implications for muscle fatigue. *The Journal of Physiology*, 575(Pt 3), 887–899.
<https://doi.org/10.1113/jphysiol.2006.106732>
- Korhonen, M. T., Cristea, A., Alén, M., Häkkinen, K., Sipilä, S., Mero, A., Viitasalo, J. T., Larsson, L., & Suominen, H. (2006). Aging, muscle fiber type, and contractile function in sprint-trained athletes. *Journal of Applied Physiology (Bethesda, Md.: 1985)*, 101(3), 906–917. <https://doi.org/10.1152/jappphysiol.00299.2006>
- Lai, S., Collins, B. C., Colson, B. A., Kararigas, G., & Lowe, D. A. (2016). Estradiol modulates myosin regulatory light chain phosphorylation and contractility in skeletal muscle of female mice. *American Journal of Physiology-Endocrinology and Metabolism*, 310(9), E724–E733. <https://doi.org/10.1152/ajpendo.00439.2015>
- Lamb, G. D., & Posterino, G. S. (2002). *Effects of oxidation and reduction on contractile function in skeletal muscle fibres of the rat.*
<https://doi.org/10.1113/jphysiol.2002.027896>

- Lanza, I. R., Larsen, R. G., & Kent-Braun, J. A. (2007). Effects of old age on human skeletal muscle energetics during fatiguing contractions with and without blood flow. *The Journal of Physiology*, 583(Pt 3), 1093–1105.
<https://doi.org/10.1113/jphysiol.2007.138362>
- Larsson, L., Li, X., & Frontera, W. R. (1997). Effects of aging on shortening velocity and myosin isoform composition in single human skeletal muscle cells. *The American Journal of Physiology*, 272(2 Pt 1), C638-649.
<https://doi.org/10.1152/ajpcell.1997.272.2.C638>
- Lexell, J., Downham, D. Y., Larsson, Y., Bruhn, E., & Morsing, B. (1995). Heavy-resistance training in older Scandinavian men and women: Short- and long-term effects on arm and leg muscles. *Scandinavian Journal of Medicine & Science in Sports*, 5(6), 329–341. <https://doi.org/10.1111/j.1600-0838.1995.tb00055.x>
- Lexell, J., Henriksson-Larsén, K., Winblad, B., & Sjöström, M. (1983). Distribution of different fiber types in human skeletal muscles: Effects of aging studied in whole muscle cross sections. *Muscle & Nerve*, 6(8), 588–595.
<https://doi.org/10.1002/mus.880060809>
- Lexell, J., Taylor, C. C., & Sjöström, M. (1988). What is the cause of the ageing atrophy? Total number, size and proportion of different fiber types studied in whole vastus lateralis muscle from 15- to 83-year-old men. *Journal of the Neurological Sciences*, 84(2–3), 275–294. [https://doi.org/10.1016/0022-510x\(88\)90132-3](https://doi.org/10.1016/0022-510x(88)90132-3)
- Li, A., Nelson, S. R., Rahmanseresht, S., Braet, F., Cornachione, A. S., Previs, S. B., O’Leary, T. S., McNamara, J. W., Rassier, D. E., Sadayappan, S., Previs, M. J., & Warshaw, D.

- M. (2019). Skeletal MyBP-C isoforms tune the molecular contractility of divergent skeletal muscle systems. *Proceedings of the National Academy of Sciences*, 116(43), 21882–21892. <https://doi.org/10.1073/pnas.1910549116>
- Liu, Y., Gampert, L., Nething, K., & Steinacker, J. M. (2006). Response and function of skeletal muscle heat shock protein 70. *Frontiers in Bioscience: A Journal and Virtual Library*, 11, 2802–2827. <https://doi.org/10.2741/2011>
- Manning, D. R., & Stull, J. T. (1982). Myosin light chain phosphorylation-dephosphorylation in mammalian skeletal muscle. *The American Journal of Physiology*, 242(3), C234–241. <https://doi.org/10.1152/ajpcell.1982.242.3.C234>
- Mashouri, P., Saboune, J., Pyle, W. G., & Power, G. A. (2024). Effects of chemically induced ovarian failure on single muscle fiber contractility in a mouse model of menopause. *Maturitas*, 180, 107885. <https://doi.org/10.1016/j.maturitas.2023.107885>
- McDonald, K. S. (2000). Ca²⁺ dependence of loaded shortening in rat skinned cardiac myocytes and skeletal muscle fibres. *The Journal of Physiology*, 525 Pt 1(Pt 1), 169–181. <https://doi.org/10.1111/j.1469-7793.2000.00169.x>
- McNeil, C. J., Doherty, T. J., Stashuk, D. W., & Rice, C. L. (2005). Motor unit number estimates in the tibialis anterior muscle of young, old, and very old men. *Muscle & Nerve*, 31(4), 461–467. <https://doi.org/10.1002/mus.20276>
- McNeil, C. J., & Rice, C. L. (2007). Fatigability Is Increased With Age During Velocity-Dependent Contractions of the Dorsiflexors. *The Journals of Gerontology: Series A*, 62(6), 624–629. <https://doi.org/10.1093/gerona/62.6.624>

- McNulty, K. L., Elliott-Sale, K. J., Dolan, E., Swinton, P. A., Ansdell, P., Goodall, S., Thomas, K., & Hicks, K. M. (2020). The Effects of Menstrual Cycle Phase on Exercise Performance in Eumenorrheic Women: A Systematic Review and Meta-Analysis. *Sports Medicine*, 50(10), 1813–1827. <https://doi.org/10.1007/s40279-020-01319-3>
- Meijer, J. P., Jaspers, R. T., Rittweger, J., Seynnes, O. R., Kamandulis, S., Brazaitis, M., Skurvydas, A., Pišot, R., Šimunič, B., Narici, M. V., & Degens, H. (2015). Single muscle fibre contractile properties differ between body-builders, power athletes and control subjects. *Experimental Physiology*, 100(11), 1331–1341. <https://doi.org/10.1113/EP085267>
- Metter, E. J., Talbot, L. A., Schrage, M., & Conwit, R. A. (2004). Arm-cranking muscle power and arm isometric muscle strength are independent predictors of all-cause mortality in men. *Journal of Applied Physiology (Bethesda, Md.: 1985)*, 96(2), 814–821. <https://doi.org/10.1152/jappphysiol.00370.2003>
- Metzger, J. M., Greaser, M. L., & Moss, R. L. (1989). Variations in cross-bridge attachment rate and tension with phosphorylation of myosin in mammalian skinned skeletal muscle fibers. Implications for twitch potentiation in intact muscle. *The Journal of General Physiology*, 93(5), 855–883. <https://doi.org/10.1085/jgp.93.5.855>
- Miller, A. E., MacDougall, J. D., Tarnopolsky, M. A., & Sale, D. G. (1993). Gender differences in strength and muscle fiber characteristics. *European Journal of Applied Physiology and Occupational Physiology*, 66(3), 254–262. <https://doi.org/10.1007/BF00235103>
- Miller, M. S., Bedrin, N. G., Callahan, D. M., Previs, M. J., Jennings, M. E., Ades, P. A., Maughan, D. W., Palmer, B. M., & Toth, M. J. (2013a). Age-related slowing of myosin

- actin cross-bridge kinetics is sex specific and predicts decrements in whole skeletal muscle performance in humans. *Journal of Applied Physiology*, 115(7), 1004–1014.
<https://doi.org/10.1152/jappphysiol.00563.2013>
- Miller, M. S., Bedrin, N. G., Callahan, D. M., Previs, M. J., Jennings, M. E., Ades, P. A., Maughan, D. W., Palmer, B. M., & Toth, M. J. (2013b). Age-related slowing of myosin actin cross-bridge kinetics is sex specific and predicts decrements in whole skeletal muscle performance in humans. *Journal of Applied Physiology*, 115(7), 1004–1014.
<https://doi.org/10.1152/jappphysiol.00563.2013>
- Momenzadeh, A., Jiang, Y., Kreimer, S., Teigen, L. E., Zepeda, C. S., Haghani, A., Mastali, M., Song, Y., Hutton, A., Parker, S. J., Van Eyk, J. E., Sundberg, C. W., & Meyer, J. G. (2023). A Complete Workflow for High Throughput Human Single Skeletal Muscle Fiber Proteomics. *Journal of the American Society for Mass Spectrometry*, 34(9), 1858–1867. <https://doi.org/10.1021/jasms.3c00072>
- Monti, E., Franchi, M. V., Badiali, F., Quinlan, J. I., Longo, S., & Narici, M. V. (2020). The Time-Course of Changes in Muscle Mass, Architecture and Power During 6 Weeks of Plyometric Training. *Frontiers in Physiology*, 11, 946.
<https://doi.org/10.3389/fphys.2020.00946>
- Moore, R. L., & Stull, J. T. (1984). Myosin light chain phosphorylation in fast and slow skeletal muscles in situ. *The American Journal of Physiology*, 247(5 Pt 1), C462-471.
<https://doi.org/10.1152/ajpcell.1984.247.5.C462>
- Moran, A. L., Nelson, S. A., Landisch, R. M., Warren, G. L., & Lowe, D. A. (2007). Estradiol replacement reverses ovariectomy-induced muscle contractile and myosin

- dysfunction in mature female mice. *Journal of Applied Physiology (Bethesda, Md.: 1985)*, 102(4), 1387–1393. <https://doi.org/10.1152/jappphysiol.01305.2006>
- Moss, R. L. (1979). Sarcomere length-tension relations of frog skinned muscle fibres during calcium activation at short lengths. *The Journal of Physiology*, 292, 177–192. <https://doi.org/10.1113/jphysiol.1979.sp012845>
- Mueller-Schotte, S., Bleijenberg, Nienke, van der Schouw, Yvonne T, & Schuurmans, M. J. (2016). Fatigue as a long-term risk factor for limitations in instrumental activities of daily living and/or mobility performance in older adults after 10 years. *Clinical Interventions in Aging*, 11, 1579–1587. <https://doi.org/10.2147/CIA.S116741>
- Nelson, C. R., Debold, E. P., & Fitts, R. H. (2014). Phosphate and acidosis act synergistically to depress peak power in rat muscle fibers. *American Journal of Physiology-Cell Physiology*, 307(10), C939–C950. <https://doi.org/10.1152/ajpcell.00206.2014>
- Nelson, C. R., & Fitts, R. H. (2014). Effects of low cell pH and elevated inorganic phosphate on the pCa-force relationship in single muscle fibers at near-physiological temperatures. *American Journal of Physiology. Cell Physiology*, 306(7), C670-678. <https://doi.org/10.1152/ajpcell.00347.2013>
- Ochala, J., Frontera, W. R., Dorer, D. J., Van Hoecke, J., & Krivickas, L. S. (2007). Single skeletal muscle fiber elastic and contractile characteristics in young and older men. *The Journals of Gerontology. Series A, Biological Sciences and Medical Sciences*, 62(4), 375–381. <https://doi.org/10.1093/gerona/62.4.375>
- O’Leary, M., Greed, E., Pritchard, J., Struszczak, L., Bozbaş, E., & Bowtell, J. (2024). The skeletal muscle proteomic determinants of neuromuscular function in young and

- older women following 8 weeks of resistance training. *Experimental Physiology*, 110(3), 438–453. <https://doi.org/10.1113/EP092328>
- Palmer, B. M., & Moore, R. L. (1989). Myosin light chain phosphorylation and tension potentiation in mouse skeletal muscle. *The American Journal of Physiology*, 257(5 Pt 1), C1012-1019. <https://doi.org/10.1152/ajpcell.1989.257.5.C1012>
- Parente, V., D'Antona, G., Adami, R., Miotti, D., Capodaglio, P., De Vito, G., & Bottinelli, R. (2008). Long-term resistance training improves force and unloaded shortening velocity of single muscle fibres of elderly women. *European Journal of Applied Physiology*, 104(5), 885–893. <https://doi.org/10.1007/s00421-008-0845-0>
- Parsons, B., Szczesna, D., Zhao, J., Van Slooten, G., Kerrick, W. G., Putkey, J. A., & Potter, J. D. (1997). The effect of pH on the Ca²⁺ affinity of the Ca²⁺ regulatory sites of skeletal and cardiac troponin C in skinned muscle fibres. *Journal of Muscle Research and Cell Motility*, 18(5), 599–609. <https://doi.org/10.1023/a:1018623604365>
- Pellegrino, A., Tiidus, P. M., & Vandenboom, R. (2022). Mechanisms of Estrogen Influence on Skeletal Muscle: Mass, Regeneration, and Mitochondrial Function. *Sports Medicine*, 52(12), 2853–2869. <https://doi.org/10.1007/s40279-022-01733-9>
- Perez-Gomez, J., Rodriguez, G. V., Ara, I., Olmedillas, H., Chavarren, J., González-Henriquez, J. J., Dorado, C., & Calbet, J. A. L. (2008). Role of muscle mass on sprint performance: Gender differences? *European Journal of Applied Physiology*, 102(6), 685–694. <https://doi.org/10.1007/s00421-007-0648-8>

- Persechini, A., Stull, J. T., & Cooke, R. (1985). The effect of myosin phosphorylation on the contractile properties of skinned rabbit skeletal muscle fibers. *The Journal of Biological Chemistry*, 260(13), 7951–7954.
- Petrella, R. J., Cunningham, D. A., Vandervoort, A. A., & Paterson, D. H. (1989). Comparison of twitch potentiation in the gastrocnemius of young and elderly men. *European Journal of Applied Physiology and Occupational Physiology*, 58(4), 395–399.
<https://doi.org/10.1007/BF00643515>
- Piasecki, J., Guo, Y., Jones, E. J., Phillips, B. E., Stashuk, D. W., Atherton, P. J., & Piasecki, M. (2023). Menstrual Cycle Associated Alteration of Vastus Lateralis Motor Unit Function. *Sports Medicine - Open*, 9(1), 97. <https://doi.org/10.1186/s40798-023-00639-8>
- Plubell, D. L., Wilmarth, P. A., Zhao, Y., Fenton, A. M., Minnier, J., Reddy, A. P., Klimek, J., Yang, X., David, L. L., & Pamir, N. (2017). Extended Multiplexing of Tandem Mass Tags (TMT) Labeling Reveals Age and High Fat Diet Specific Proteome Changes in Mouse Epididymal Adipose Tissue. *Molecular & Cellular Proteomics: MCP*, 16(5), 873–890.
<https://doi.org/10.1074/mcp.M116.065524>
- Pöllänen, E., Ronkainen, P. H. A., Horttanainen, M., Takala, T., Puolakka, J., Suominen, H., Sipilä, S., & Kovanen, V. (2010). Effects of combined hormone replacement therapy or its effective agents on the IGF-1 pathway in skeletal muscle. *Growth Hormone & IGF Research*, 20(5), 372–379. <https://doi.org/10.1016/j.ghir.2010.07.003>
- Power, G. A., Allen, M. D., Booth, W. J., Thompson, R. T., Marsh, G. D., & Rice, C. L. (2014). The influence on sarcopenia of muscle quality and quantity derived from magnetic

resonance imaging and neuromuscular properties. *Age*, 36(3), 9642.

<https://doi.org/10.1007/s11357-014-9642-3>

Previs, M. J., Mun, J. Y., Michalek, A. J., Previs, S. B., Gulick, J., Robbins, J., Warshaw, D. M., & Craig, R. (2016). Phosphorylation and calcium antagonistically tune myosin-binding protein C's structure and function. *Proceedings of the National Academy of Sciences of the United States of America*, 113(12), 3239–3244.

<https://doi.org/10.1073/pnas.1522236113>

Privett, G. E., Ricci, A. W., David, L. L., Wiedenfeld Needham, K., Tan, Y. H., Nakayama, K. H., & Callahan, D. M. (2024). Fatiguing exercise reduces cellular passive Young's modulus in human vastus lateralis muscle. *Experimental Physiology*, 109(11), 1922–1937. <https://doi.org/10.1113/EP092072>

Privett, G. E., Ricci, A. W., Needham, K. W., & Callahan, D. M. (2024). *Chronic and Acute Mediators of Passive Viscoelasticity in Human Skeletal Muscle Fibers* (p. 2024.08.13.607865). bioRxiv. <https://doi.org/10.1101/2024.08.13.607865>

Privett, G. E., Ricci, A. W., Ortiz-Delatorre, J., & Callahan, D. M. (2024). Predicting myosin heavy chain isoform from postdissection fiber length in human skeletal muscle fibers. *American Journal of Physiology - Cell Physiology*, 326(3), C749–C755. <https://doi.org/10.1152/ajpcell.00700.2023>

Rayment, I., Rypniewski, W. R., Schmidt-Bäse, K., Smith, R., Tomchick, D. R., Benning, M. M., Winkelmann, D. A., Wesenberg, G., & Holden, H. M. (1993). Three-dimensional structure of myosin subfragment-1: A molecular motor. *Science (New York, N.Y.)*, 261(5117), 50–58. <https://doi.org/10.1126/science.8316857>

Robinett, J. C., Hanft, L. M., Geist, J., Kontrogianni-Konstantopoulos, A., & McDonald, K. S.

(2019). Regulation of myofilament force and loaded shortening by skeletal myosin binding protein C. *The Journal of General Physiology*, 151(5), 645–659.

<https://doi.org/10.1085/jgp.201812200>

Rodriguez, L. A., Casey, E., Crossley, E., Williams, N., & Dhafer, Y. Y. (2024). The hormonal profile in women using combined monophasic oral contraceptive pills varies across the pill cycle: A temporal analysis of serum endogenous and exogenous hormones using liquid chromatography with tandem mass spectroscopy. *American Journal of Physiology-Endocrinology and Metabolism*, 327(1), E121–E133.

<https://doi.org/10.1152/ajpendo.00418.2023>

Rose, A. J., Michell, B. J., Kemp, B. E., & Hargreaves, M. (2004). Effect of exercise on protein kinase C activity and localization in human skeletal muscle. *The Journal of Physiology*, 561(Pt 3), 861–870. <https://doi.org/10.1113/jphysiol.2004.075549>

Schoenfeld, B. J. (2010). The Mechanisms of Muscle Hypertrophy and Their Application to Resistance Training. *The Journal of Strength & Conditioning Research*, 24(10), 2857. <https://doi.org/10.1519/JSC.0b013e3181e840f3>

Schoenfeld, B. J., Grgic, J., Ogborn, D., & Krieger, J. W. (2017). Strength and Hypertrophy Adaptations Between Low- vs. High-Load Resistance Training: A Systematic Review and Meta-analysis. *The Journal of Strength & Conditioning Research*, 31(12), 3508. <https://doi.org/10.1519/JSC.0000000000002200>

- Seals, D. R., Chase, P. B., & Taylor, J. A. (1988). Autonomic mediation of the pressor responses to isometric exercise in humans. *Journal of Applied Physiology*, *64*(5), 2190–2196. <https://doi.org/10.1152/jappl.1988.64.5.2190>
- Senefeld, J., Yoon, T., Bement, M. H., & Hunter, S. K. (2013). Fatigue and recovery from dynamic contractions in men and women differ for arm and leg muscles. *Muscle & Nerve*, *48*(3), 436–439. <https://doi.org/10.1002/mus.23836>
- Shoepe, T. C., Stelzer, J. E., Garner, D. P., & Widrick, J. J. (2003). Functional Adaptability of Muscle Fibers to Long-Term Resistance Exercise: *Medicine & Science in Sports & Exercise*, *35*(6), 944–951. <https://doi.org/10.1249/01.MSS.0000069756.17841.9E>
- Sipilä, S., Narici, M., Kjaer, M., Pöllänen, E., Atkinson, R. A., Hansen, M., & Kovanen, V. (2013). Sex hormones and skeletal muscle weakness. *Biogerontology*, *14*(3), 231–245. <https://doi.org/10.1007/s10522-013-9425-8>
- Stuart, D. S., Lingley, M. D., Grange, R. W., & Houston, M. E. (1988). Myosin light chain phosphorylation and contractile performance of human skeletal muscle. *Canadian Journal of Physiology and Pharmacology*, *66*(1), 49–54. <https://doi.org/10.1139/y88-009>
- Stull, J. T., Kamm, K. E., & Vandenoorn, R. (2011). Myosin light chain kinase and the role of myosin light chain phosphorylation in skeletal muscle. *Archives of Biochemistry and Biophysics*, *510*(2), 120–128. <https://doi.org/10.1016/j.abb.2011.01.017>
- Sweeney, H. L., & Stull, J. T. (1986). Phosphorylation of myosin in permeabilized mammalian cardiac and skeletal muscle cells. *The American Journal of Physiology*, *250*(4 Pt 1), C657–660. <https://doi.org/10.1152/ajpcell.1986.250.4.C657>

- Sweeney, H. L., & Stull, J. T. (1990). Alteration of cross-bridge kinetics by myosin light chain phosphorylation in rabbit skeletal muscle: Implications for regulation of actin-myosin interaction. *Proceedings of the National Academy of Sciences of the United States of America*, 87(1), 414–418. <https://doi.org/10.1073/pnas.87.1.414>
- Taaffe, D. R., Sipilä, S., Cheng, S., Puolakka, J., Toivanen, J., & Suominen, H. (2005). The effect of hormone replacement therapy and/or exercise on skeletal muscle attenuation in postmenopausal women: A yearlong intervention. *Clinical Physiology and Functional Imaging*, 25(5), 297–304. <https://doi.org/10.1111/j.1475-097X.2005.00628.x>
- Takagi, Y., Shuman, H., & Goldman, Y. E. (2004). Coupling between phosphate release and force generation in muscle actomyosin. *Philosophical Transactions of the Royal Society of London. Series B, Biological Sciences*, 359(1452), 1913–1920. <https://doi.org/10.1098/rstb.2004.1561>
- Taylor, M. Y., Osborne, J. O., Topranin, V. D. M., Engseth, T. P., Solli, G. S., Valsdottir, D., Andersson, E., Øistuen, G. F., Flatby, I., Welde, B., Morseth, B., Haugen, T., Sandbakk, Ø., & Noordhof, D. A. (2024). Menstrual Cycle Phase has no Influence on Performance-Determining Variables in Endurance-Trained Athletes: The FENDURA Project. *Medicine & Science in Sports & Exercise*. <https://doi.org/10.1249/MSS.0000000000003447>
- Trappe, S., Gallagher, P., Harber, M., Carrithers, J., Fluckey, J., & Trappe, T. (2003). Single Muscle Fibre Contractile Properties in Young and Old Men and Women. *The Journal of Physiology*, 552(1), 47–58. <https://doi.org/10.1113/jphysiol.2003.044966>

- Trappe, S., Godard, M., Gallagher, P., Carroll, C., Rowden, G., & Porter, D. (2001). Resistance training improves single muscle fiber contractile function in older women. *American Journal of Physiology-Cell Physiology*, 281(2), C398–C406. <https://doi.org/10.1152/ajpcell.2001.281.2.C398>
- Trappe, S., Williamson, D., Godard, M., Porter, D., Rowden, G., & Costill, D. (2000). *Effect of resistance training on single muscle fiber contractile function in older men.*
- Venturelli, M., Saggin, P., Muti, E., Naro, F., Cancellara, L., Toniolo, L., Tarperi, C., Calabria, E., Richardson, R. S., Reggiani, C., & Schena, F. (2015). In vivo and in vitro evidence that intrinsic upper- and lower-limb skeletal muscle function is unaffected by ageing and disuse in oldest-old humans. *Acta Physiologica (Oxford, England)*, 215(1), 58–71. <https://doi.org/10.1111/apha.12524>
- Wattanapernpool, J., & Reiser, P. J. (1999). Differential effects of ovariectomy on calcium activation of cardiac and soleus myofilaments. *American Journal of Physiology-Heart and Circulatory Physiology*, 277(2), H467–H473. <https://doi.org/10.1152/ajpheart.1999.277.2.H467>
- Westcott, W. L. (2012). Resistance training is medicine: Effects of strength training on health. *Current Sports Medicine Reports*, 11(4), 209–216. <https://doi.org/10.1249/JSR.0b013e31825dabb8>
- Westwood, S. A., Hudlicka, O., & Perry, S. V. (1984). Phosphorylation in vivo of the P light chain of myosin in rabbit fast and slow skeletal muscles. *The Biochemical Journal*, 218(3), 841–847. <https://doi.org/10.1042/bj2180841>

- Widrick, J. J., Stelzer, J. E., Shoepe, T. C., & Garner, D. P. (2002). Functional properties of human muscle fibers after short-term resistance exercise training. *American Journal of Physiology-Regulatory, Integrative and Comparative Physiology*, 283(2), R408–R416. <https://doi.org/10.1152/ajpregu.00120.2002>
- Wrucke, D. J., Kuplic, A., Adam, M. D., Hunter, S. K., & Sundberg, C. W. (2024). Neural and muscular contributions to the age-related differences in peak power of the knee extensors in men and women. *Journal of Applied Physiology*, 137(4), 1021–1040. <https://doi.org/10.1152/jappphysiol.00773.2023>
- Xeni, J., Gittings, W. B., Caterini, D., Huang, J., Houston, M. E., Grange, R. W., & Vandenboom, R. (2011). Myosin light-chain phosphorylation and potentiation of dynamic function in mouse fast muscle. *Pflügers Archiv - European Journal of Physiology*, 462(2), 349–358. <https://doi.org/10.1007/s00424-011-0965-y>
- Yoon, T., De-Lap, B. S., Griffith, E. E., & Hunter, S. K. (2008). Age-related muscle fatigue after a low-force fatiguing contraction is explained by central fatigue. *Muscle & Nerve*, 37(4), 457–466. <https://doi.org/10.1002/mus.20969>
- Yoon, T., Doyel, R., Widule, C., & Hunter, S. K. (2015). Sex differences with aging in the fatigability of dynamic contractions. *Experimental Gerontology*, 70, 1–10. <https://doi.org/10.1016/j.exger.2015.07.001>
- Yu, F., Hedström, M., Cristea, A., Dalén, N., & Larsson, L. (2007). Effects of ageing and gender on contractile properties in human skeletal muscle and single fibres. *Acta Physiologica (Oxford, England)*, 190(3), 229–241. <https://doi.org/10.1111/j.1748-1716.2007.01699.x>

Zhi, G., Ryder, J. W., Huang, J., Ding, P., Chen, Y., Zhao, Y., Kamm, K. E., & Stull, J. T. (2005). Myosin light chain kinase and myosin phosphorylation effect frequency-dependent potentiation of skeletal muscle contraction. *Proceedings of the National Academy of Sciences of the United States of America*, *102*(48), 17519–17524.
<https://doi.org/10.1073/pnas.0506846102>